NAVAL POSTGRADUATE SCHOOL
Monterey, California

THESIS

STATIC AND DYNAMIC FLOW VISUALIZATION
STUDIES OF TWO DOUBLE-DELTA WING MODELS
AT HIGH ANGLES OF ATTACK

by

LI, FENG-HSI

March 1992

Thesis Advisor:	S. K. Hebbar
Co-Advisor:	M. F. Platzer

Approved for public release; distribution is unlimited

REPORT DOCUMENTATION PAGE

1a. REPORT SECURITY CLASSIFICATION Unclassified	1b. RESTRICTIVE MARKINGS

2a. SECURITY CLASSIFICATION AUTHORITY	3. DISTRIBUTION/AVAILABILITY OF REPORT
2b. DECLASSIFICATION/DOWNGRADING SCHEDULE	Approved for public release; distribution is unlimited.

4. PERFORMING ORGANIZATION REPORT NUMBER(S)	5. MONITORING ORGANIZATION REPORT NUMBER(S)

6a. NAME OF PERFORMING ORGANIZATION Naval Postgraduate School	6b. OFFICE SYMBOL (If applicable) AA	7a. NAME OF MONITORING ORGANIZATION Naval Postgraduate School

6c. ADDRESS (City, State, and ZIP Code) Monterey, CA 93943-5000	7b. ADDRESS (City, State, and ZIP Code) Monterey, CA 93943-5000

8a. NAME OF FUNDING/SPONSORING ORGANIZATION	8b. OFFICE SYMBOL (If applicable)	9. PROCUREMENT INSTRUMENT IDENTIFICATION NUMBER

8c. ADDRESS (City, State, and ZIP Code)	10. SOURCE OF FUNDING NUMBERS			
	Program Element No.	Project No.	Task No.	Work Unit Accession Number

11. TITLE (Include Security Classification)
Static and Dynamic Flow Visualization Studies of Two Double-Delta Wing Models at High Angles of Attack, (Unclassified)

12. PERSONAL AUTHOR(S) Li, Feng-Hsi

13a. TYPE OF REPORT Master's Thesis	13b. TIME COVERED From To	14. DATE OF REPORT (year, month, day) March 1992	15. PAGE COUNT 107

16. SUPPLEMENTARY NOTATION
The views expressed in this thesis are those of the author and do not reflect the official policy or position of the Department of Defense or the U.S. Government.

17. COSATI CODES			18. SUBJECT TERMS (continue on reverse if necessary and identify by block number)
FIELD	GROUP	SUBGROUP	High angle of attack aerodynamics, effect of static AOA, pitch rate dynamic motion, flow visualization by dye injection, vortex development and bursting, water tunnel studies, effect of fillet, baseline or modified double-delta wing

19. ABSTRACT (continue on reverse if necessary and identify by block number)

A water tunnel flow visualization was performed to study the vortex development and bursting phenomena on a baseline double delta wing model and a modified double delta wing model. The primary focus of this study was two-fold: First, to study the static and dynamic effects of pitch and pitch rate on the vortical flowfield of the individual models. Second, to compare the vortex breakdown characteristics of these two models under static and dynamic conditions. Results indicate that the vortex burst location moves forward with increasing AOA for both the models relative to the static case, the bursting is delayed during pitch-up motion with the vortex burst lag increasing with the pitch rate. Compared with the baseline model, the small geometry modification at the strake/wing junction of the modified model changes the local flowfiel by developing the wing vortex earlier and promoting earlier coiling-up of strake and wing vortices.

20. DISTRIBUTION/AVAILABILITY OF ABSTRACT			21. ABSTRACT SECURITY CLASSIFICATION
☒ UNCLASSIFIED/UNLIMITED	☐ SAME AS REPORT	☐ DTIC USERS	Unclassified

22a. NAME OF RESPONSIBLE INDIVIDUAL S. K. Hebbar	22b. TELEPHONE (Include Area code) (408) 646-2997	22c. OFFICE SYMBOL AA/HB

DD FORM 1473, 84 MAR   83 APR edition may be used until exhausted   SECURITY CLASSIFICATION OF THIS PAGE
All other editions are obsolete   UNCLASSIFIED

Static and Dynamic Flow Visualization Studies
of Two Double-Delta Wing Models at High Angles of Attack

by

Li,Feng-Hsi
Commander, ROC Navy
B.S., ROC Naval Academy,1977

Submitted in partial fulfillment
of the requirements for the degree of

MASTER OF SCIENCE IN AERONAUTICS

from the

NAVAL POSTGRADUATE SCHOOL
March 1992

ABSTRACT

A water tunnel flow visualization was performed to study the vortex development and bursting phenomena on a baseline double delta wing model and a modified double delta wing model. The primary focus of this study was two-fold: First, to study the static and dynamic effects of pitch and pitch rate on the vortical flowfield of the individual models. Second, to compare the vortex breakdown characteristics of these two models under static and dynamic conditions. Results indicate that the vortex burst location moves forward with increasing AOA for both the models relative to the static case, the bursting is delayed during pitch-up motion with the vortex burst lag increasing with the pitch rate. Compared with the baseline model, the small geometry modification at the strake/wing junction of the modified model changes the local flowfield by developing the wing vortex earlier and promoting earlier coiling-up of strake and wing vortices.

TABLE OF CONTENTS

ACKNOWLEDGEMENT

I. INTRODUCTION

A. BACKGROUND

What will be the limitations on the performance envelope of an advanced fighter of the future? The pilot requires a fast fighter with good low speed flight capabilities for combat . Meeting these contradictory requirements is the goal of today's aircraft designer. A pilot in an agile fighter will be able to gain and maintain an advantageous position or disengage at will.

Since the 1950's, most fighter designs had wings optimized for high speed. In fact, the German engineers researched the delta-wing planform in the early 1940's. At least two companies designed delta-winged aircraft before 1952: French Dassault used the delta wing on Mirage III fighter (Fig. 1), and in the U.S. Convair produced the XF-92/F-102 (Fig. 2). One of the significant advantages of the delta- wing design was that the leading edge vortex flows were effective in reducing pre-stall buffet levels to give a more gradual loss of lift above the angle of attack (AOA) for maximum lift coefficient [Ref. 1]. The disadvantages of the single-delta wing were low wing loading and poor maneuverability. Dassault did not favor the delta planform to design a fighter with reduced landing speeds, improved maneuverability and a heavier weapon load. The Mirage F-1 had a tapered swept wing instead of a delta wing (Fig. 3). Today's advanced fighter aircraft require improved performance in the high alpha aerodynamics,
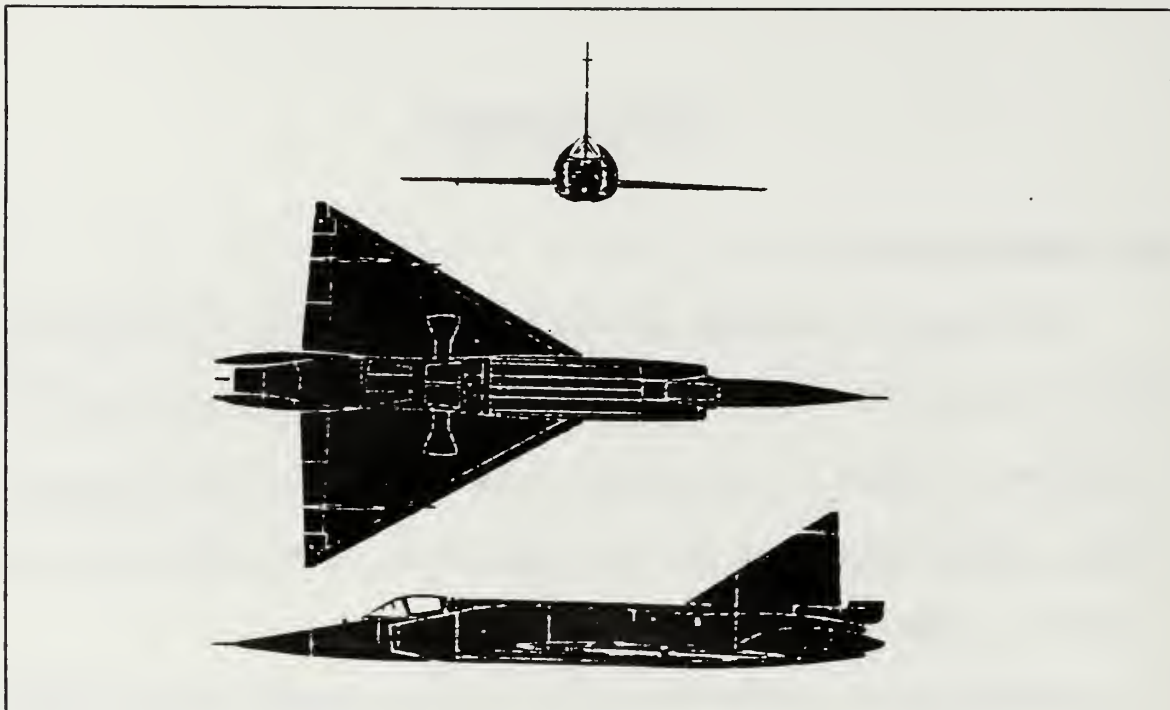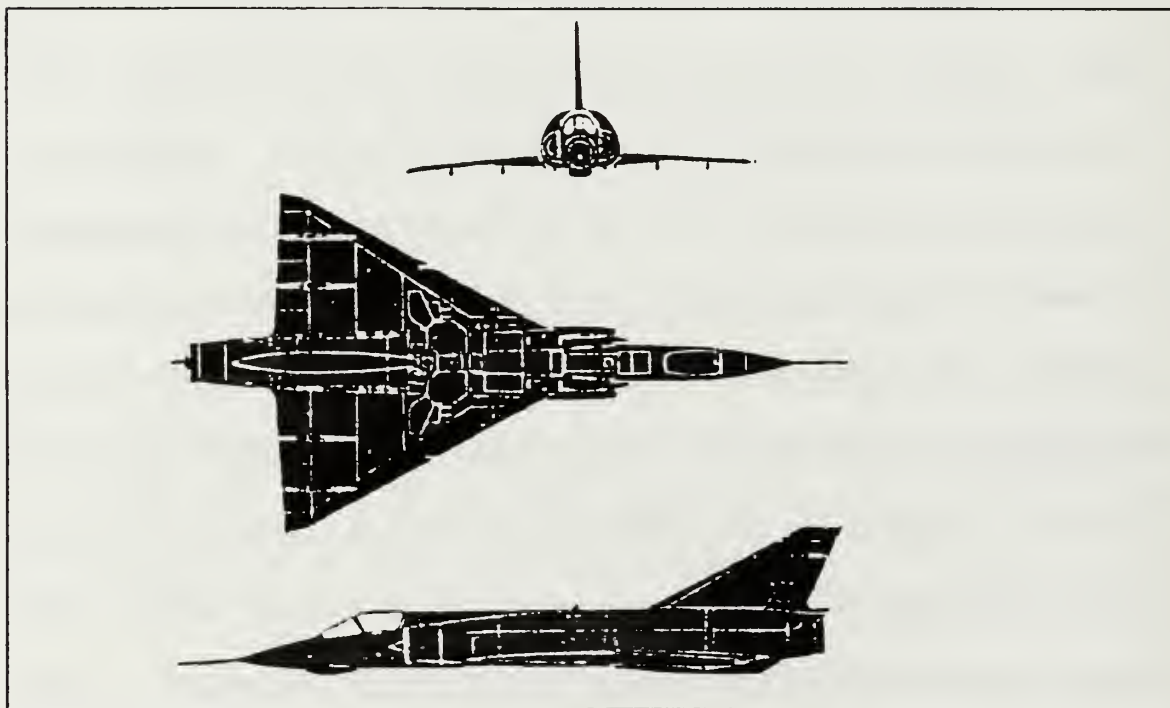
Figure 1. Dassault Mirage III
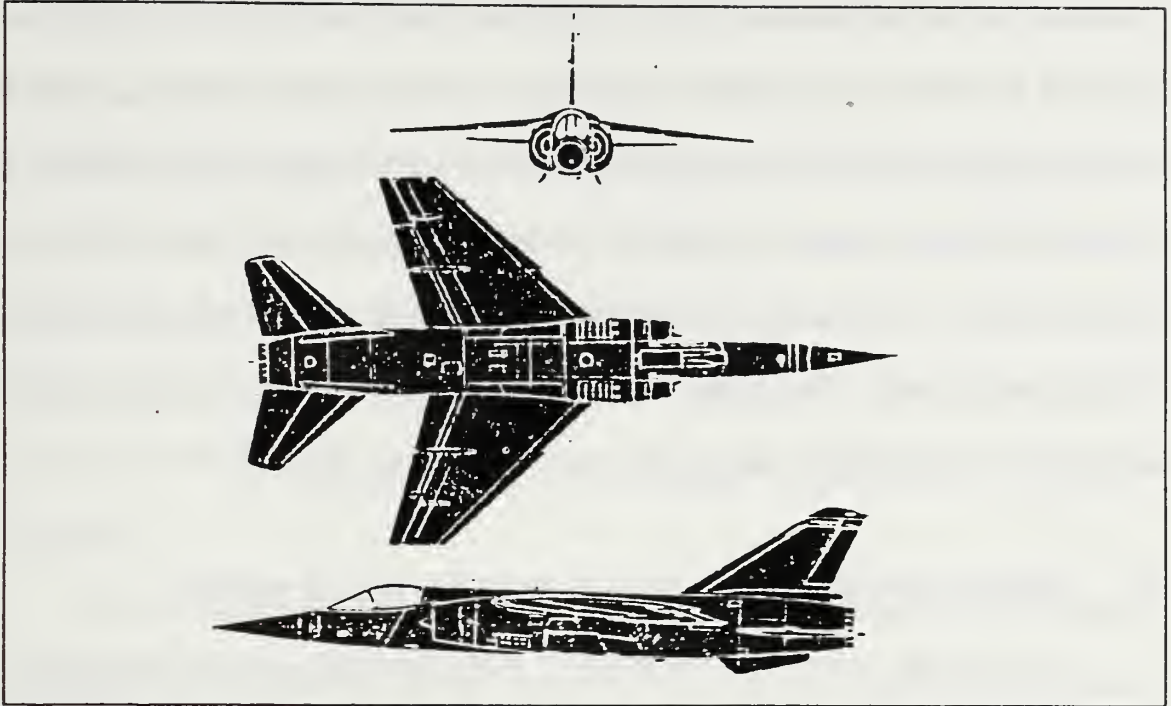

Figure 2. Convair F-102 Delta Dagger

2

Figure 3. Mirage F-1

supermaneuverability and post-stall (PST) capability, to gain airborne tactical superiority.

The National Aeronautics and Space Administration (NASA) is currently conducting a High-Alpha Technology Program (HATP) to provide new design guidelines and concepts for vortex control on advanced, highly maneuverable aircraft at high angles of attack. This program integrates the F/A-18 flight test and wind tunnel data with Computational Fluid Dynamics (CFD). An in-flight flow visualization study was conducted as part of this program [Refs. 2 - 4].

The concept of flow control through vortex manipulation began in the 1950's. Lawrence suggested the use of asymmetric edge shape effects to achieve roll

3

control of low aspect ratio wings at high angle of attack [Ref. 5]. In the 1960's the SAAB of Sweden used canards to delay the main wing upper surface separation on the Viggen fighter [Ref. 6]. In the 1970's, the use of leading edge extensions or strakes was developed. These devices are now employed on the F/A-18 and F-16 aircraft. The growing interest in high angle of attack maneuvering has refocussed the attention of the research community on delta planforms with emphasis on double-delta wing planforms and their derivatives.

B.   AERODYNAMICS OF DELTA AND DOUBLE-DELTA WINGS

It is desirable to increase the angle of attack envelope of delta-wing aircraft to improve maneuverability. The basic aerodynamic phenomenon of a delta wing includes formation of leading edge vortices, their development and subsequent breakdown (burst).

At high angles of attack, the flow does not attach to the wing surface. The maximum lift AOA for an airfoil is about 15 degrees but a 70-degree swept delta wing shows increasing lift to an AOA of 40 degrees [Ref. 7]. The leading edge vortices of the delta wing play a significant role in this enhanced lift. Typically, the vortices may account for as much as 30 % of the total wing lift and become more important as AOA increases beyond the range of a conventional wing [Ref.8].

Leading edge vortex flows have been under study since the late 1950's. Generally, two symmetric leading edge vortices are generated on wings with sweep angles greater than 45 degrees as the wing pitches up.

4

At moderate AOA, the flow attaches to the lower surface and then turns towards the swept leading edge. Unable to negotiate the sharp turn the flow separates and a vortex sheet is formed. The spanwise pressure gradient causes the vortex to move inward and roll up, eventually forming a concentrated vortex called the primary vortex (Figs. 4-5, reproduced from Ref. [17]). The size of the primary vortex is generally on the order of the half span. The primary vortex causes the flow over the upper surface to accelerate producing extra lift called vortex lift.

The flow over the upper surface encounters the primary vortex, sweeps downward, and reattaches to the surface of the wing outboard of the primary vortex. The boundary layer of a reverse pressure gradient causes the flow to separate, creating a smaller counter rotating vortex called the secondary vortex.

At high AOA, the core flow of the primary vortex suddenly stagnates and expands in size. This phenomenon is called vortex burst or breakdown. The position of the burst is affected by wing sweep, AOA and the shape of the leading edge [Ref. 9].

A particular form of the strake/wing configuration is the double-delta wing. It has similar geometric characteristics to a delta wing-except it has a discontinuity or kink in its leading edge, meaning that at some point the leading-edge sweep angle abruptly changes to a lower angle.

The flow over a double-delta wing is very similar to that over a delta wing, but more complicated. The vortex, generated by the apex of the strake, called the
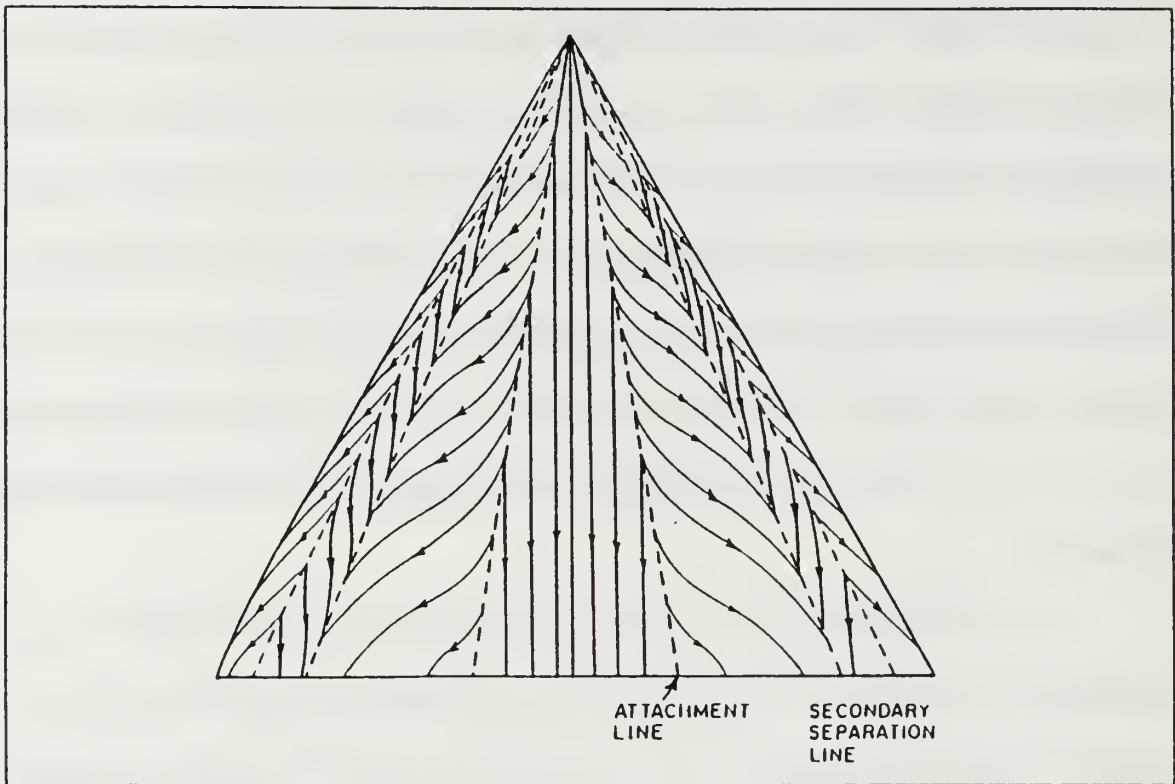
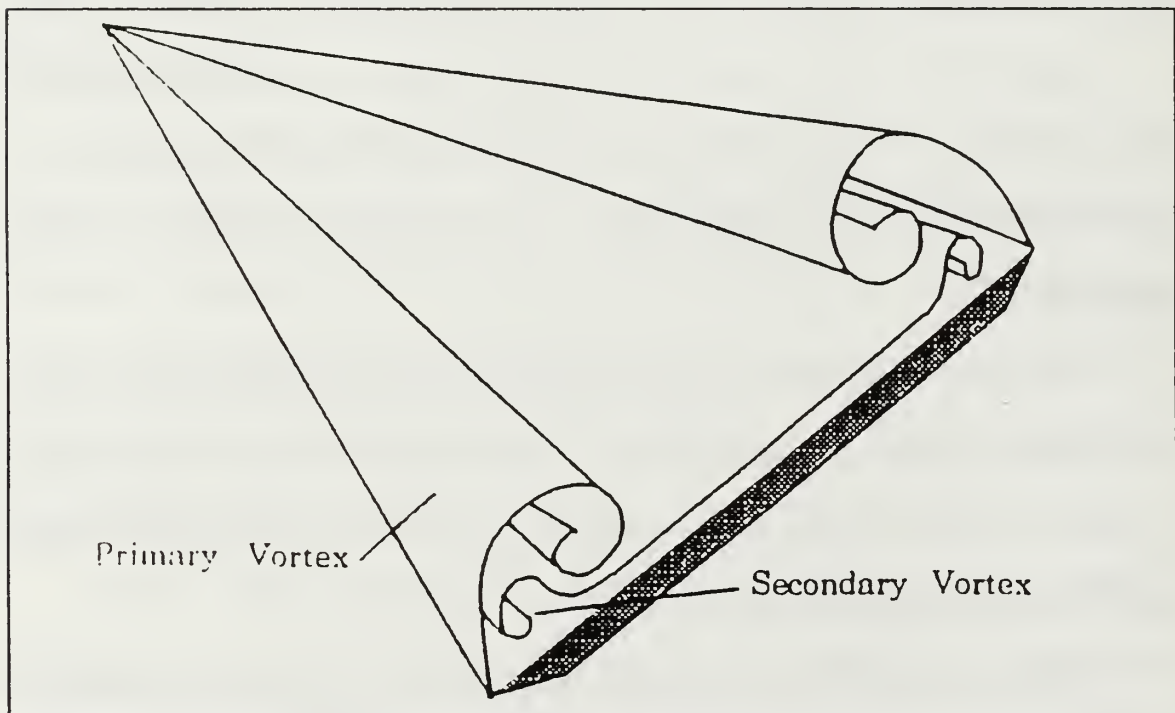**Figure 4.** Surface Flow Pattern Over A Single Delta-Wing

Figure 5. Typical Vortex Structure Over A Delta Wing at AOA

6

inner vortex or the strake vortex, roughly parallels the strake leading edge (LEX) at low angles of attack ($\alpha < 10$ deg). Simultaneously another vortex called the outer vortex or wing vortex is produced at the strake/wing junction and parallels the wing leading edge. At high AOA ($\alpha > 10$ deg) the two vortices begin to merge and parallel the leading edge. The vortex burst phenomenon is influenced by various factors similar to those in the case of a single delta wing (Fig. 6). When a strake is added to a delta wing, it not only increases the lifting area of the wing, but also creats its own leading edge vortices which persist over the main wing.

Studies related to vortex aerodynamics and vortex burst on single delta wings have generally focussed on static conditions [Refs.9-13]. An investigation on the coiled-up vortices on a double delta wing was conducted in the water tunnel by Yu, et al. [Ref. 14]. Included in this study were the vortex flow structures above the wing surface, showing the coiling-up of the primary and secondary vortices . Low-speed unsteady aerodynamics of a pitching straked wing at high incidence was examined by den Boer, and Cunningham [Ref. 15]. Measurements of unsteady overall airloads and pressure distributions were obtained from wind tunnel tests covering a wide range of incidence (-8 to +50 degrees) and amplitudes (1-16 degrees). Smoke and laser sheet techniques were used for flow visualization. A numerical investigation of the flow over a double delta wing at high incidence was carried out by Ekaterinam's et al.[Ref. 16], for flow conditions matching the experimental conditions of Ref.[15]. A numerical investigation of flow control

7

through small geometric modifications at the strake/wing junction of a cropped double-delta wing was carried out by Kern [Ref. 17].
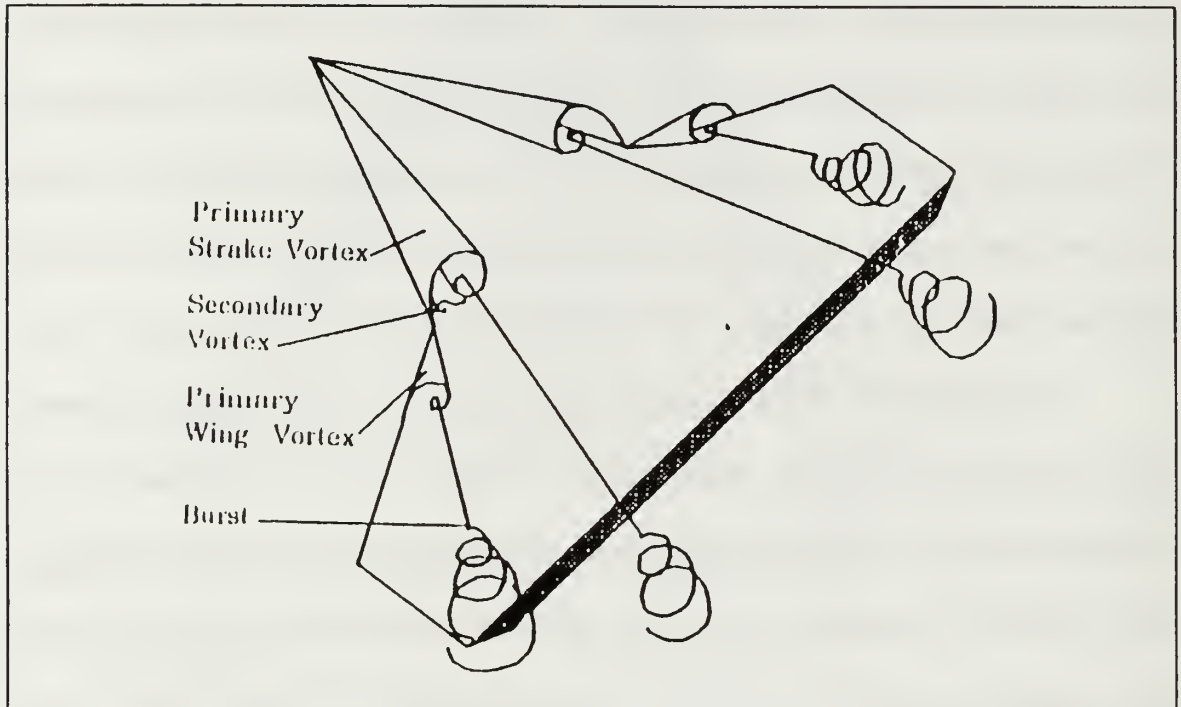

Figure 6. Double-Delta Wing Vortex Burst Phenomenon

It is clear that the data available on double-delta wings is scarce and is restricted to static conditions of the flowfield. The data available on double-delta wings in dynamic motion or the data on the effects of geometric modifications is scarcer. Thus, there is a great need to better understand the physics of vortical flows over double delta-wings. The present investigation was undertaken to meet this need and was carried out in the NPS water tunnel in two phases.

8

a. Study of vortex interaction and vortex breakdown characteristics. This phase consists of static and dynamic visualization of the vortical flow field of a basic double-delta wing in the 0-50 degree angle-of-attack range.

b. Study of the effect of geometric modification. This phase consists of static and dynamic visualization of the vortical flow field of a modified double-delta wing over the same angle-of-attack range followed by a critical comparison of the two flow fields.

II. EXPERIMENTAL APPARATUS

A. THE WATER TUNNEL

The experiments were conducted in the Naval Postgraduate School flow visualization water tunnel. This is a closed circuit facility appropriate for studying a wide range of aerodynamic and fluid dynamic phenomena(Fig. 7).

The key design features of the water tunnel are good flow quality and horizontal orientation. The horizontal configuration facilitates model access,

KEY:
1. PUMP
2. PERFORATED INLET
3. DELIVERY PLENUM
4. FLOW CONDITIONING ELEMENTS
5. CONTRACTION SECTION
6. DYE LINES
7. TEST SECTION
8. MODEL SUPPORT
9. DISCHARGE PLENUM
10. RETURN PIPING
11. FILTER SYSTEM
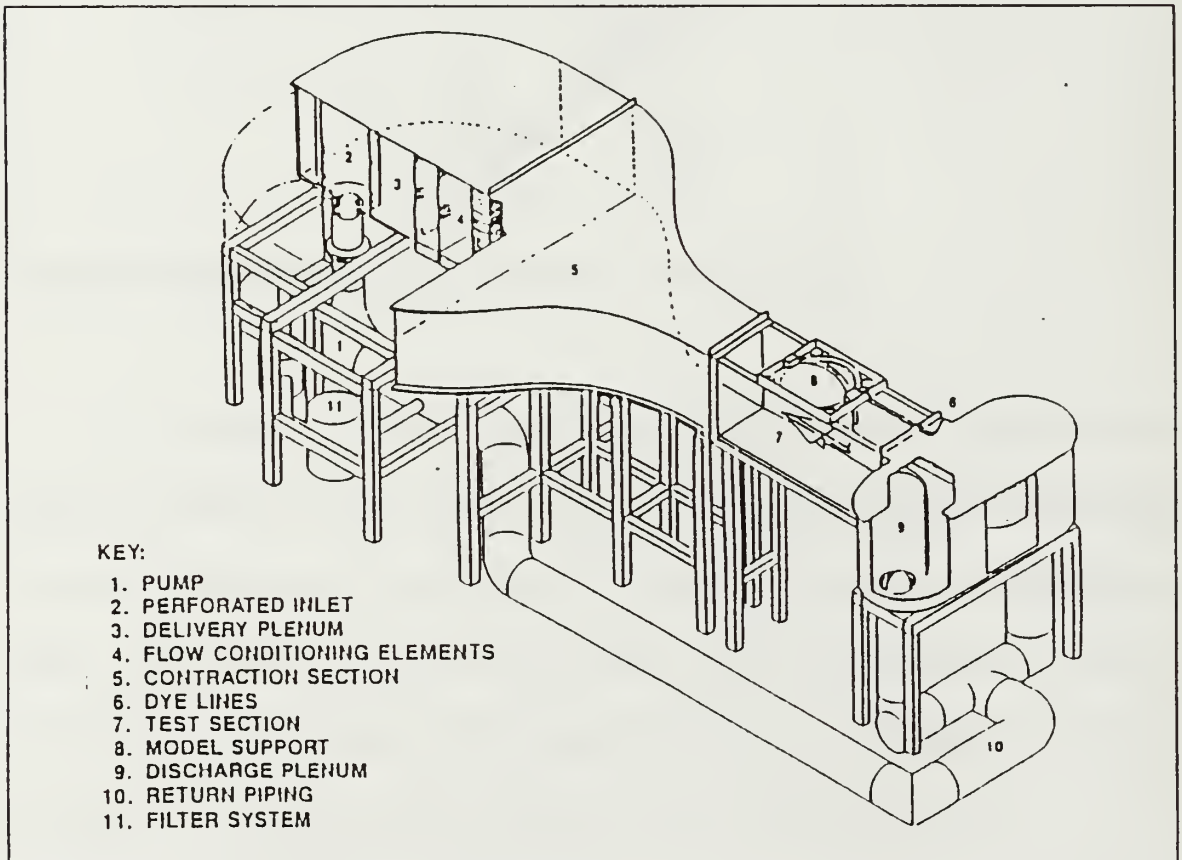
Figure 7. Water Tunnel Facility at NPS

10

enables models to be readily changed without draining the water from the tunnel, and provides for visualization of the flow axially from a downstream transverse window. The facility is operated as a continuous flow channel, and the water level is adjusted to be approximately 2" below the top of the walls. The entire circuit is constructed of noncorrosive materials supported by a structural steel framework.

The test section of the water tunnel is nominally 15 in. wide, 20 in. high and 60 in. long and is constructed of glass to allow simultaneous viewing of the model flowfield from the bottom, from both sides and from the rear. Viewing from the rear is specially advantageous when studying flow structures in the cross-flow plane. There is enough space underneath the test section for convenient viewing and setup space for either direct or indirect (with a mirror) visual access for photography through the bottom of the test section. The test section flow velocity is variable from 0 up to 1.0 ft/sec.

The level of flow quality over the range of test section velocities is as follows:

Turbulence intensity level= < 1.0% RMS

Velocity uniformity= < ±2%

Mean flow angularity= < 1.0° in both pitch and yaw angle

A pressurized six-color dye system designed to use water-soluble food coloring is provided with individually routed lines from the dye canisters to the model support system. A small compressor and a pressure regulator are used to pressurize the dye canisters to control the pressure level. The value of a

11

pressurized system is finer control to regulate the dye emission and to provide a means of blowing air out of the dye lines going to the model.

The model support system was designed for specific needs of high angle-of-attack aerodynamic research studies, with angle-of-attack and sideslip capability through the following ranges:

α = -10 deg to + 70 deg

β = -20 deg to + 20 deg

Angle of attack is set by pitching the model in the vertical plane on a C-strut arrangement and sideslip angles are achieved by rotating the model support assembly on a turntable. Both pitch and yaw motions are controlled by a remote switch for ease of operation and observation. The high pitch rate and low pitch rate correspond to 4.8 deg/sec and 2.2 deg/sec, respectively.

B. THE MODELS

Two different shapes of double-delta wing were used during the investigation. The geometry of the baseline model is indicated in Fig. 8. whose planform is similar to that of the model of Ref. 15 that consisted of a 76-degree swept strake and a 40-degree swept wing with sharp, bevelled leading edges. A derivative of the baseline wing is shown in Fig. 9. and was obtained by incorporating certain geometric modifications near the kink of the baseline model. The planform areas are 36.91 square inches for the baseline model, and 38.49 square inches for the

12
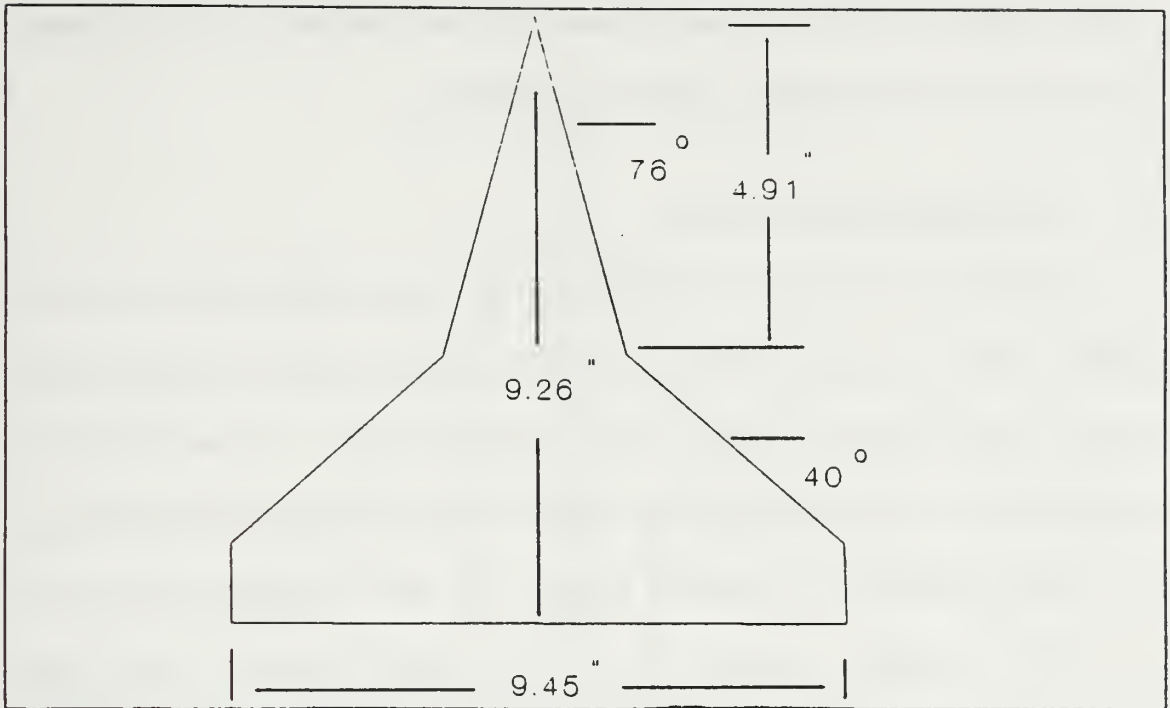
Figure 8. The Geometry of the Baseline Model
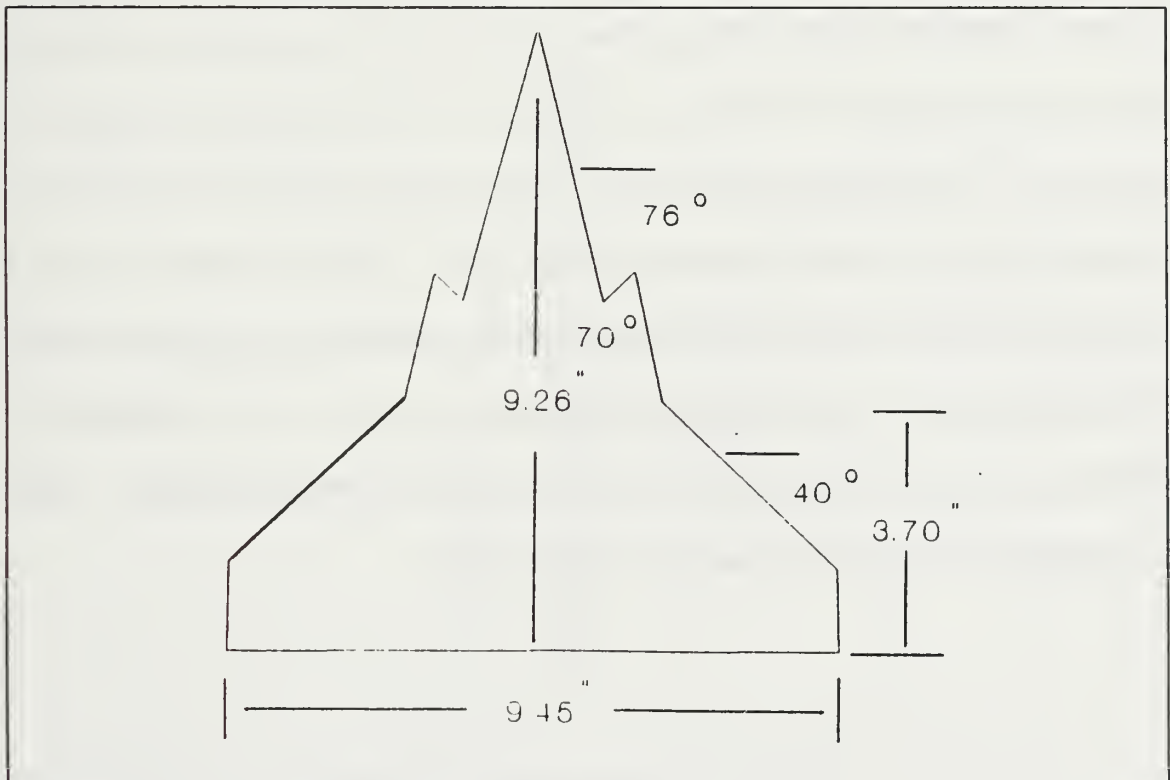
Figure 9. A Derivative of the Baseline Model

13

modified model. This means a 4% increase in the area due to the modification. Each model has a centerline chord of 9.26 inches.

C. DYE TUBE INSTALLATION

Dye tubes consisting of small brass tubes were installed on the lower wing surface. Both the location of the dye injector and the injection rate are crucial to obtain a good flow visualization of the model flow field. The pressurized dye system helped to control the injection rate. The right location for the tip of the dye tube was determined by moving around the tube and observing the dye streamlines at angles of attack of 10°, 20°, 30° and 40°. Figures 10 and 11 show two different positions of the dye tube. In position 1, a straight dye tube is located on the underneath of the wing surface with the tip sitting squarely on the flat surface below the apex. This location was found to yield satisfactory results. In position 2, a straight dye tube was used as in the previous position, but the tip was pushed a little bit forward (about 0.75 inches). Position 2 was found less satisfactory in that the dye streamlines at angles of attack looked more like a wide band and not as a concentrated, well defined vortex core. For convenience of direct visualization, different color dyes were selected for different locations. Table 1 indicates the locations of dye tube and dye colors.
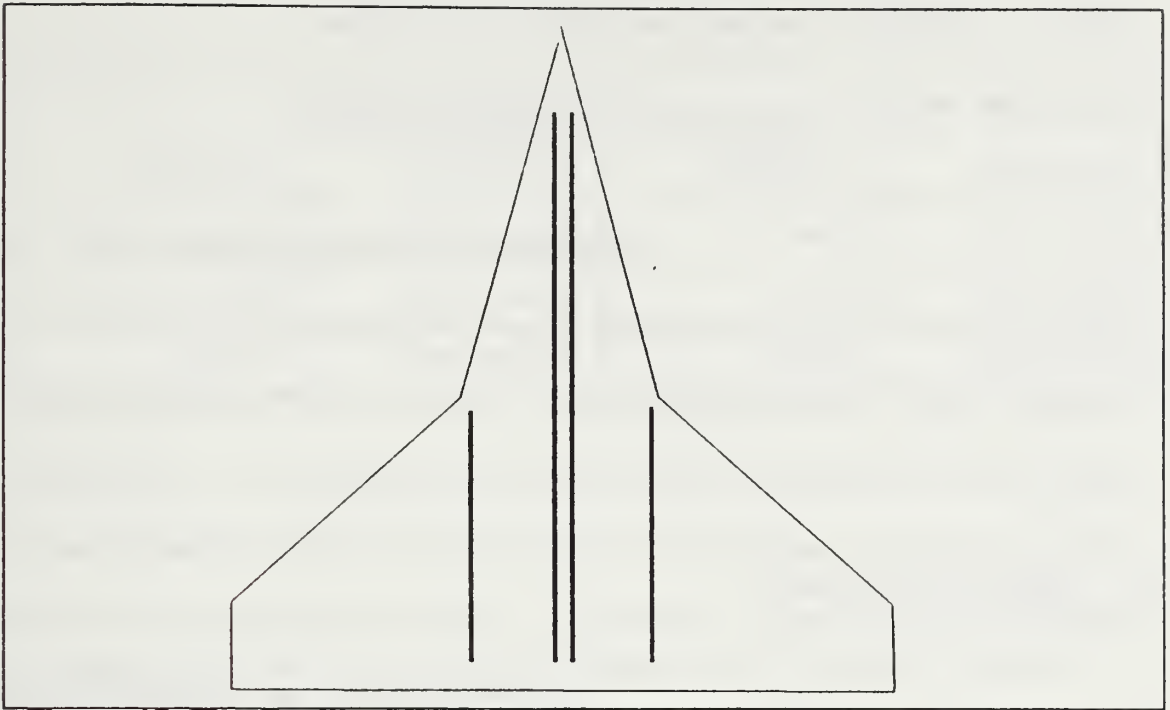
Figure 10. The Position 1 of the Dye Tube
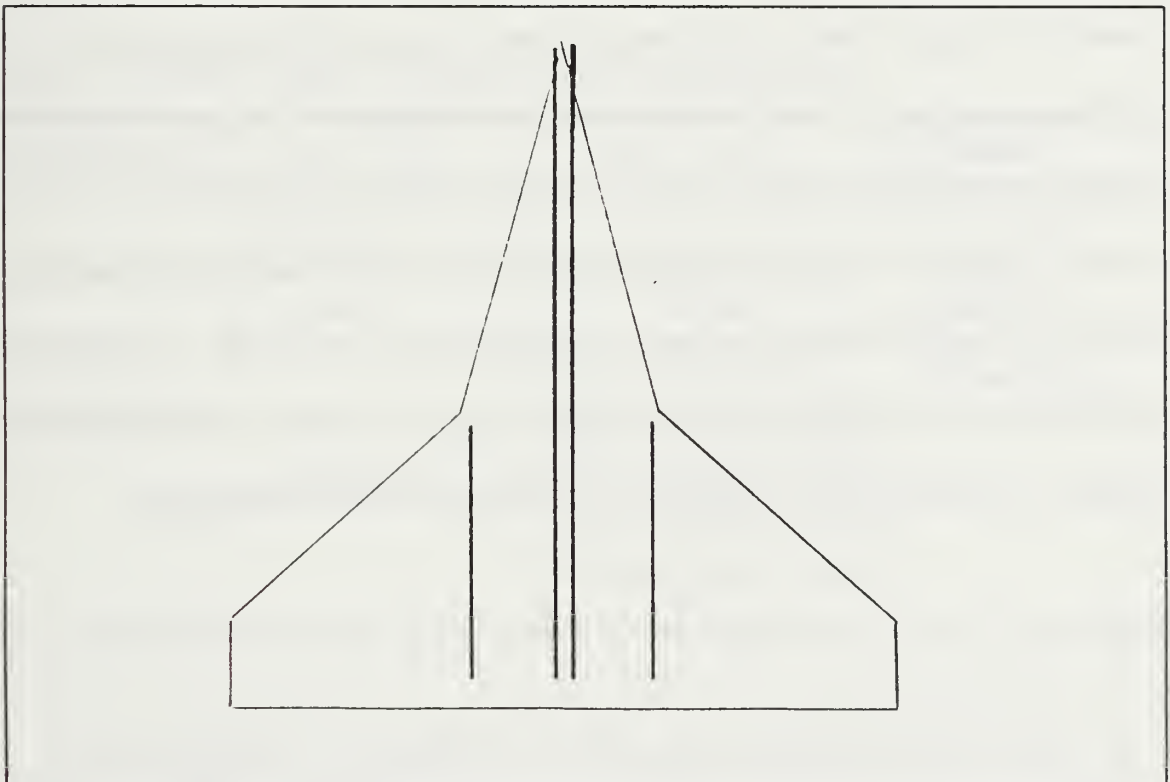
Figure 11. The Position 2 of the Dye Tube

15

TABLE 1. DYE COLORS AND INJECTION LOCATION

BASELINE MODEL		MODIFIED MODEL	
LOCATION	COLOR(S)	LOCATION	COLOR(S)
Apex (R)	Blue	Apex (R)	Blue
Apex (L)	Red	Apex (L)	Red
Kink (R)	Green	Starboard	Green

D.   MODEL MOUNTING

It is very important to insure that the model is mounted horizontally in the water tunnel with zero pitch, zero yaw and zero roll. Details of model mounting are given in Ref. [19]. Briefly, the model sting was secured to the sting holder of the model support system and introduced into the test section. The center-line of the model was aligned with the freestream (tunnel centerline), thus ensuring zero pitch angle. The zero yaw was checked by setting the model apex equidistant from either side wall of the test section. To assure that no roll exists, the heights of both left and right wing tips from the bottom of the test section were checked for equality. The pitch axis was located at 5 inches aft of the model apex.

III. EXPERIMENTAL PROCEDURE

A. FLOW VISUALIZATION EXPERIMENTS

The goal of this investigation was to study the vortical flow past two sharp-edged double-delta wings, one with a simple baseline geometry and the other with a modified kink. The experiments consisted of flow visualization of these models with zero sideslip in static condition and for two pitch rates, with AOA (α) varying from 0° to 50° (simple pitch-up motion) and 50° to 0° (simple pitch-down motion). Table 2 illustrates different test conditions.

Table 2. STRAKE/ WING VORTEX FLOW VISUALIZATION

AOA (Degrees)	CONDITION	PITCH RATE	REMARKS
0° to 50° at 5° increments	Static	******	Sideview Topview Photos and Videotape
	Dynamic	Low pitch rate down	
		Low pitch rate up	
		High pitch rate down	
		High pitch rate up	

Both still-picture photography and videotape recording were used for documentation of dye flow visualization of the models. The flow velocity was kept

17

nearly constant at 0.25 ft/sec that corresponded to a nominal Reynolds Number of 23000/ft. Reynolds Number effects are expected to be negligible on burst positions of vortices shed off thin sharp edged delta wings at these angles of attack [Ref.20].

B.   REDUCED PITCH RATE SIMULATION

An aircraft encounters unsteadiness under all flight conditions whether due to inputs of dynamic motion (i.e., pitch-up/down, yaw increase/decrease), or of natural disturbances (i.e., wind shear,gusts). Therefore, to understand the stability of an aircraft operating in these conditions, a knowledge of its response to flow unsteadiness is essential. In other words, the parameter characterizing the flow unsteadiness governs a dynamic flowfield.

The guiding non-dimensional parameter during pitching motions is the reduced pitch rate, k, given by:

$$k = \frac{\dot{\alpha}\, C}{2\, U_\infty}$$

where ,

    k = reduced pitch rate,non-dimensional

    $\dot{\alpha}$ = pitch rate, rad/sec

18

c = characteristic length of the body, ft

U_∞= free-stream velocity, ft/sec

In the case of a wing pitching about its mid-chord location, it can be interpreted as the ratio of the vertical motion of the leading edge to its longitudinal motion.

Based on this formula, the reduced pitch rates for the present models are 0.06 for low pitch rate and 0.13 for high pitch rate.

C. BLOCKAGE

The so-called "blockage" effects are caused by the presence of the model in a finite test section. The dynamic motion is affected by the projected area of the model normal to the flow direction. The following equation can be used for calculating model blockage in percentage.

$$B = \frac{A\cos(90-\alpha)}{S}(100)$$

where:

B = blockage (%)

A = surface area of the model (in^2)

α = angle of attack (deg)

S = cross section area of the test section (in^2)

The model blockage is thus dependent on incidence. The blockage at 50° angle of attack was 9.4% for the baseline model, and 9.8% for the modified model.

D.   DATA ACQUISITION AND PHOTOGRAPHY APPROACH

The data collection consisted of taking photographs providing a simultaneous sideview (starboard side) and top view of the vortical flow field originating at the apex and the kink of the double-delta wing models in both static and dynamic conditions.   This was accomplished by using two 35 mm cameras.   A video camera was also used to record the flow phenomenon for later playback during the data reduction phase.   The data collection phase was preceded by direct visual observation of the flow field.

Four Smith-Victor 600 watt photographic lights,and a 500-watt floodlight fixed below the test section were used for illumination.   The placing of the lights is important in that it should not only provide sufficient illumination but also minimize the shadow of the model and the reflections of the light in the pictures.   For the sideview photographs, two of the lights were placed at a distance of three feet and at a 45-degree angle from the test section. One of the lights placed below the test section in front of the model and another one near the rear of the model in

20

conjunction with the fixed floodlight provided sufficient lighting for the topview photographs (Fig. 12).
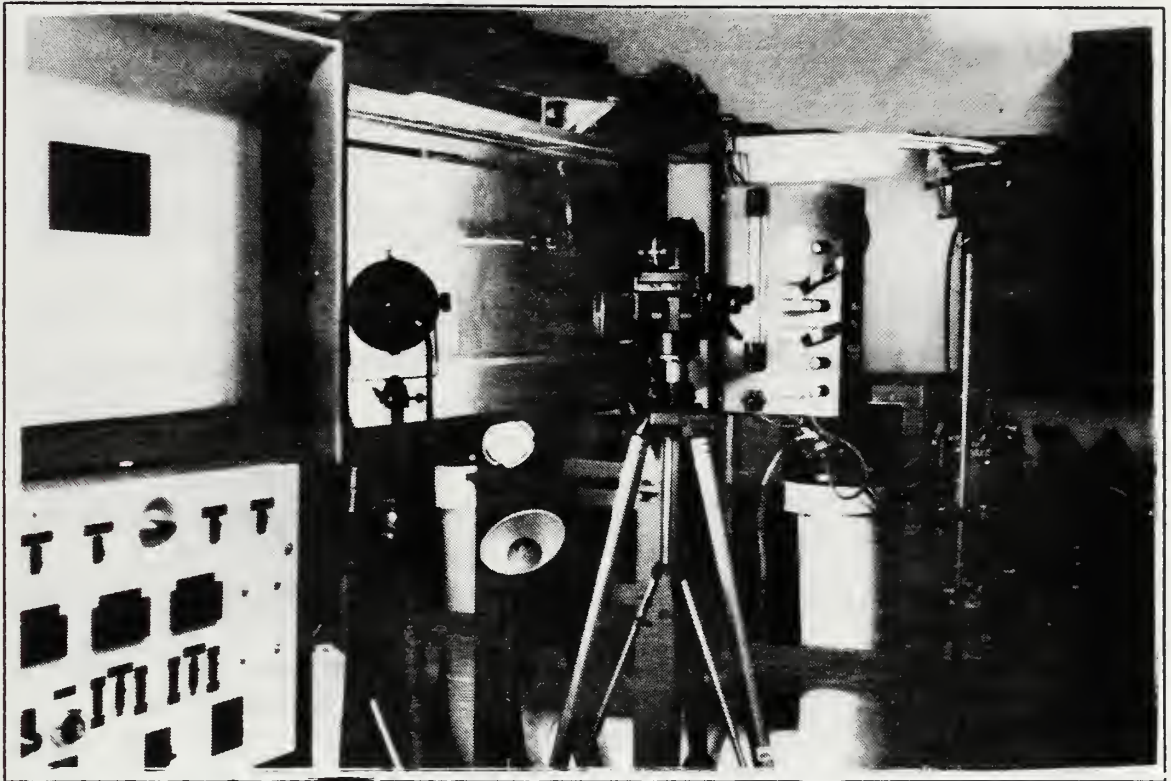
Figure 12. Illustration for Water Tunnel Test Section

An angle-of-attack scale was fixed to the rear side wall of the tunnel to help in reading the instantaneous angle of attack in the sideview photographs.

IV. RESULTS AND DISCUSSION

Several rolls of 35mm black and white films were exposed and also several hours of videotape recorded during the experiment. The results of this investigation are presented here in the form of flow visualization photographs in Appendix A (Figures 13 through 66). Each figure contains a sideview and a topview.

The flow visualization photographs will be examined and discussed in two parts. The first part will include a discussion of static flowfield characteristics and comparison of vortical flow patterns for the basic and the modified double-delta wings. The second part of the discussion is related to the dynamic flow field characteristics and comparison of flow patterns for the two wing planforms. Finally, with the aid of burst location plots, the effects of pitch rate on the development/bursting of strake vortices will be discussed for each model and then compared. The percent location used in the following discussion refers to the ratio of the distance of the vortex burst location from the apex to the centerline chord length multiplied by 100.

It must be pointed out here that some preliminary experiments were carried out to determine the optimum position for the dye tube location. A dye tube located flat on the buttom surface of the model with its tip as close to the apex as

possible was fround to give satisfactory dye injection for vortex visualization purpose.

A. EFFECTS OF ANGLE OF ATTACK ON STRAKE VORTEX CORE BREAKDOWN (OR BURSTING)

There were situations where the breakdown was not visible on the upper surface either because it occured in the wake behind the trailing edge or because dispension of the dye made it difficult to track the vortex core before breakdown occured.

1. Static Conditions

Figures 13 through 31, show flow visualization photographs for both the baseline and the modified models under static condition.

a. Baseline Model

At lower angles of attack ($<10°$) the flow is smooth and attached (Fig.13). The vortical flow field over the wing surface develops as the angle of attack is increased. At 15° AOA (Fig.14), both strake and wing vortices are already well developed and coiled-up with each other. The strake vortex core is nearly conical over the strake portion of the wing and is drawn outboard by the wing vortex. At the same time, the wing vortex core is also drawn away from the wing leading edge by the strake vortex. The bursting of the merged vortices occurs near the wing trailing edge. As AOA is increased from 15° to 20° (Fig.15) the coiling up of the two vortices occurs earlier and the burst location moves

23

forward (83.8% location). At 25° AOA, even before the coiling up of the two vortices, the strake vortex core bursts at 64.9% location(Fig.16). The strake vortex induces an upward and inboard movement of the wing vortex. Conversely, the wing vortex induces a downward and outboard movement of the strake vortex. The interaction of the two vortices causes them to intertwine upstream with increasing AOA. At $\alpha = 50°$ (Fig.21) the strake vortex burst location has moved forward close to the apex (24.3% location).

b. Modified Model

Figures 22 through 31 show the vortical flow field over the modified model under the static condition. At $\alpha = 5°$ (Fig.22) a weak wing vortex core is seen, with no strake vortex developed yet from the apex. At $\alpha = 10°$ (Fig.23) the wing vortex core has become stronger, with the strake vortex core just developing. There is no interaction between these two vortex cores. As the AOA is increased, they merge together, and the burst location moves upstream (Figs.24,25). With further increase in the AOA, the strake vortex core bursts before interacting with the wing vortex core, and the bursting position moves upstream until it is close to the apex at 50° AOA(Figs 26-31).

c. Effect of fillet

The flow is smooth and attached for both the models at low AOAs ($\alpha < 5°$), but at 5° AOA, the wing vortex starts to develop on the modified model (Fig.22). Based on the basic principle of vortex flow, an additional lift can be

24

expected at this angle of attack. This phenomenon can be attributed to the effect of the shape of the modification. From the geometry of the modified (filleted) region, it can be observed that near the secondary apex, the wing is locally yawed (about 23°) with respect to the incoming flow. This reduces the effective sweep of the windward leading edge but increases the effective sweep of the leeward leading edge causing the vortex to develop as early as at 5° AOA on the modified model. On the baseline model, the develoment of this vortex is delayed until α = 10°.

Another difference to be noted in the vortical field between these two models is the AOA for separation of coiled-up vortices. The coiled-up vortices separate at α = 25° (Fig.16) for the baseline model and at α = 30° for the modified model (Fig.27).

The flow phenomenon is similar for both models at higher angles of attack (α > 30°).

2. Dynamic Conditions

All the photographs were taken at approximately 5° interval during simple pitch-up and pitch-down motions at two reduced pitch rates for the two models at zero yaw (Figs 32-66). It was often difficult to identify vortex core burst location from the photographs for lack of clarity, particularly so if the compressor was on and its vibration affected the model. In such cases, video recording was used for determing burst location.

25

a. Baseline model

Figures 32 through 36 show the model flow field during simple pitch-up motion at $\kappa = 0.06$. At low angles of attack ($\alpha < 10°$), the vortices are not formed yet. A developed strake vortex is seen at $\alpha=15°$ (Fig.32). With increasing AOA (from 20° to 50°) the vortex core is seen to be getting tight. It increases in strength and the bursting point approaches the apex. The behavior of the bursting location during pitch-up motion can be examined by comparing with the behavior for the static condition at the same AOA. Thus comparing Figures 33 and 15 at the same AOA of 20°, it is clearly seen that the bursting location during dynamic motion lags that for the static condition. This indicates that during pitch-up motion, the bursting location occurs at a point further downstream than would occur for the static condition, resulting in a vortex system which is equivalent to a static system at a reduced angle of attack. Similar results of dynamic lag effects have been obtained by other investigators [Refs. 20-23].

Figures 37 through Figures 40 show the flowfield during simple pitch-down motion at $\kappa=-0.06$ with AOA decreasing from 50° to 0°. The vortex core grows with the burst location moving rearward and outboard as AOA decreases. During the pitch-down motion, the burst location occurs earlier compared to the static case.

Figures 41 through 44 exhibit the flow patterns during simple high rate pitch-up motion with $\kappa = 0.13$. They show the model flowfield during pitch-up motion with AOA increasing from 20° to 50°. The flow features are analogous to

26

those observed during the low rate pitch up motion, but with increased lag effects. Thus, comparing Figures 42,33,and 15 all at same AOA of 20°, it is seen that the burst location for the high rate pitch-up motion lags that for the static case and that the lag effect increases with the pitch rate.

Figures 45 through 48 display the flow field during simple high rate pitch-down motion with κ=-0.13.

b. Modified Model

Figure 49 through Figure 54 show the flow field during a simple pitch-up motion with κ = 0.06. Figure 49, α = 10°, shows that the wing vortex is just starting to develop and at α = 15°, the strake vortex has developed (Fig.50). The wing vortex and the strake vortex start to interact at approximately α = 20° (Fig.51), and merge into one stable vortex. With increasing A0A, the vortex breakdown occurs and the burst location moves upstream in a fashion similar to that observed for the baseline model. The coiled-up vortices separate at about α = 35°.

Figures 55 through 58 correspond to the flow field during a simple pitch-down motion with κ=-0.06. The vortex core grows and develops as the AOA is decreased from 50° to 0°.

Figures 59 through 63 show the flow field during a simple high- rate pitch-up motion with κ = 0.13. Figure 59, α = 10°, shows that the wing vortex has already developed. It was observed during the play back of the videotape that the strake vortices developed at α = 16° and started to coil-up with the wing vortex in

27

the AOA range 20° to 40° (Figs. 50-52). The dynamic lag effects are also seen during the pitch-up motion.

Figures 64 through 66 show the flow field during a simple high rate pitch-down motion (κ=-0.13) with AOA decreasing from 50° to 0°. The burst location occurred earlier during the pitch-down motion compared to that for the static case at same AOA (Table 3).

c. Effect of fillet

An interesting result can be seen from comparing the corresponding bursting locations during dynamic motion. Generally speaking, during pitch-up motion, the strake vortex core bursts later on the baseline model than on the modified model, whereas during the pitch-down motion it occurs earlier. In other words, the strake vortex core burst location on the baseline model lags/leads that on the modified mode during pitch-up/pitch-down motion respectively.

B. BURST LOCATION PLOTS

The quantitative data on burst location reduced from the flow visualization photographs taken during the experiments and the videotape recordings are listed in Table 3. The longitudinal strake vortex core burst locations in case of static and dynamic conditions for both the models are plotted as a function of angle of attack (AOA) in Figures 67 through 73 (Appendix B).

Figure 67 compares the static condition for both the baseline and the modified models. It is seen that the burst location occurs later on the baseline

28

Table III. STRAKE VORTEX BURST LOCATIONS (% CHORD LENGTH)

Pitch Rate / Model	Angle of Attack (deg)									
	5	10	15	20	25	30	35	40	45	50
Static Case / Baseline	N	N	100	83.8	64.9	51.4	41.9	35.1	27.7	24.3
Static Case / (Modified)	N	N	89.2	79.7	62.9	47.3	39.2	33.8	26.4	23.7
Low Pitch-Up / (Baseline)	N	N	N	91.9	75.7	68.9	56.1	45.3	35.1	31.1
Low Pitch-Up / (Modified)	N	N	N	82.4	74.3	63.5	52.7	43.9	33.8	28.4
Low Pitch-Down / (Baseline)	100	89.2	73.0	59.5	51.4	41.9	31.1	27.0	24.6	24.3
Low Pitch-Down / (Modified)	100	85.1	73.0	59.5	51.4	41.9	29.7	27.0	24.3	23.7
High Pitch-Up / (Baseline)	N	N	N	N	78.4	71.6	60.1	56.1	45.3	36.5
High Pitch-Up / (Modified)	N	N	N	N	77.0	66.2	54.1	51.4	44.6	35.1
High Pitch-Dow / (Baseline)	97	85.1	71.6	58.1	48.6	40.5	29.7	27.0	24.5	24.3
High Pitch-Dow / (Modified)	95	83.8	73.0	58.1	48.6	39.2	29.1	27.0	24.1	23.7

Note: N = No Burst Location on the strake/wing area

model than on the modified model throughout the AOA range. It is also seen that

the difference between burst location for the two models is nearly constant at high

angles of attack ($30° < \alpha < 50°$).

Figures 68 and 69 illustrate the dynamic effect on burst location for the baseline and the modified model, respectively. A careful observation shows a similar trend in both figures. During pitch-up motion in the AOA range considered, the burst location always occurs later relative to the static case. During the pitch-down motion, the burst location occurs earlier relative to the static case. Further, this dynamic lag effect is seen to increase with the pitch rate. The vortex bursting response observed here for pitch rate motions is similar to the one observed by Cavazos, et al. [Ref.20] in their experimental investigation of LEX vortex bursting location on the F/A-18 model. Similar response of vortex bursting on simple delta wings has been reported by Magness et al.[Ref.22].

The effects of fillet on the burst location during simple pitch rate motions are shown in Figures 70 and 71. Figure 70 clearly shows that during a simple low-rate pitch-up motion, the burst location on the baseline model occurs later than that on the modified model with significant difference seen at low and moderate angles of attack. Figure 71 corresponds to the low pitch-down motion. For both models the burst location plots practically coincide except at very low angles of attack. Note that in these figures the difference between the plots is within the uncertainty in the experimental data which is expected to be less than 0.05.

Figure 72 displays the burst location plots for high pitch-up motion. The strake vortex bursts earlier on the modified model than on the baseline model until high angles of attack ($\approx 40°$). Since there is no coiling-up of vortices at large AOA (>40°), the strake vortex core burst locations of both models approach each other.

30

The wing vortex usually occurs at low angle of attack and then coils-up with the strake vortex; the vortices remain merged for sometime and separate (or break) afterwards. The AOAs at which this coil up and separation of vortices occurs depend on the pitch rate. These angles have been determined from videotape recordings and are listed in Table 4.

Figure 73 corresponds to the simple high pitch-down motion. The slopes of the curves are very similar to those for the low pitch-down motion discussed above.

Table 4. THE LOCATION OF COIL-UP OF VORTICES

Coil-Up of Vortices	Pitch Rate							
	Baseline Model				Modified Model			
	Pitch-Up		Pitch-Down		Pitch-Up		Pitch-DOwn	
	Low	High	Low	High	Low	High	Low	High
Start (AOA)°	15	21	20	15	14	20	19	16
Break (AOA)°	30	38	---	---	29	39	---	---

V. CONCLUSIONS AND RECOMMENDATIONS

A low speed flow visualization investigation was initiated to study the vortex development and bursting phenomena on two double-delta wing models, one a baseline model and the other a filleted model with small geometry modifications at the kink, using dye injection in the Naval Postgraduate School water tunnel. The primary focus of this research was two-fold: First, to study the static and dynamic effects of pitch on the development, interaction, and bursting of vortices shed off the strake and the wing of the baseline model. Secondly, to compare the vortex breakdown characteristics of these two models for static and dynamic conditions. The following conclusions are extracted from the results of the experimental investigation:

1. Static Conditions: The strake vortex develops at $\alpha \approx 10°$ for both models, but the wing vortex develops earlier at $\alpha = 5°$ for the modified model. The vortex burst locations move forward with increasing AOA for both the models. The fillet on the modified model promotes earlier coiling-up of vortices but has no influence at high angles of attack.

2. Dynamic Conditions: Compared to the static case, the strake vortex burst locations occur earlier during pitch-down motion for both models. On the other hand, the bursting is delayed during pitch-up motion relative

to the static case. These dynamic lag effects are found to increase with pitch rate.

3.   Effect of fillet: The small geometry modification at the strake/wing junction of the baseline model changes the local flow field by developing the wing vortex earlier and promoting earlier coiling-up of vortices.

The following recommendations are made based on this investigation:

1.   Investigation of double delta wing models with different geometry modifications at the strake/wing junction is highly recommended.

2.   Similar studies of the double delta wing models shoud be carried out in the wind tunnel and the experimental data should be compared with computational results.

3.   It is highly recommended that the above investigation be extended to include the effects of sideslip (yaw).

LIST OF REFERENCES

1. R. Whitford, Design for Air Combat, Janes publishing Company Ltd., London 1987.

2. D. F. Fisher, J. H. Del Frate, and D. M. Richwine, "In-Flight Flow Visualization of the NASA F-18 High Alpha Research Vehicle at High Angle of Attack," NASA TM-4130, May 1990.

3. J. H. Del Frate, D. F. Fisher, and F. A. Zuniga, "In-Flight Flow Visualazition with Pressure Measurements at Low Speeds on the NASA F-18 High Alpha Research Vehicle," NASA TM-101726, October 1990.

4. D. F. Fisher, J. H. Del Frate, and F. A. Zuniga, "Summary of In-Flight Flow Visualization Obtained From the NASA High Alpha Research Vehicle," NASA TM-101734, January 1991.

5. G. E. Barlett, and R. J. Vidal, "Experimental Investigation of influence of Edge Shape on the Aerodynamic Characteristics of Low Aspect Ratio Wings at Low Speeds" Journal of the Aeronautical Sciences, Volume 22,Number 8, August 1955.

6. J. E. Lamar, "Nonlinear Lift Control at High Speed and High Angle of Attack using Vortex Flow Technology," AGARD, 1986.

7. Lee, M., and Ho, C. M., Vortex Dynamics of Delta Wings, Frontiers in Experimental Fluid Mechanics, Lecture Notes in Engineering, NO. 46, Springler-Verlag, New York, 1989.

8. N.J. WOOD and L. Roberts , "Control of Vortical Lift on Delta Wings by Tangential Leading-Edge Blowing," Journal of Aircraft, Vol. 25, No. 3, March 1988.

9. M. W. Walters,"Flowfield of Bursting Vortices Over Moderately Swept Delta Wings," HTP-5 Workshop On Vortical Flow Breakdown and Structural Interactions, NASA Langley Research Center, August 15-16, 1991.

10. N.G. Verhaagen, and S.H.J. Naarding, "Experimental and Numerical Investigation of Vortex Flow over a Side slipping Delta Wing", Journal of Aircraft, Vol. 26, No. 11, November 1989.

11. J. Er-El, D. Soother, and D. Weihs, "Nonlinear Aerodynamics of a Delta Wing in Combined Pitch and Roll", Journal of Aircraft, Vol. 26, No.3, March 1989.

12. Y. Zohar, and J. Er-El, "Influence of the Aspect Ratio on the Aerodynamics of the Delta Wing at High Angle of Attack" Journal of Aircraft, Vol. 25, No. 3, March 1988.

13. K.C. Powell, and E.M. Murman, "Comparison of Experimental and Numerical Results for Delta Wings with Vortex Flaps", Journal of Aircraft, Vol. . No. , May 1988.

14. F. Yu, K. Young, and R. Chang, An Investigation on the Coiling-Up of Vortices on a Double Delta Wing, AIAA, 28th Aerospace Sciences Meeting, January 8-11,1990/Reno,Nevada.

15. R. G. Den Boer, and A. M. Cunningham Jr, "Low-Speed Unsteady Aerodynamics of a Pitching Strake Wing at High Incidence-part I: Test Program," Journal of Aircraft, Vol 27, No. 1, Jan.1990.

16. J. A. Ekaterinaris, R. L. Coutley, L. B. Schiff, and M. F. Platzer, "Numerical Investigation of the Flow Over a Double Delta Wing at High Incidence," 29th Aerospace Sciences Meeting, AIAA paper 91-0753, January 7-10,1991/Reno,Nevada.

17. S. B. Kern, "Numerical Investigation of Vortex Flow Control Through Small Geometry Modifications At the Strake/Wing Junction of a Cropped Double-Delta Wing," 30th Aerospace Sciences Meeting&Exhibit, January 6-9,1992/Reno,Nevada.

18. User's Manual, Flow Visualization Water Tunnel Operation for Model 1520, Eidelic International, Inc., Torrance, California, 1988. (Prepared for Naval Postgraduate School, Monterey, California).

19. O. Cavazos, A Flow Visualization Study of Lex Generated on a F/A-18 Fighter Aircraft at High Angle of Attack,Master's Thesis, Naval Postgraduate School, Monterey, California, June 1990.

20. S. Hebbar, M. Platzer, O. Cavazos,," A Water Tunnel Investigation of the Effects of Pitch Rate and Yaw on LEX Generated Vortices of an F/A-18 Fighter Aircraft Model" AIAA 29th Aerospace Sciences Meeting, AIAA paper no. 91-0280, January 7-10, 1991/Reno, Nevada.

21. C. Kim, Flow Visualization Studies of A Sideslipping, Canard-Configured X-31A-Like Fighter Aircraft Model, Master's Thesis, Naval Postgraduate School, Monterey, California, December 1991.

22. D. R. Magness., and D. Rockwell., 'Control of Leading Edge Vortices on A Delta Wing, AIAA-89-0900, AIAA 2nd Shear Flow Conference, March 1989.

23. D. Grismer, R. Nelson, W. Ley," An Experimental Study of Double Delta Wing in Sideslip" AIAA 9th Applied Aerodynamics Conference, September 23-25, 1991 / Baltimore,MD.

APPENDIX A. EXPERIMENTAL RESULT (PHOTOGRAPHS)

FIGURES 13 THROUGH 66
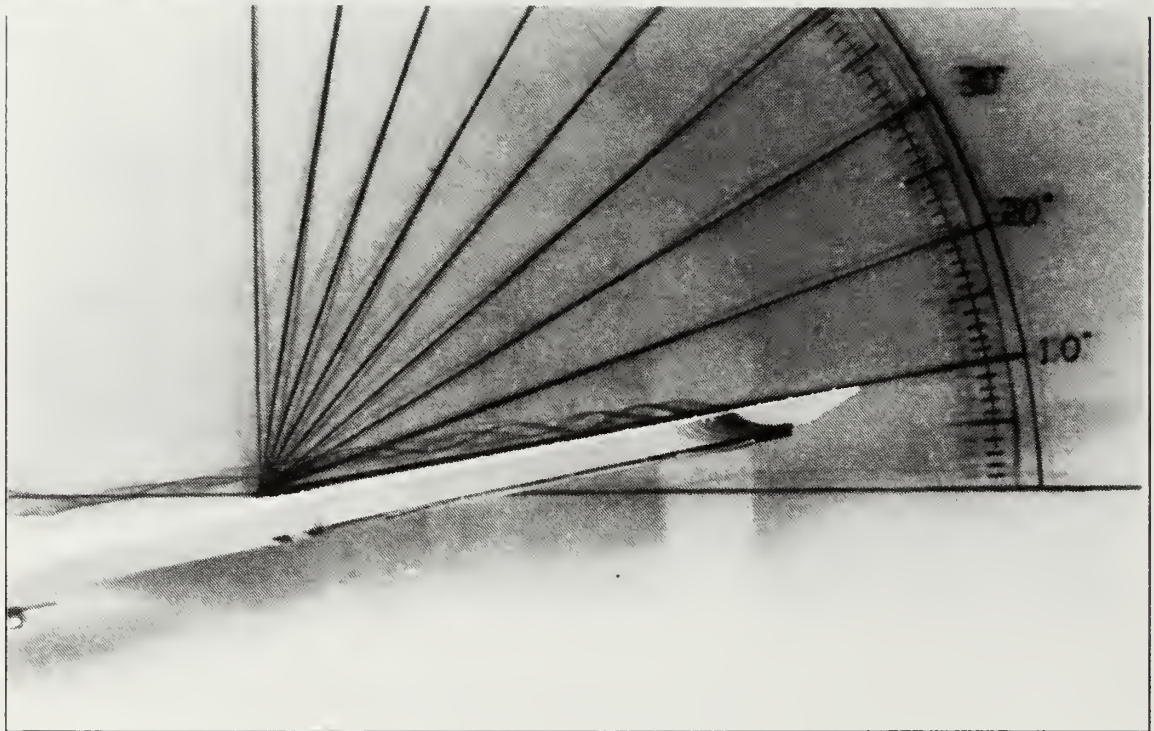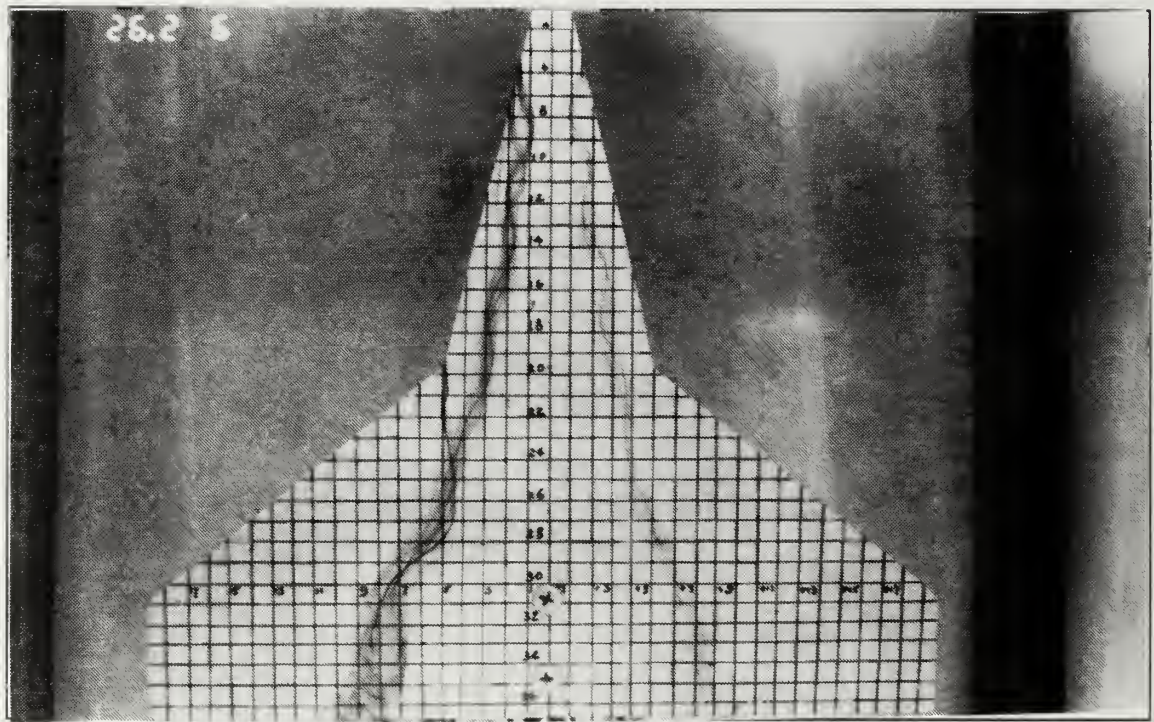
Figure 13. Strake Vortex Flow, Baseline Model,
k=0, α=10°
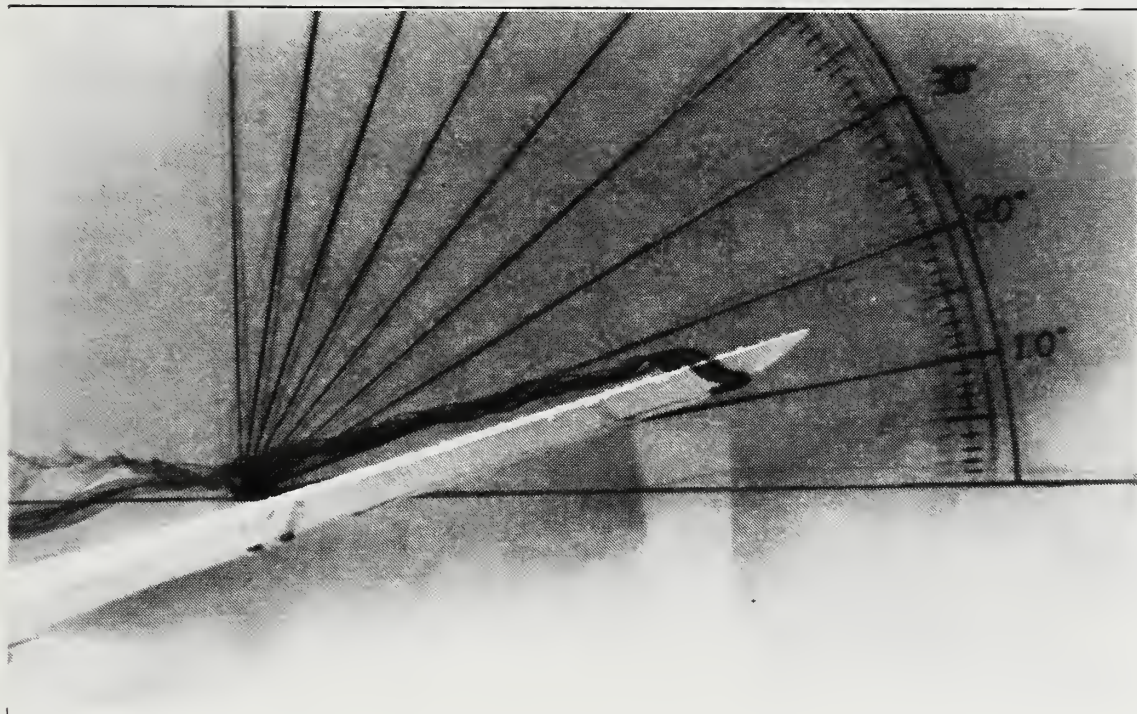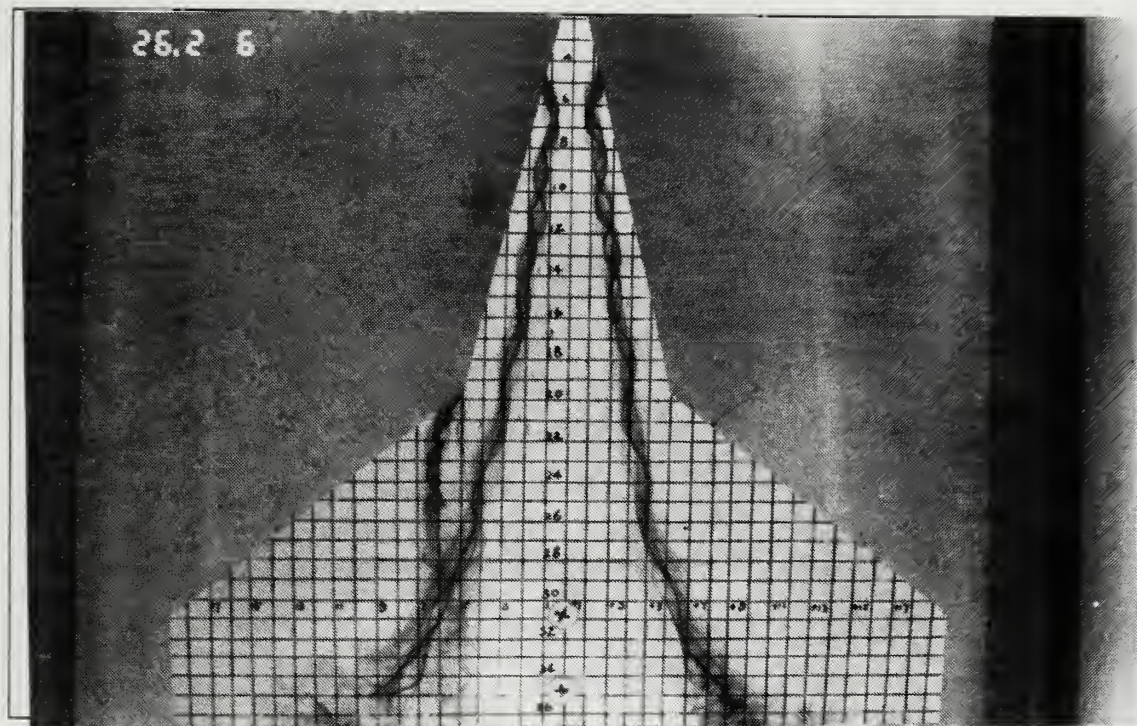
Figure 14. Strake Vortex Flow, Baseline Model,
k=0, α=15°
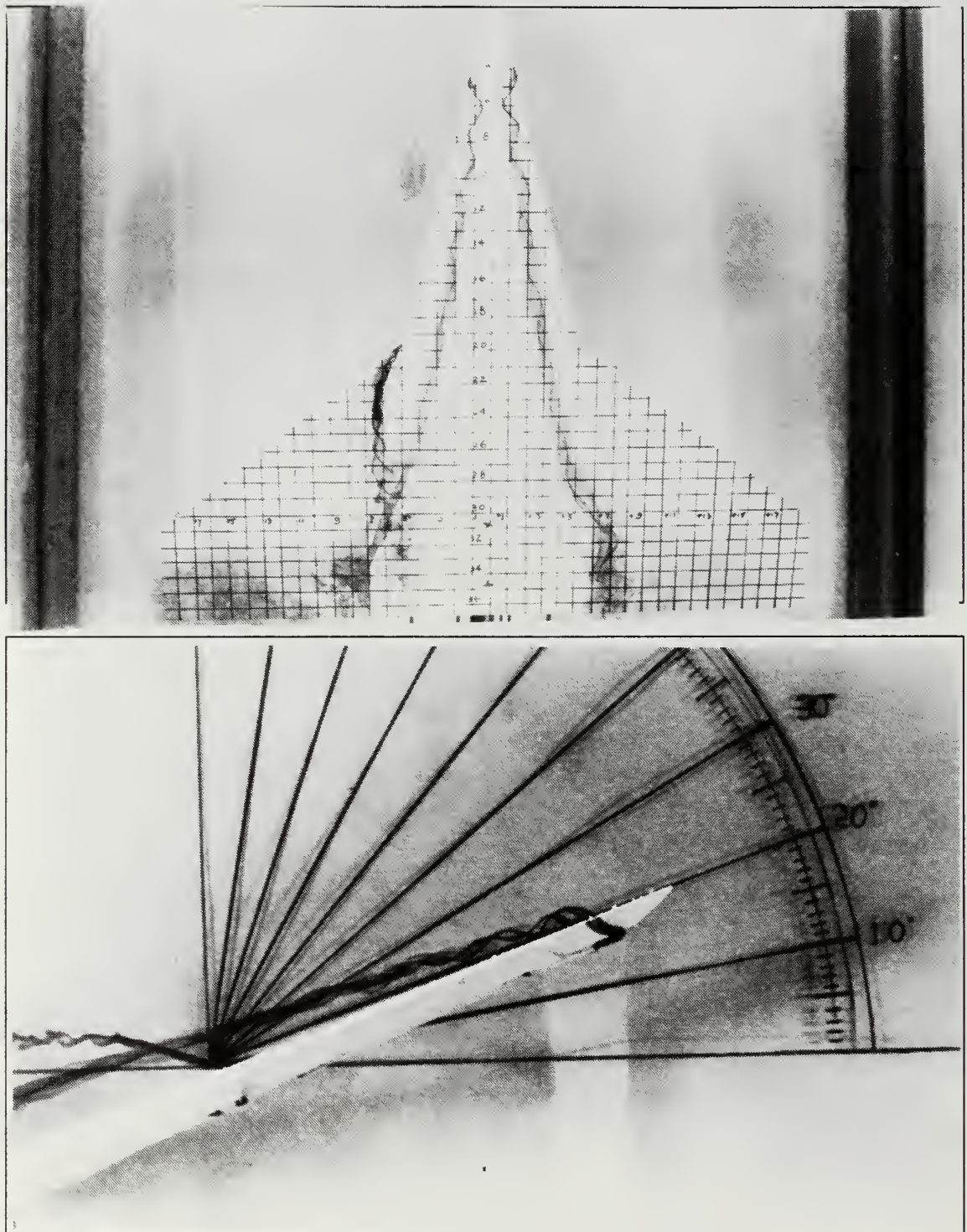
Figure 15. Strake Vortex Flow, Baseline Model,
k=0, α=20°
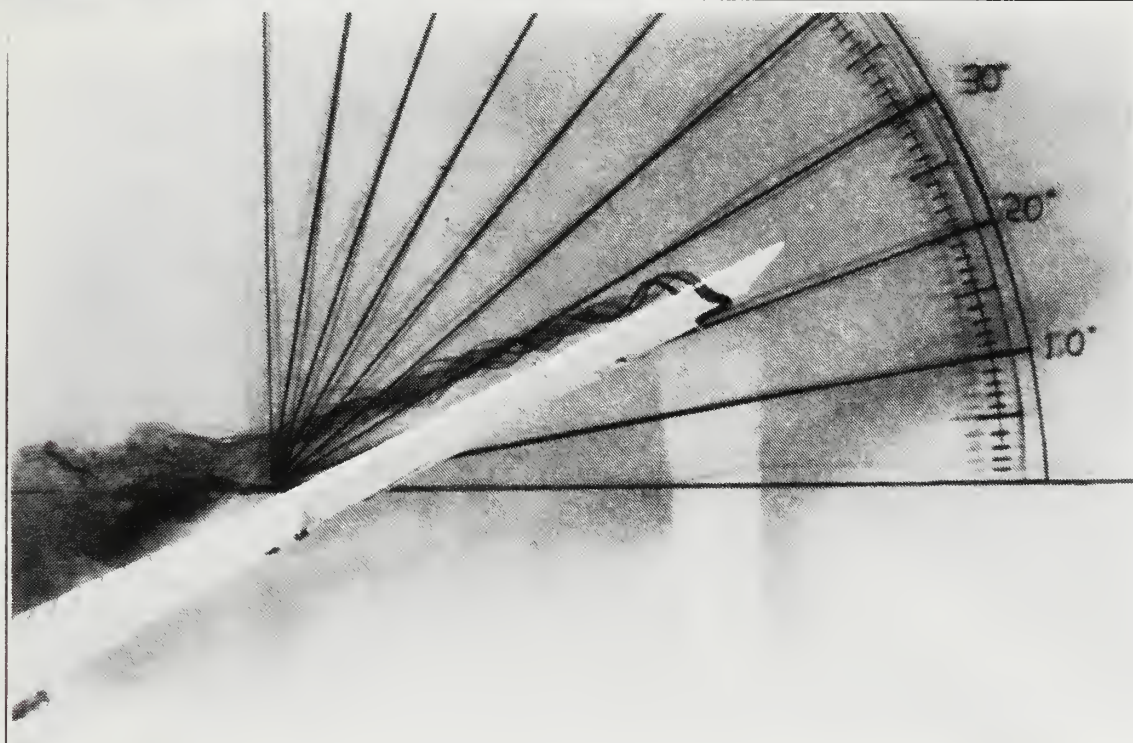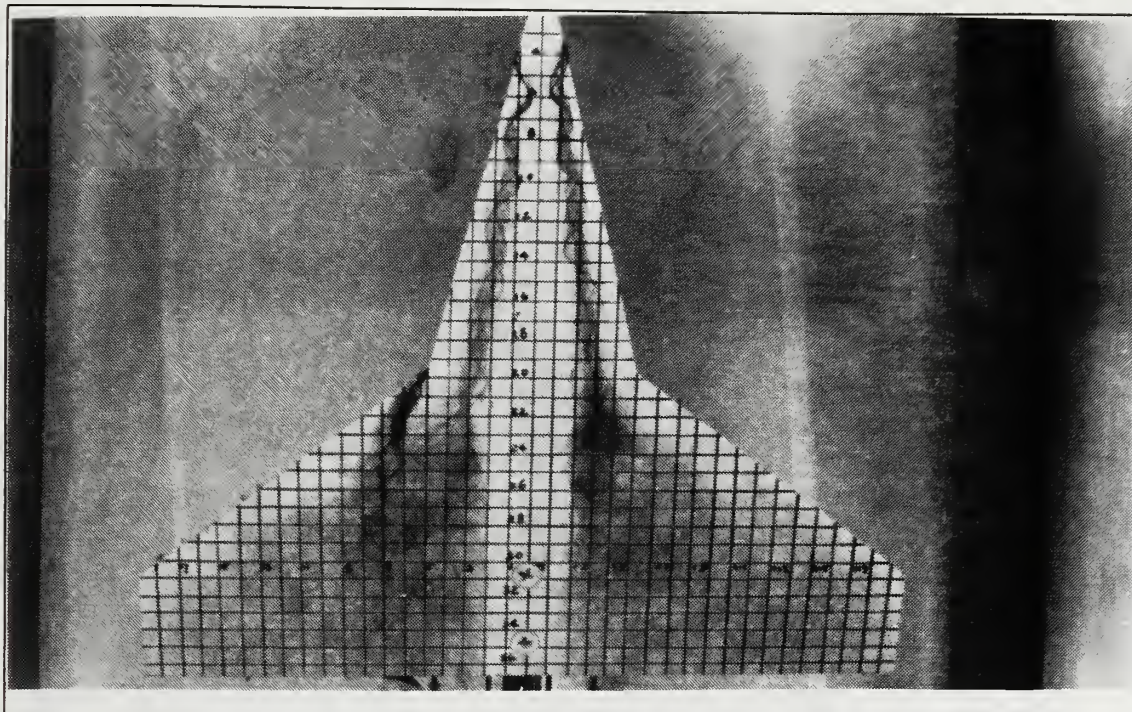
Figure 16. Strake Vortex Flow, Baseline Model,
k=0, α=25°
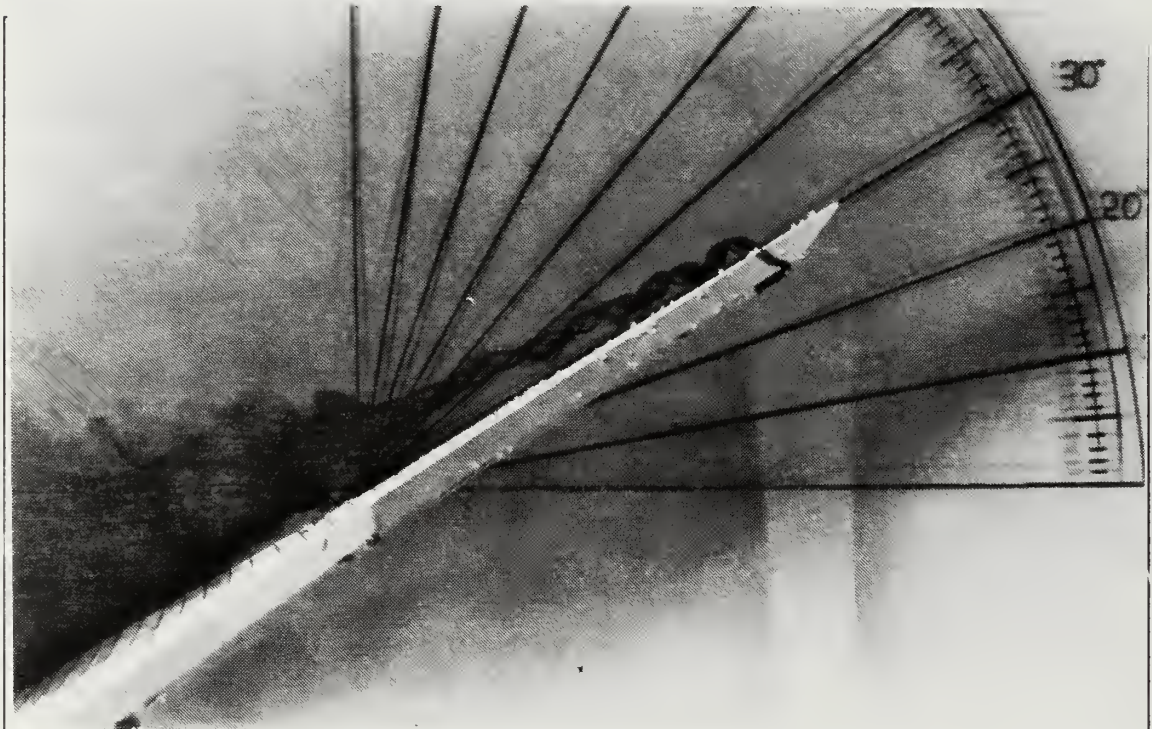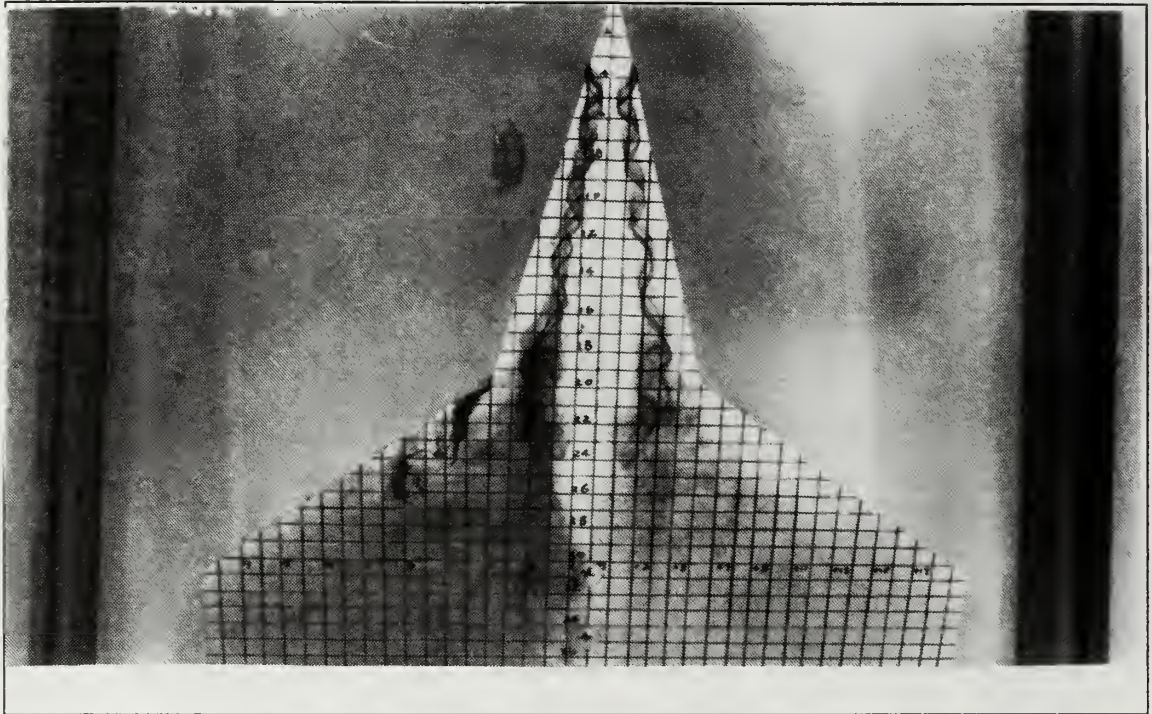
Figure 17. Strake Vortex Flow, Baseline Model,
k=0, α=30°
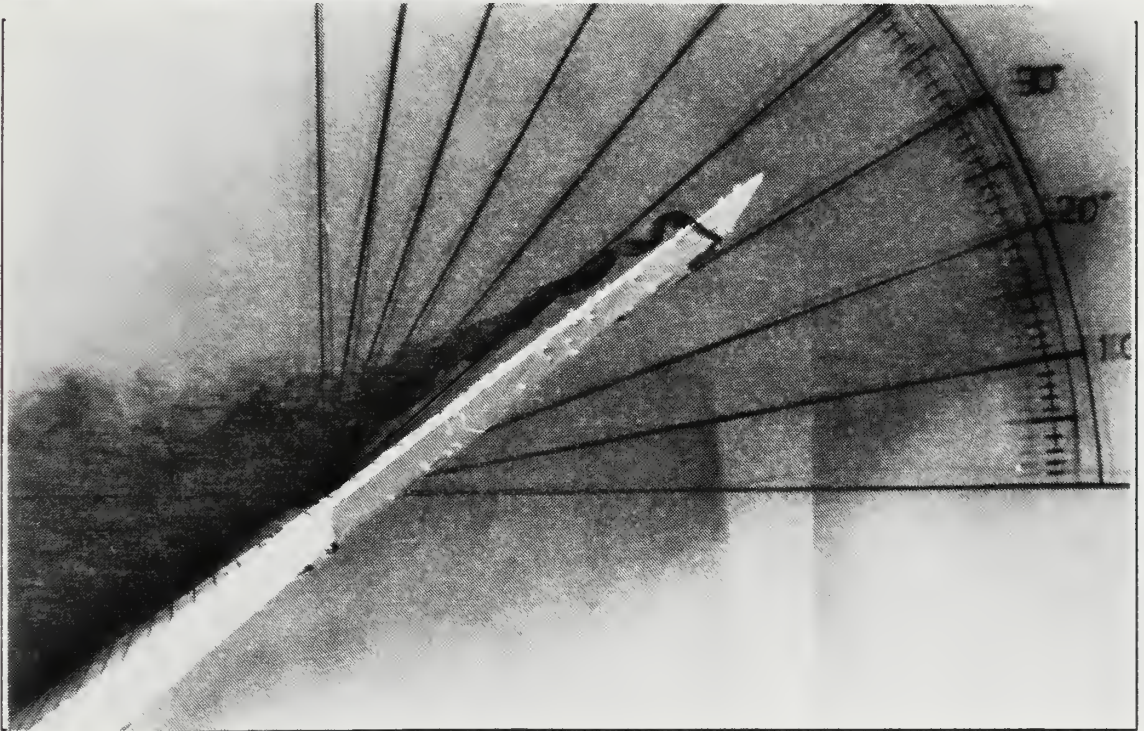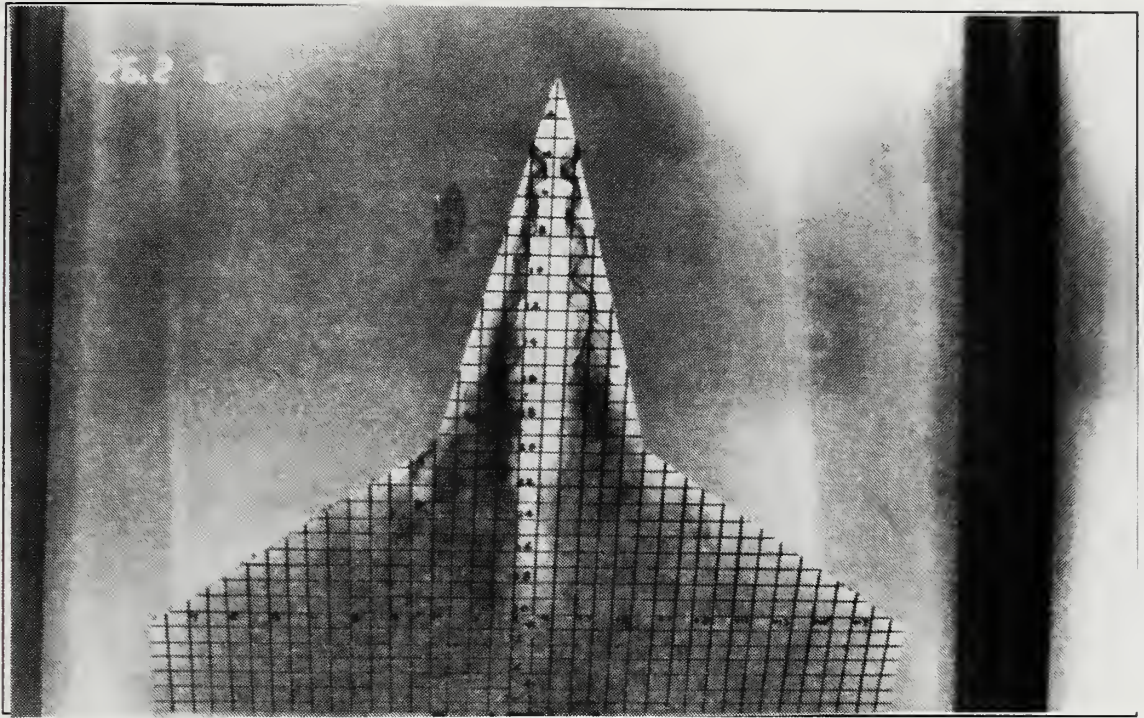
Figure 18. Strake Vortex Flow, Baseline Model,
k=0, α=35°
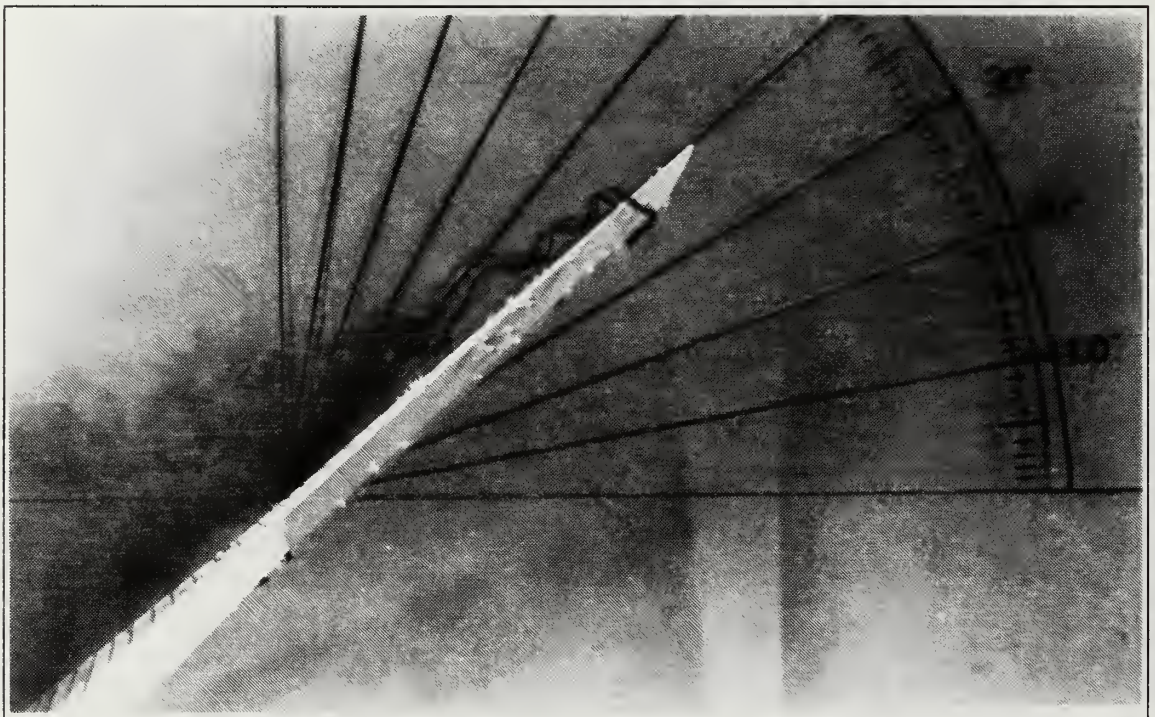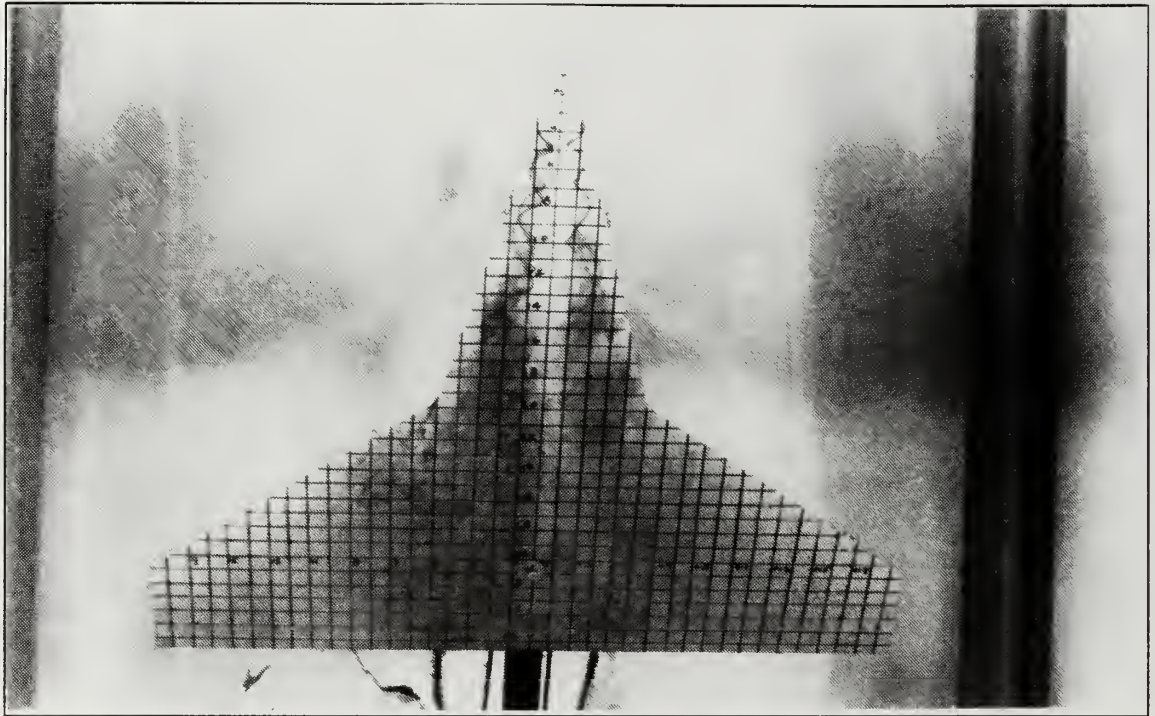
Figure 19. Strake Vortex Flow, Baseline Model,
k=0, $\alpha=40°$
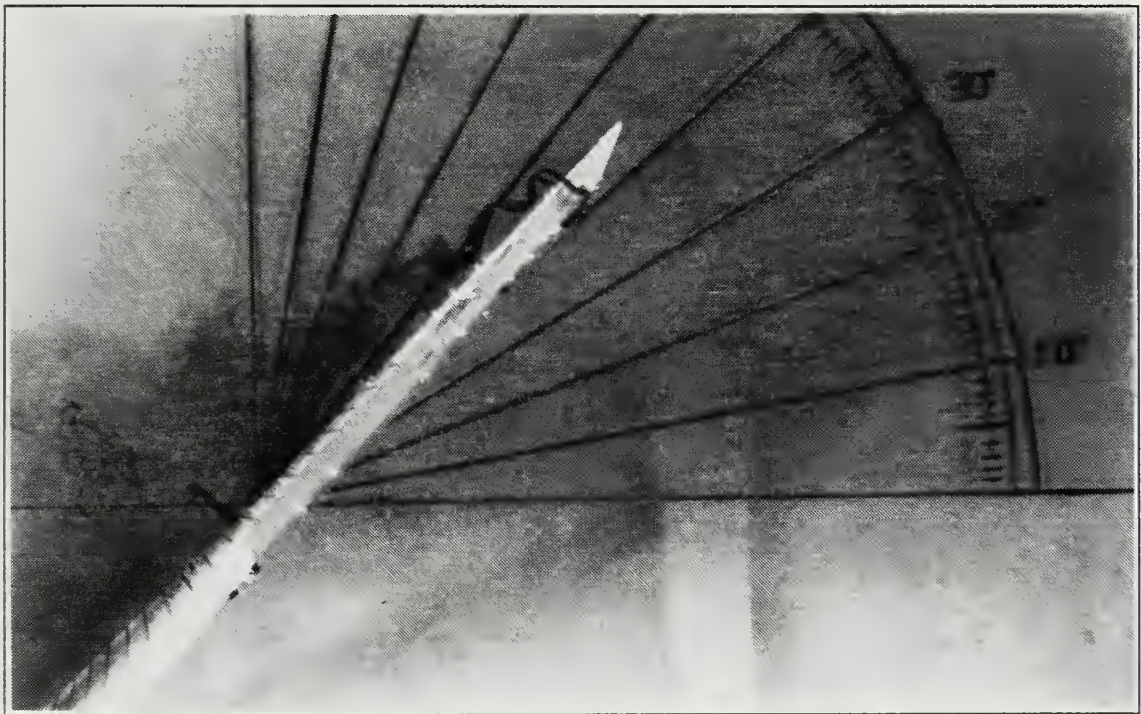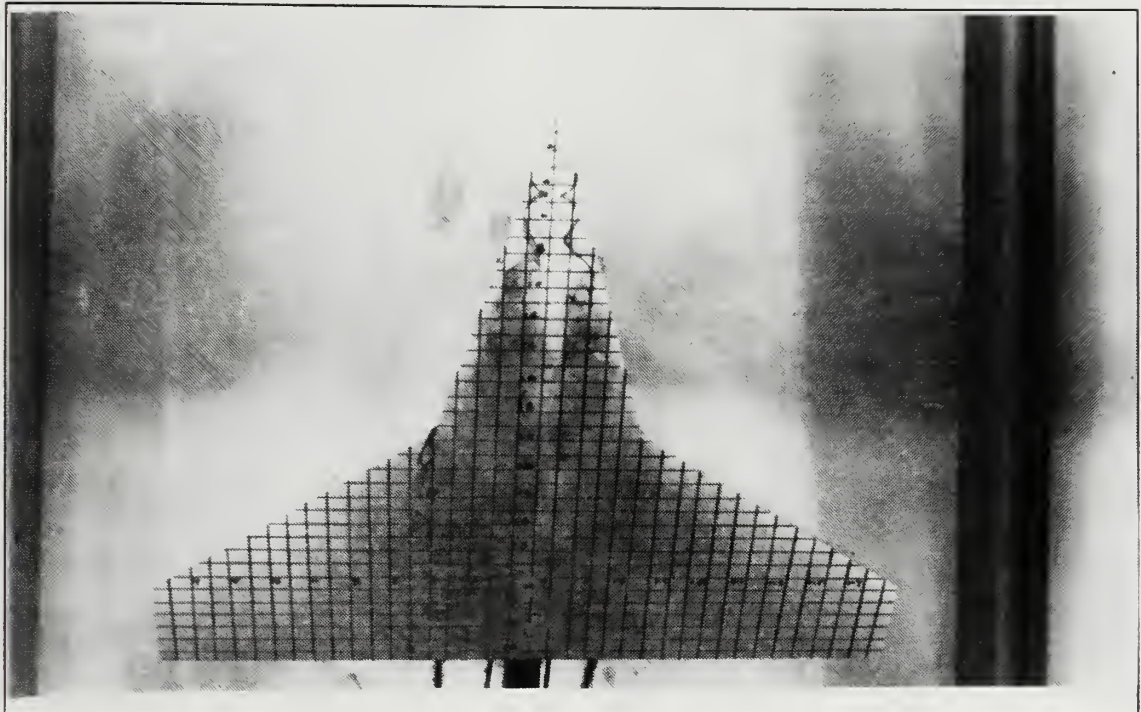
Figure 20. Strake Vortex Flow, Baseline Model, k=0, α=45°
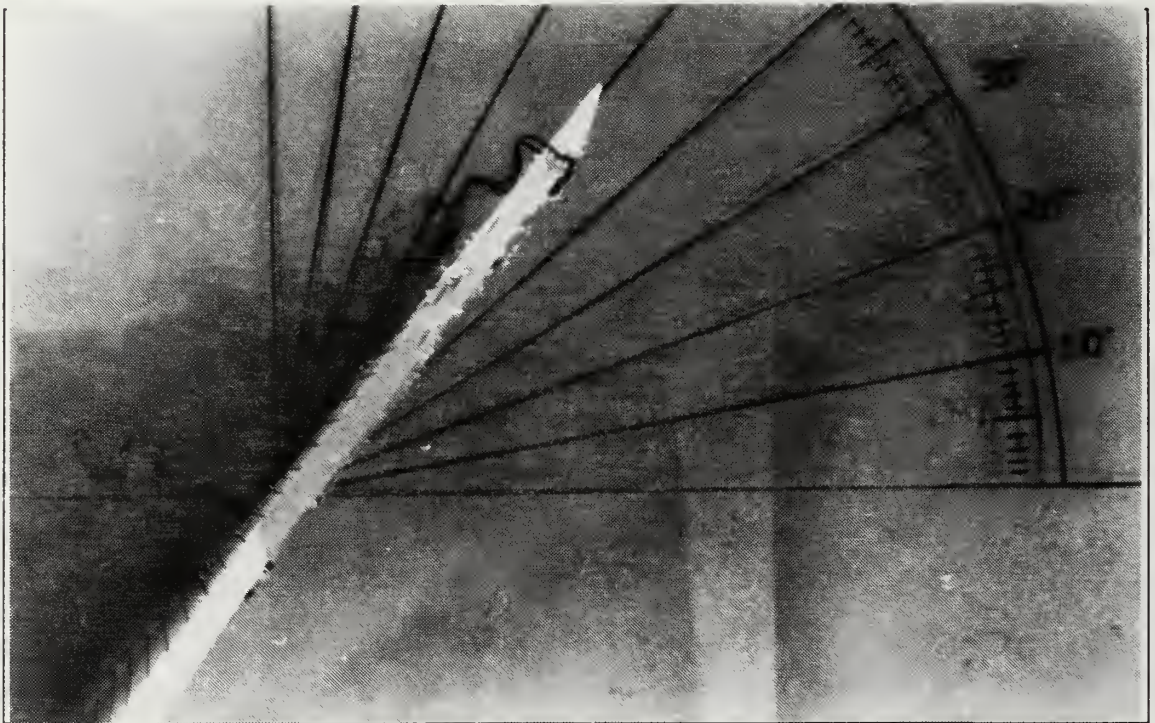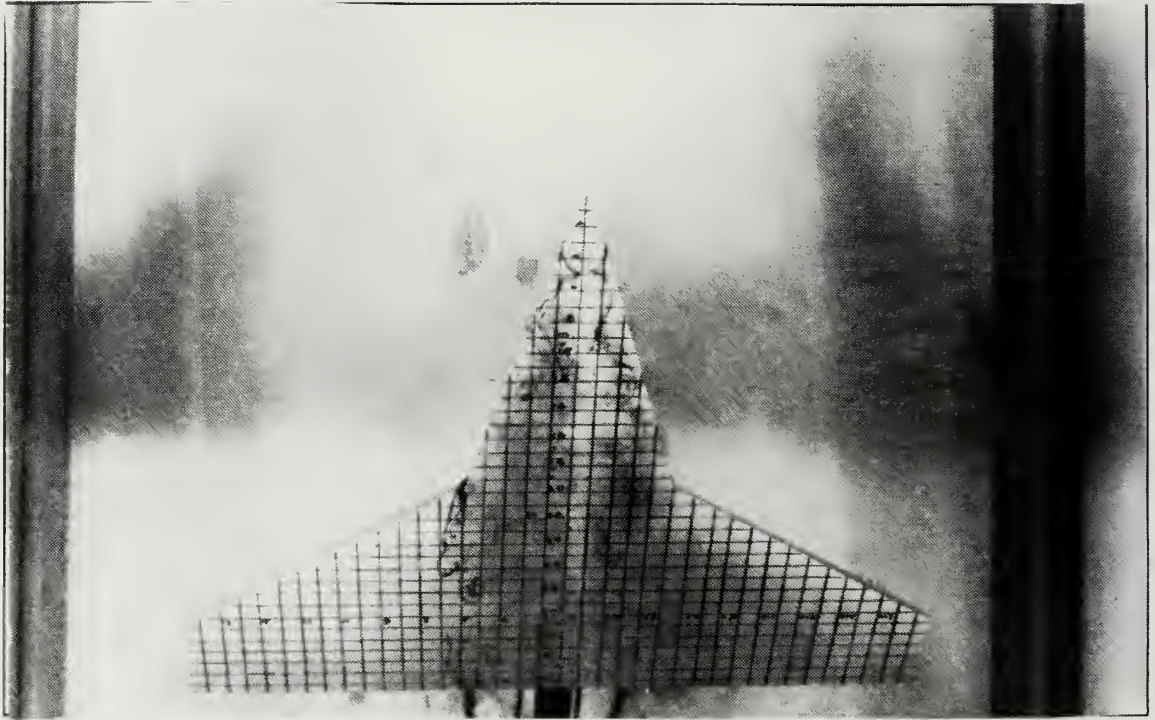
Figure 21. Strake Vortex Flow, Baseline Model,
k=0, α=50°
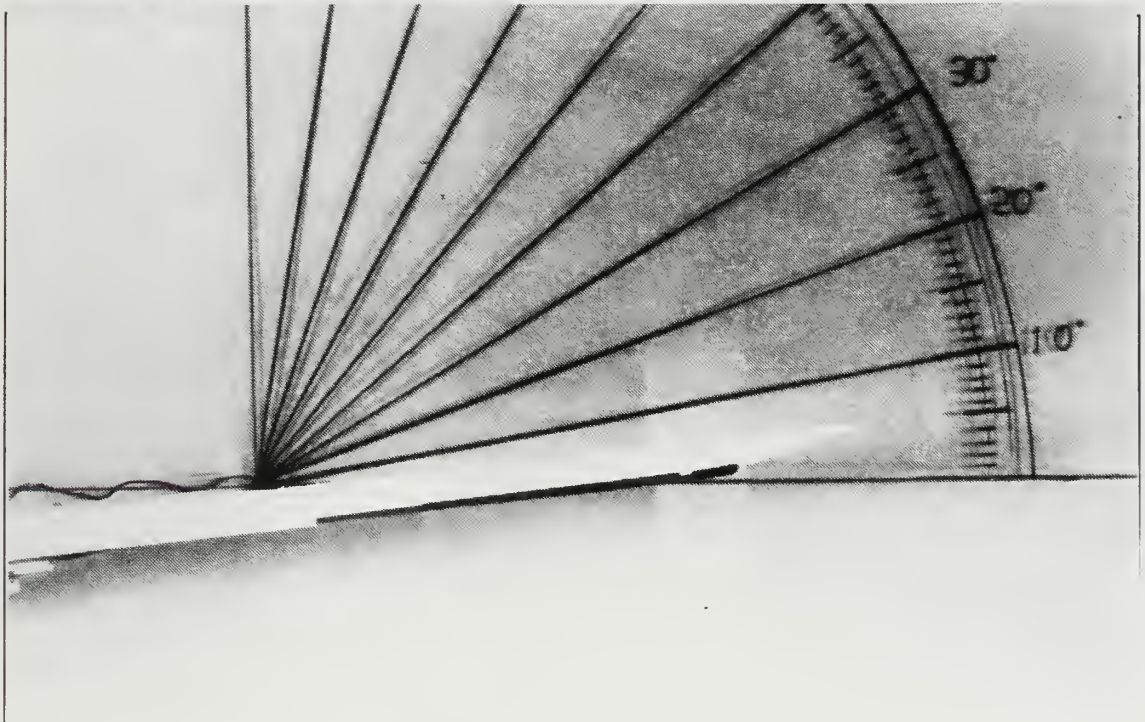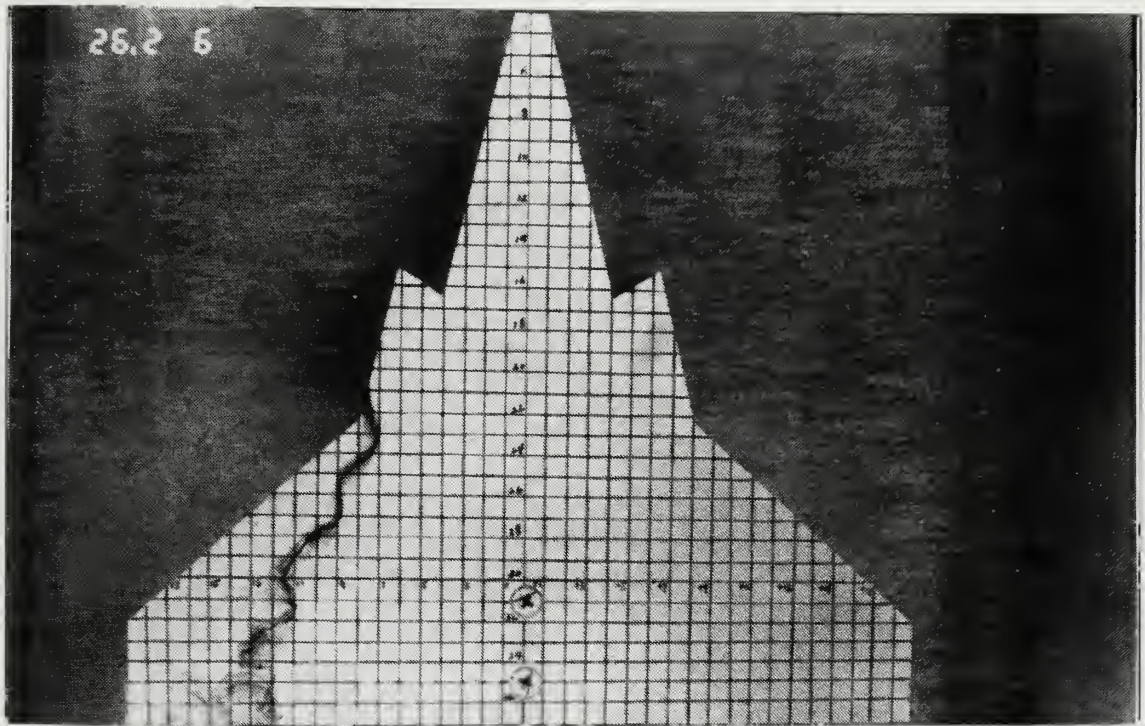
Figure 22. Strake Vortex Flow, Modified Model,
k=0, α=5°
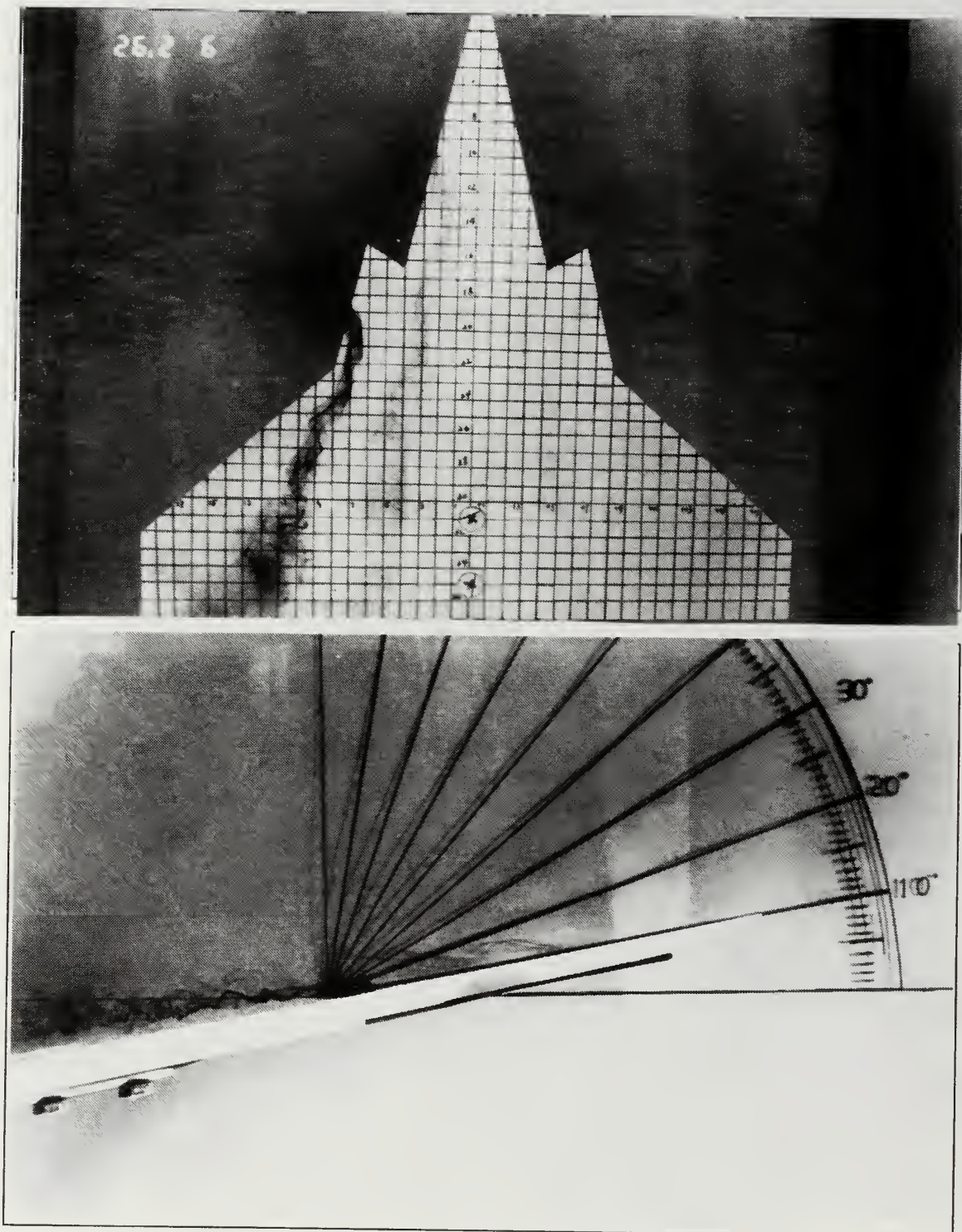
Figure 23. Strake Vortex Flow, Modified Model,
k=0, α=10°
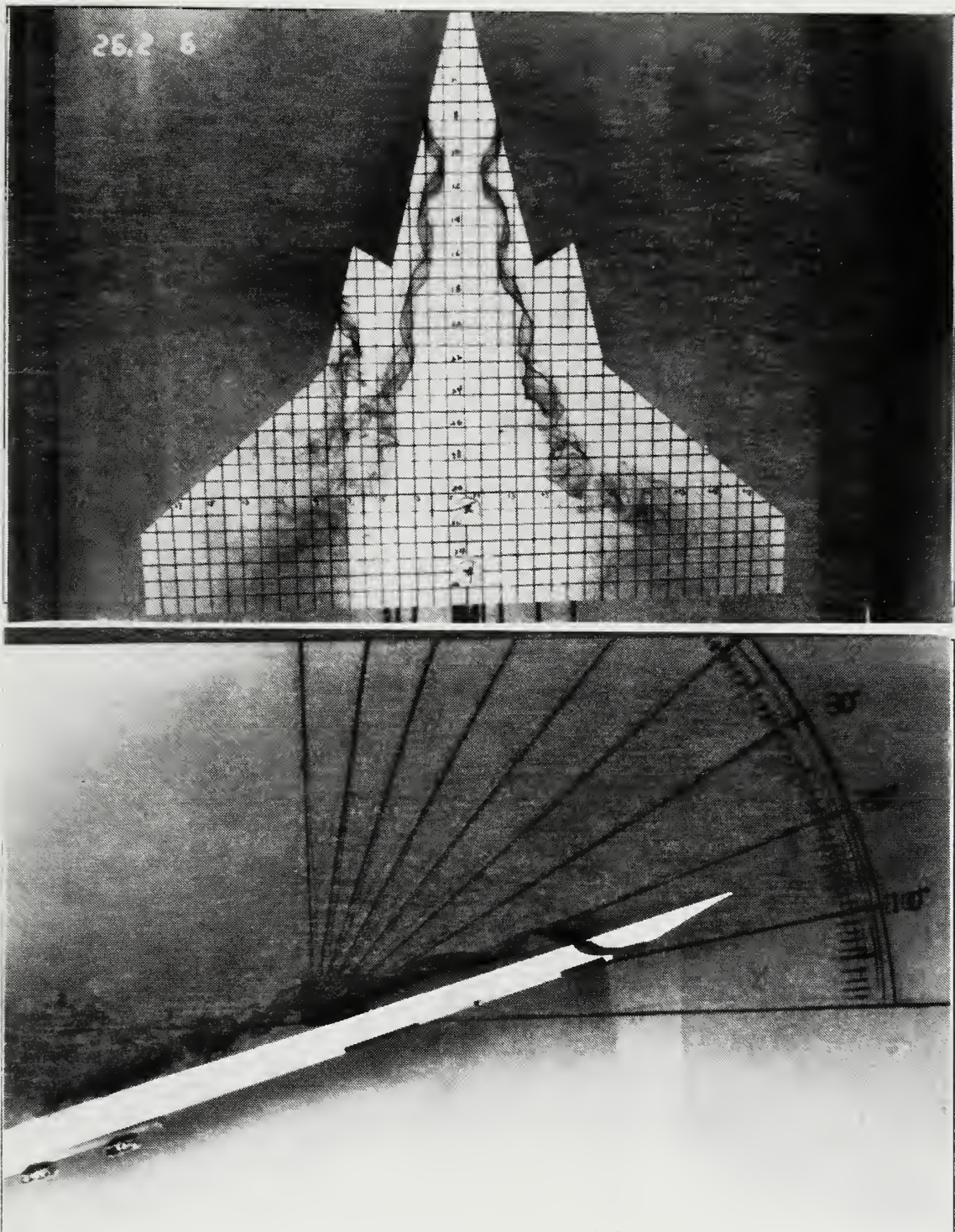
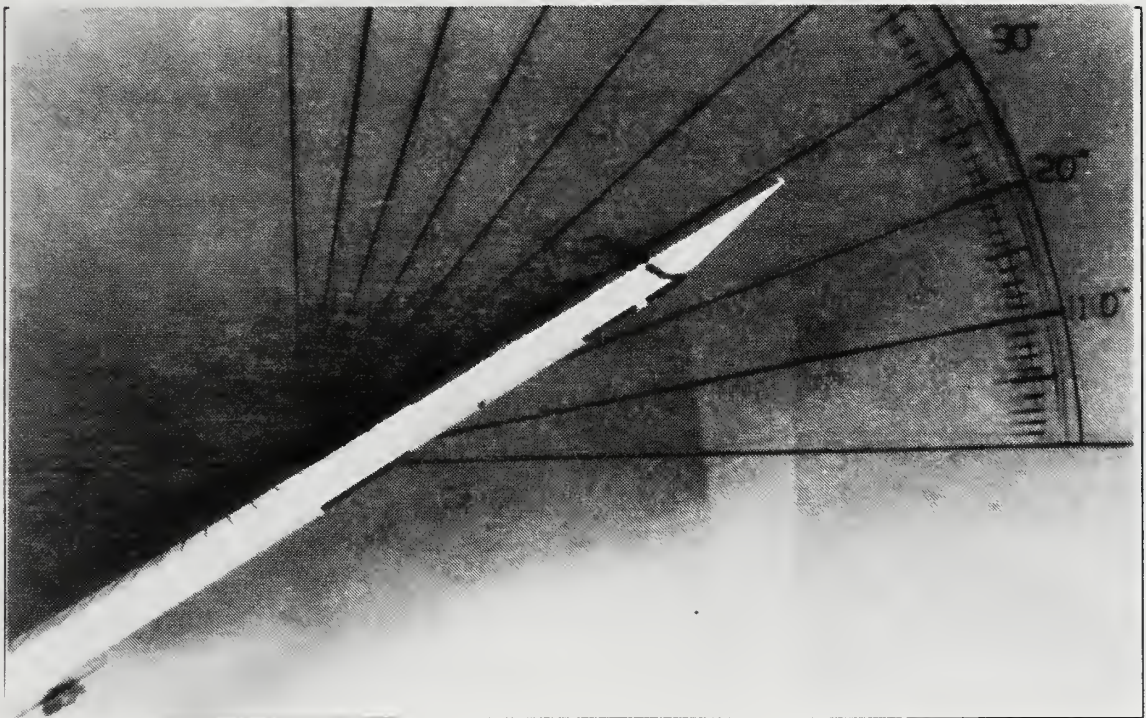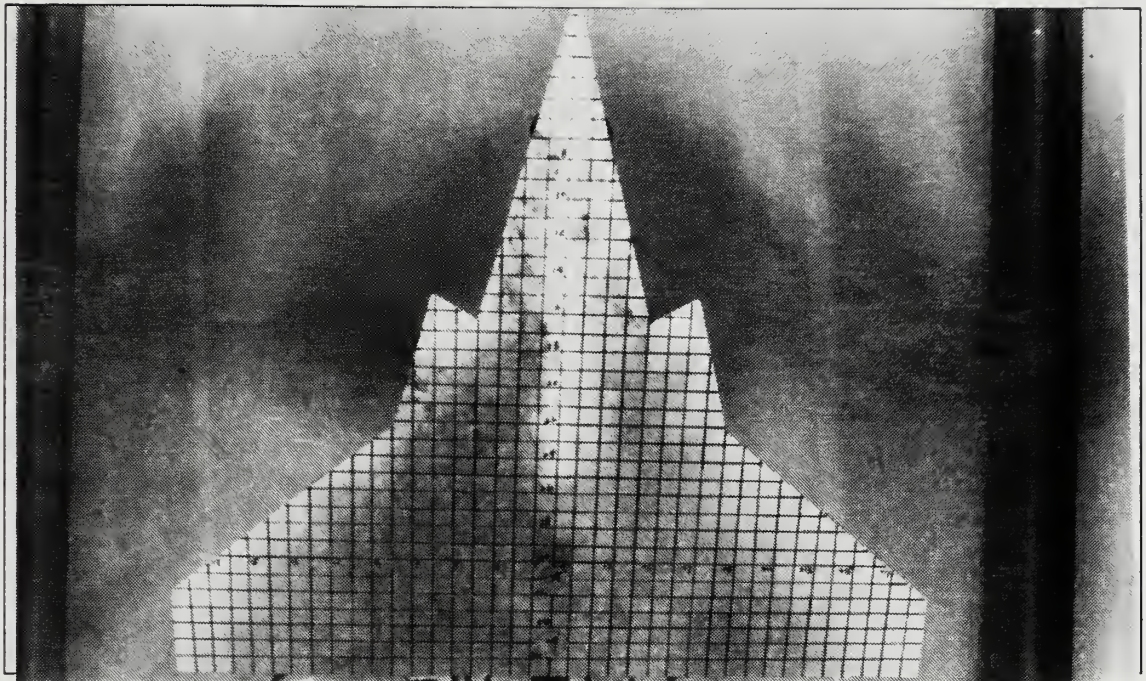Figure 24. Strake Vortex Flow, Modified Model,
k=0, α=15°
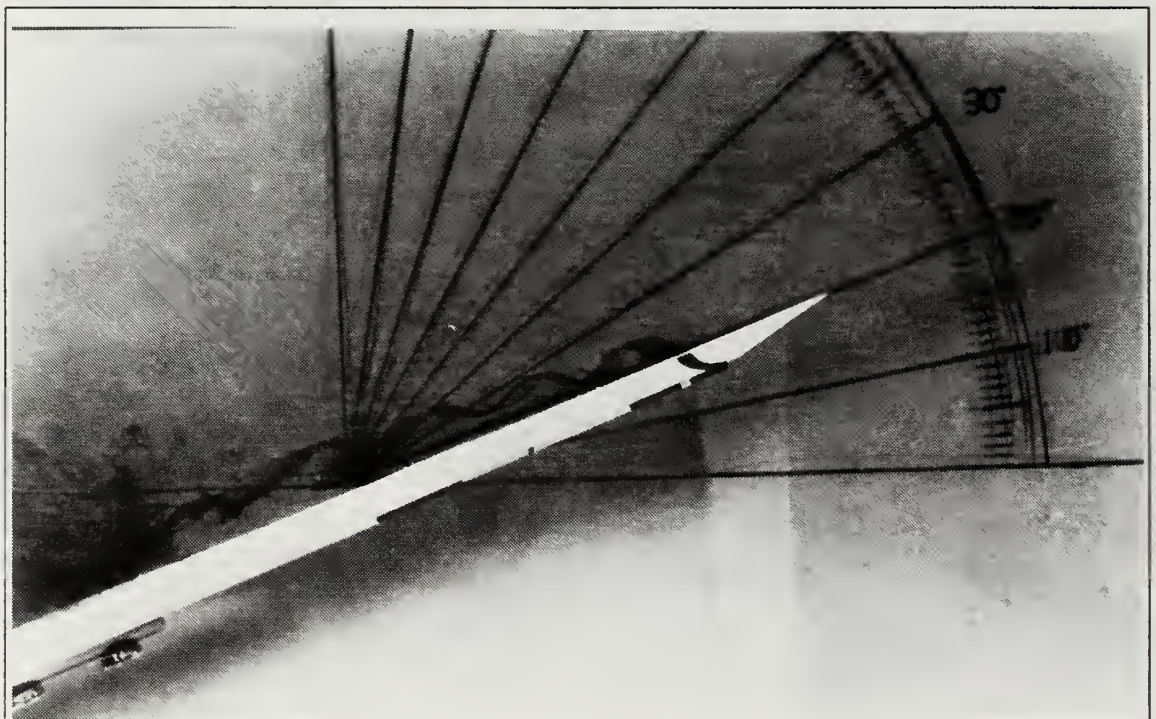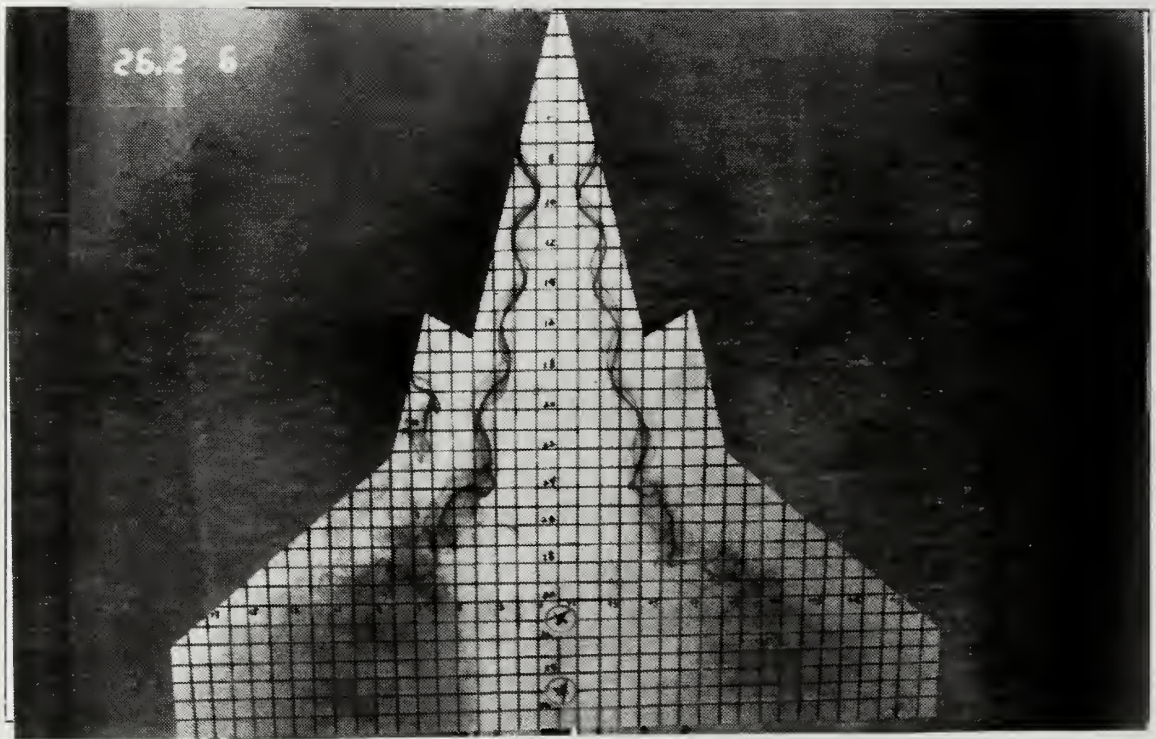
Figure 25. Strake Vortex Flow, Modified Model, k=0, α=20°
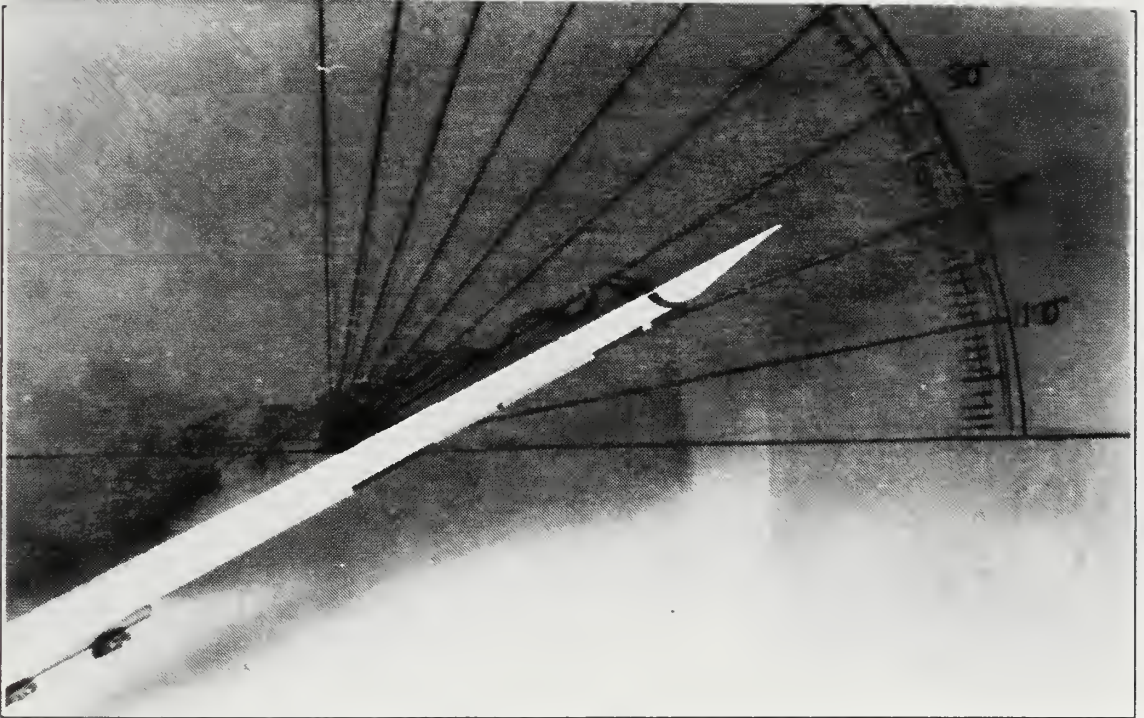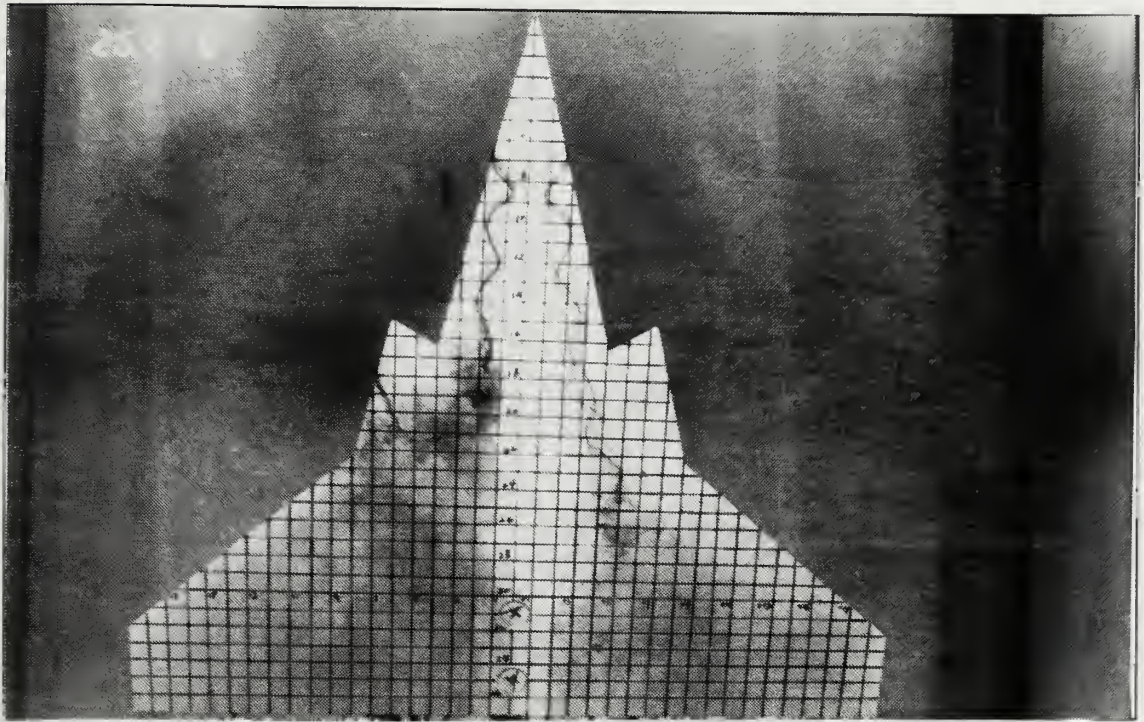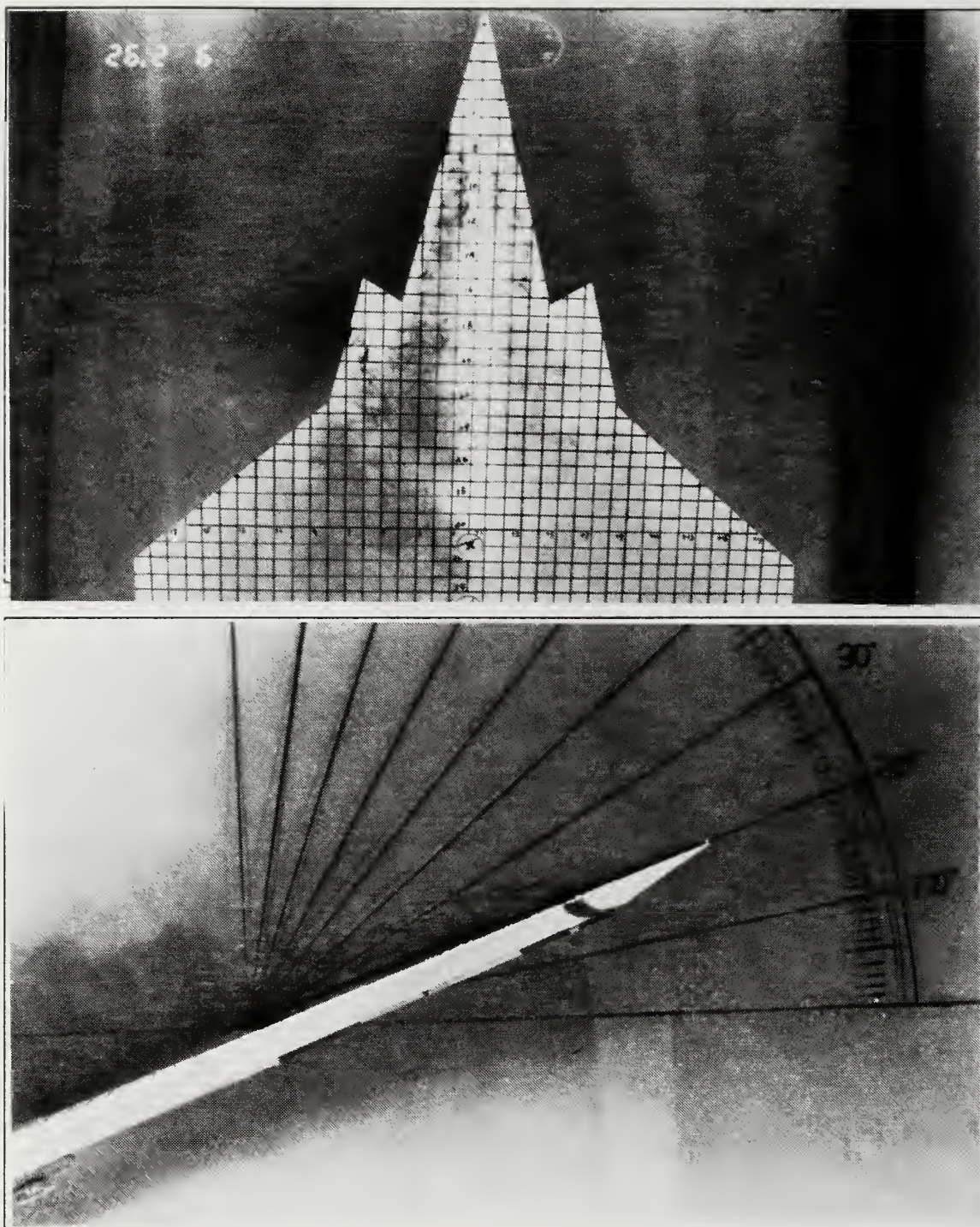
Figure 26. Strake Vortex Flow, Modified Model,
k=0, α=25°
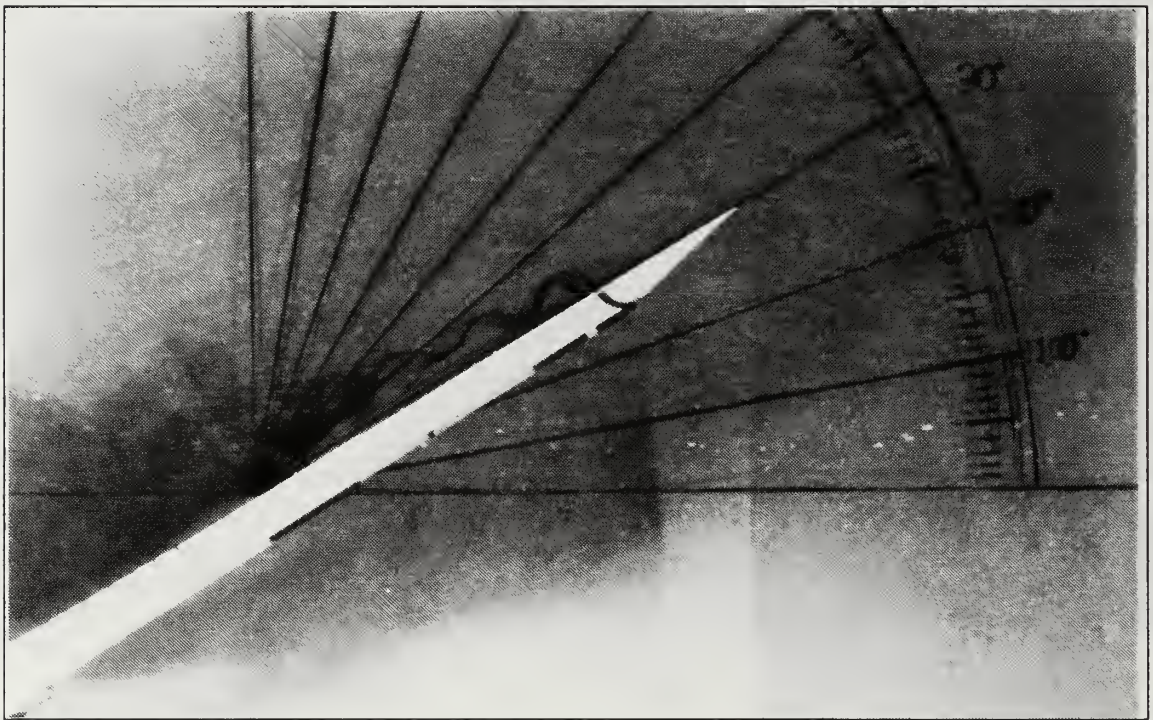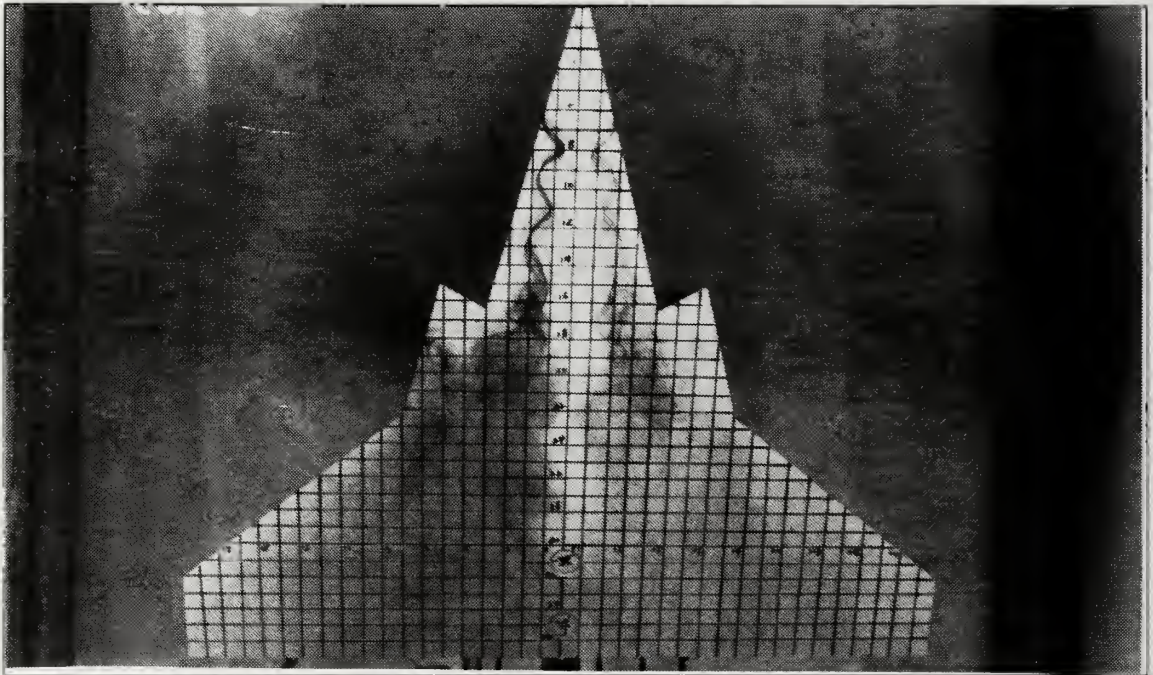
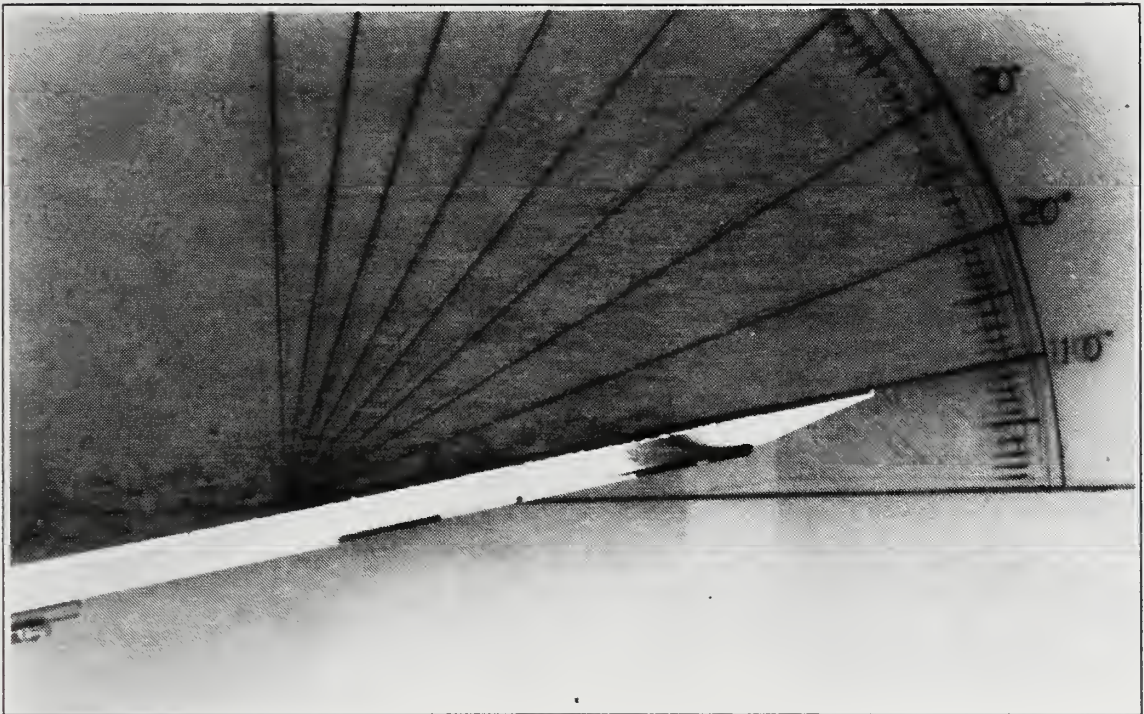Figure 27. Strake Vortex Flow, Modified Model,
k=0, α=30°
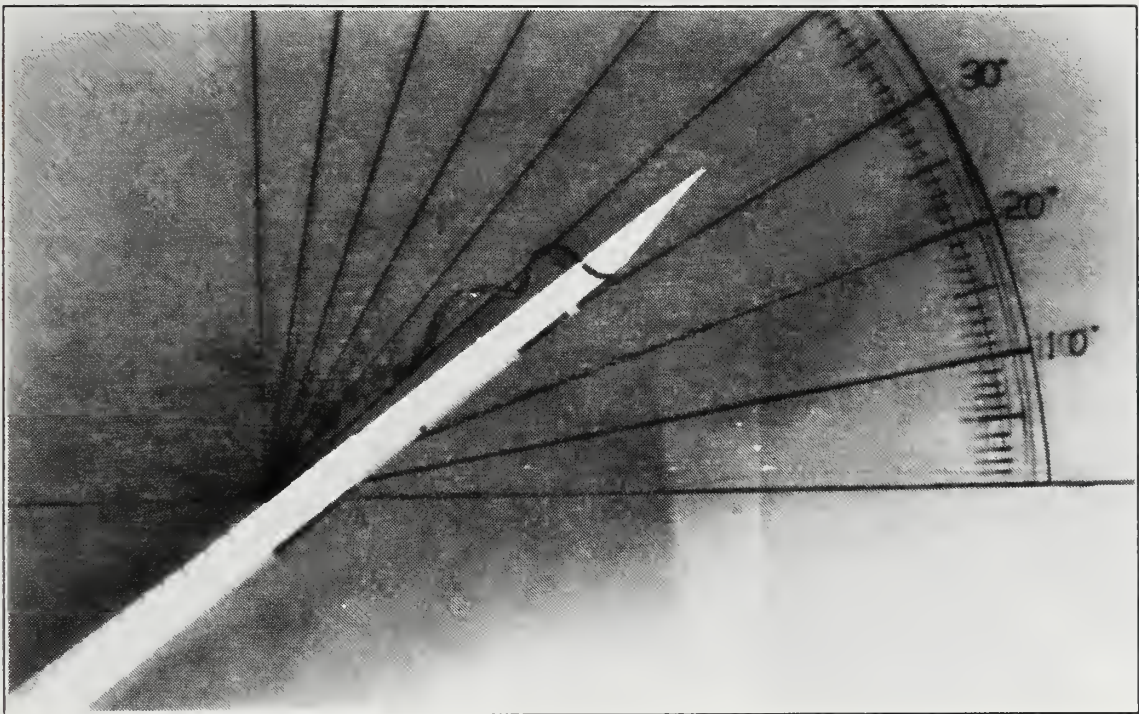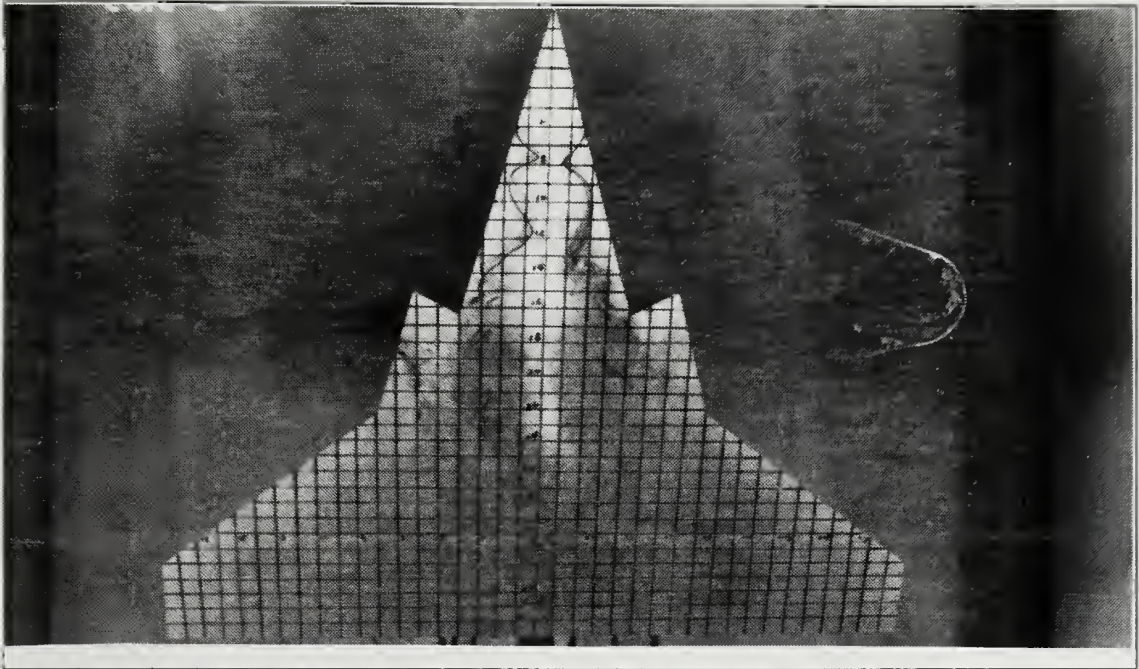
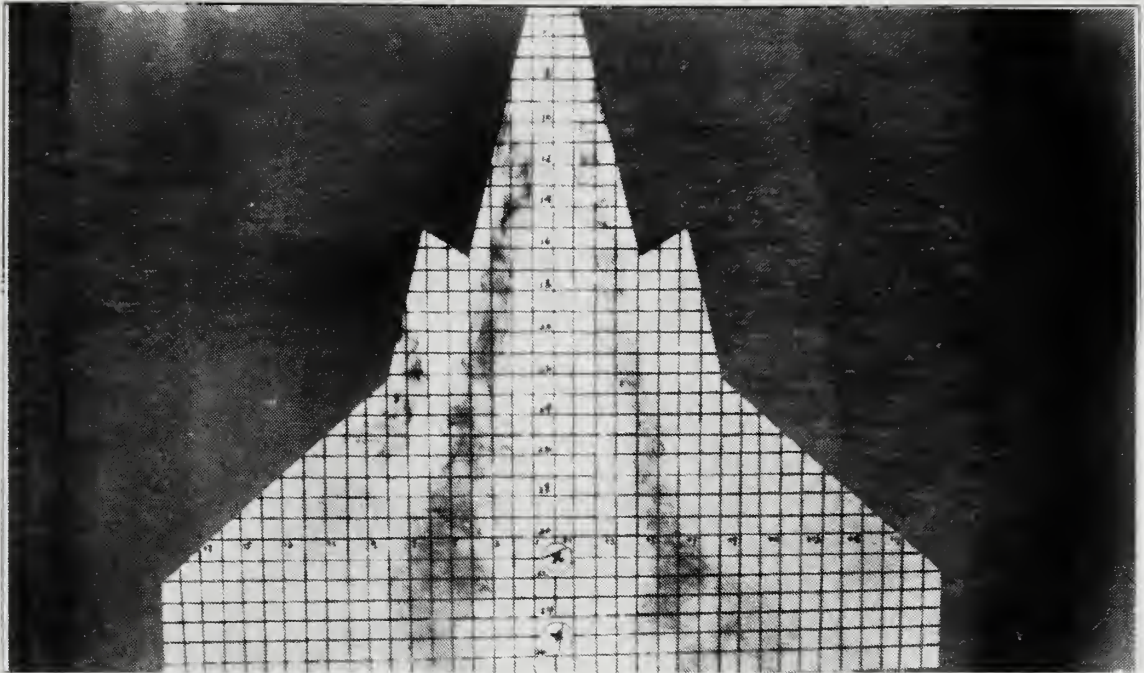Figure 28. Strake Vortex Flow, Modified Model, k=0, α=35°
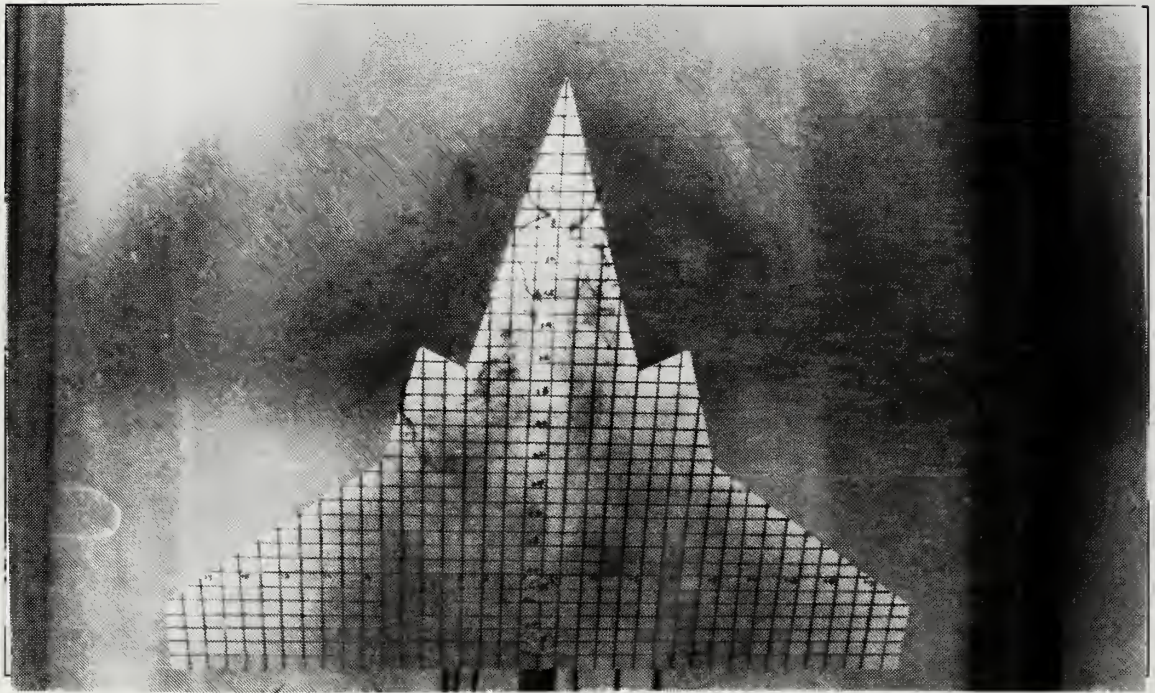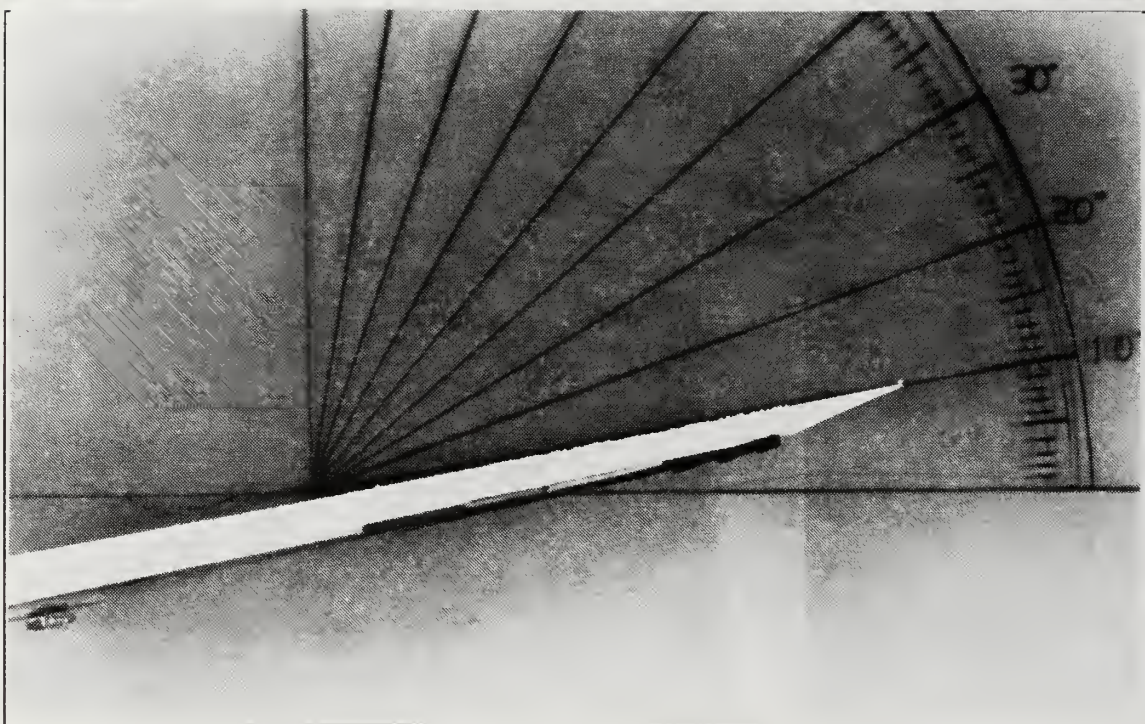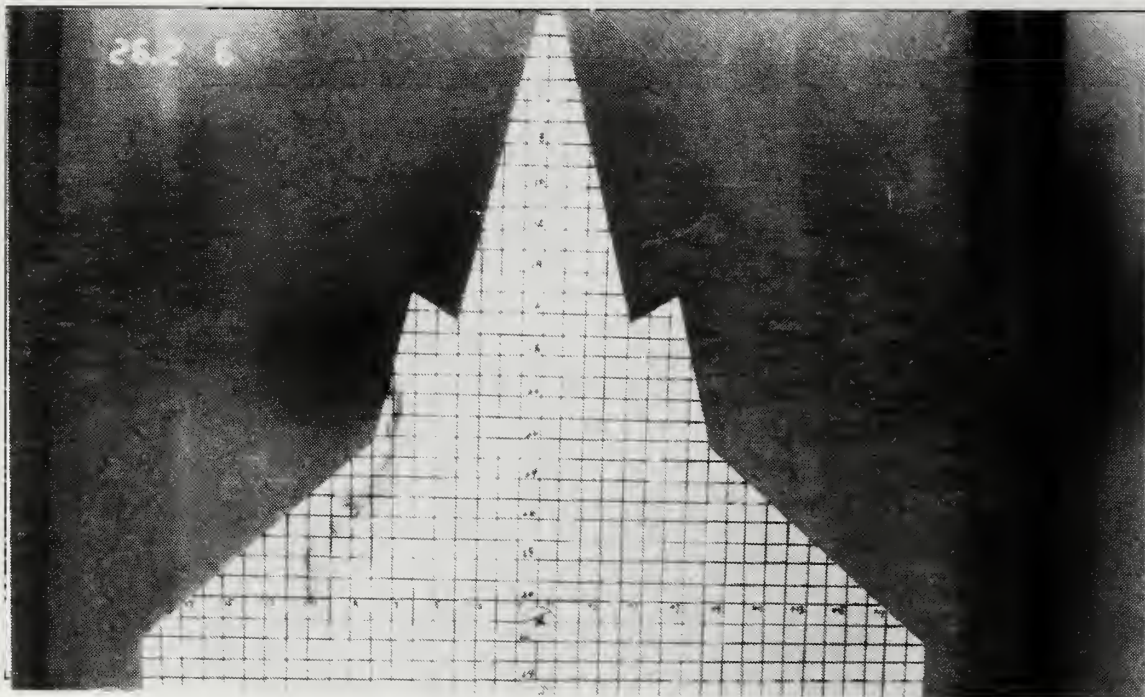
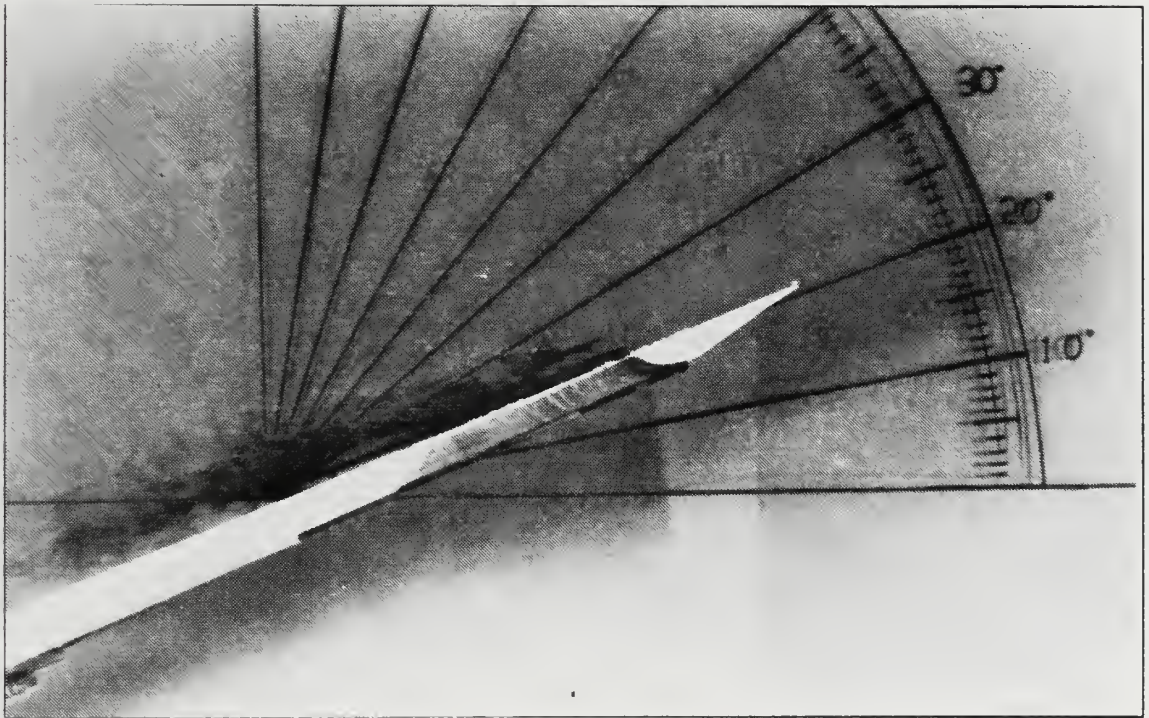Figure 29. Strake Vortex Flow, Modified Model,
k=0, α=40°
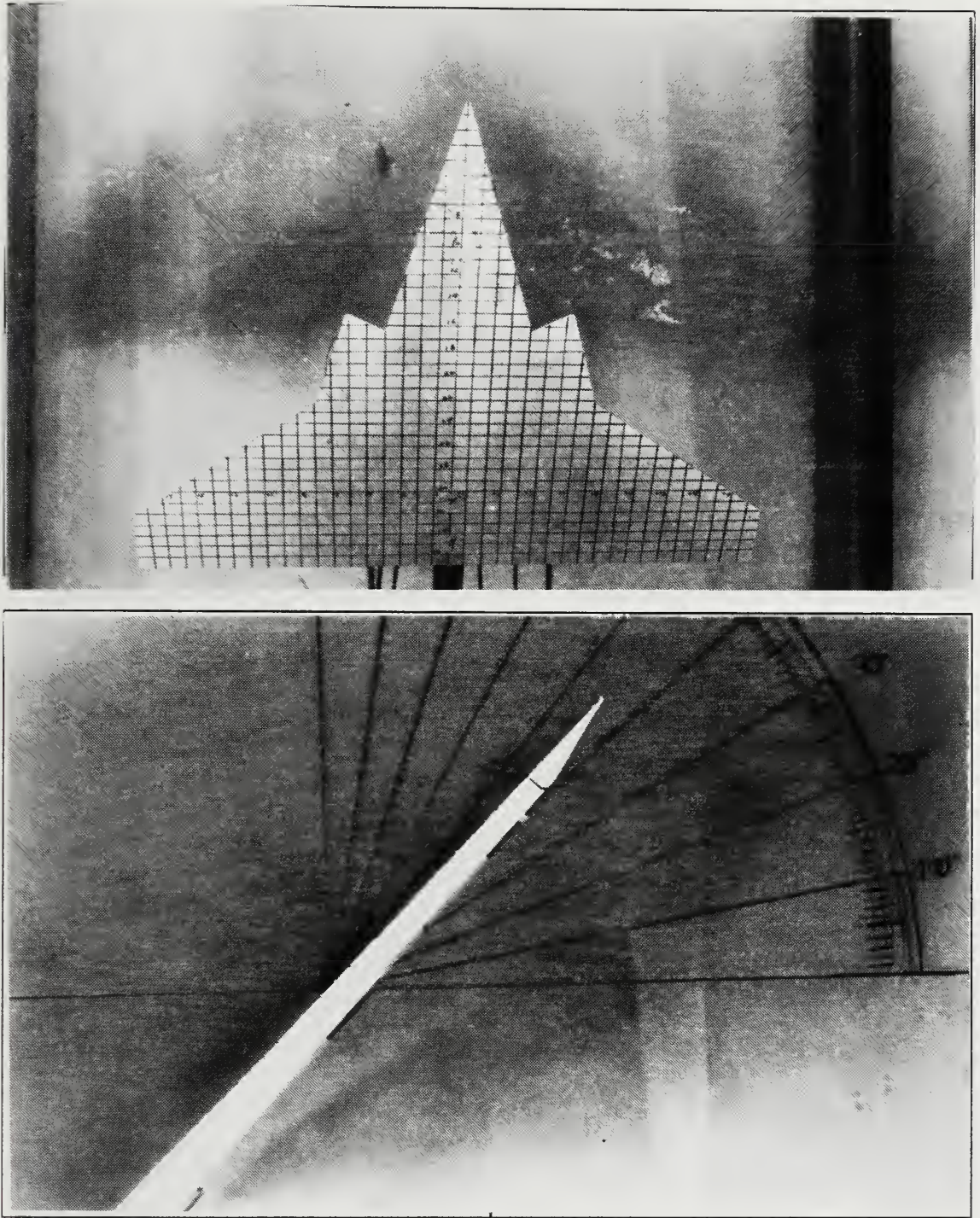
Figure 30. Strake Vortex Flow, Modified Model,
k=0, α=45°
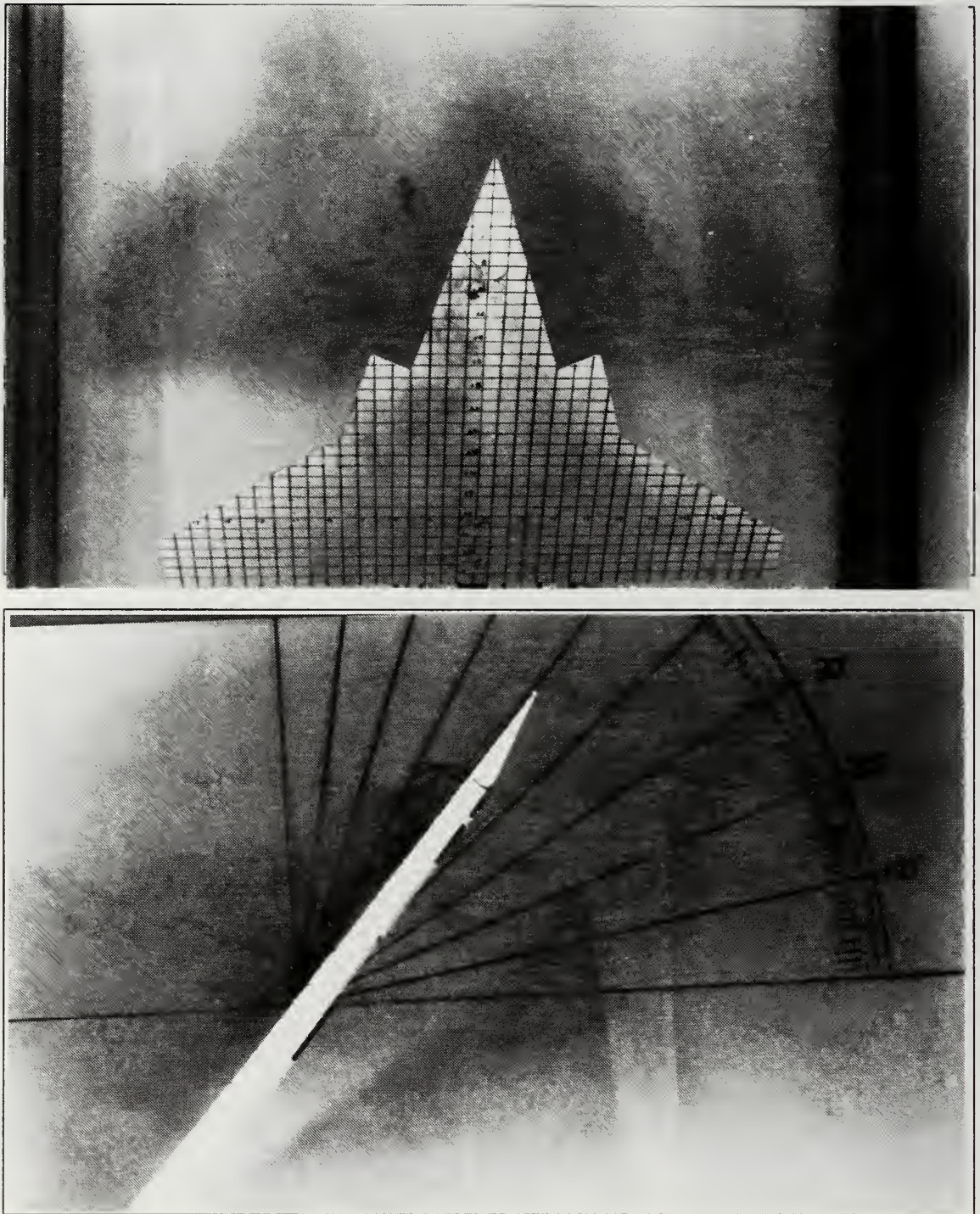
Figure 31. Strake Vortex Flow, Modified Model,
k=0, α=50°
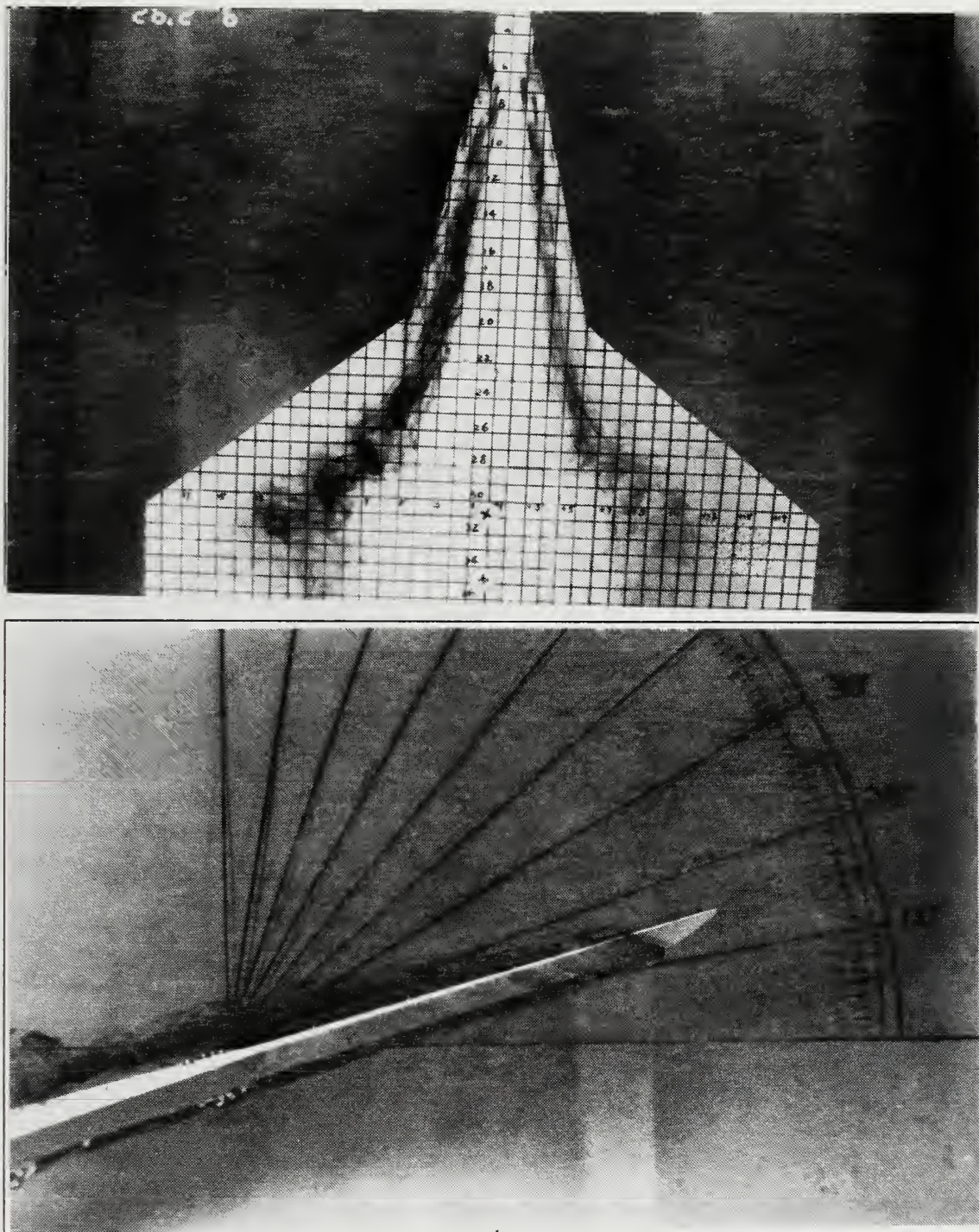
Figure 32. Strake Vortex Flow, Baseline Model,
k=0.06, α=15°
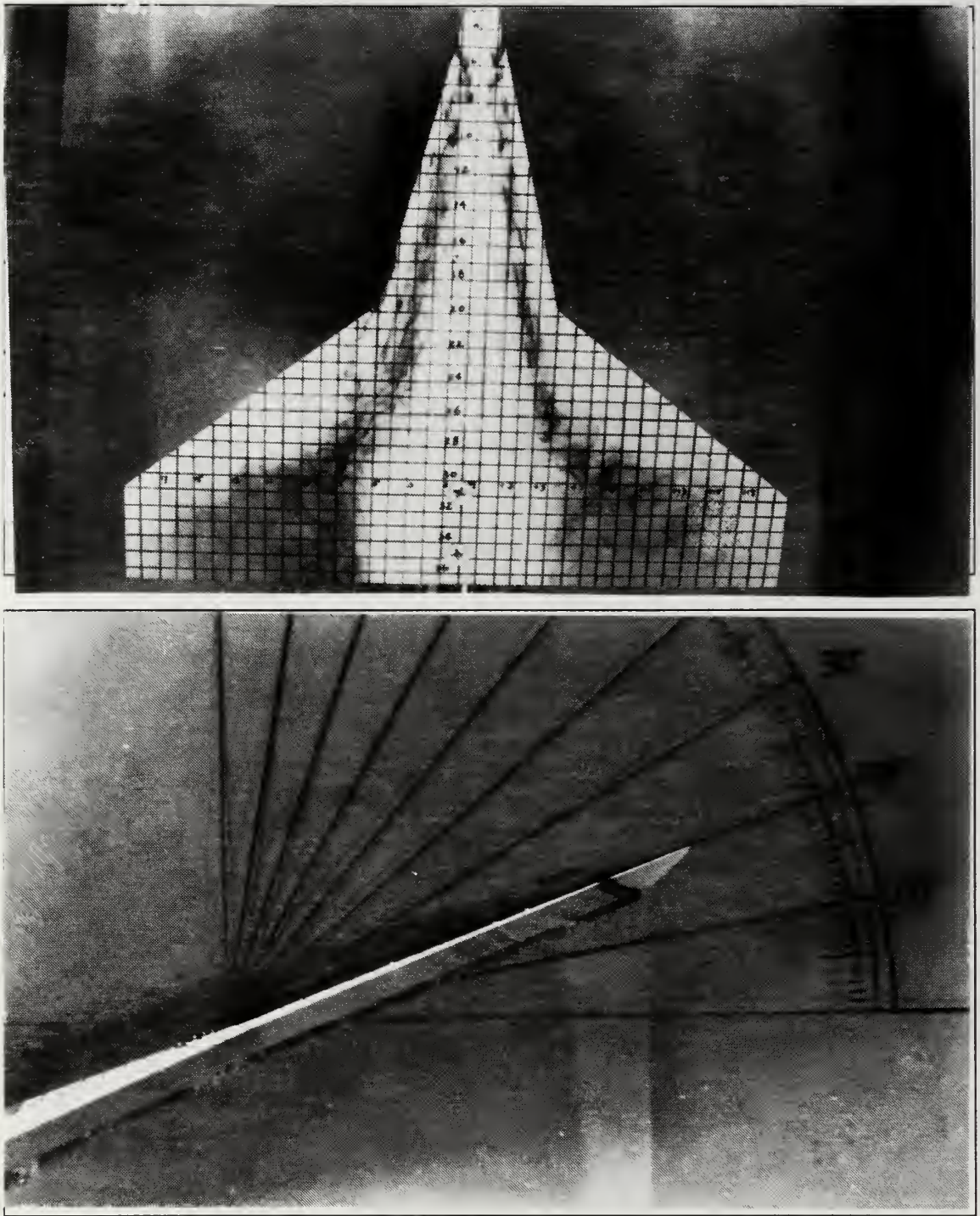
Figure 33. Strake Vortex Flow, Baseline Model,
k=0.06, $\alpha=20°$
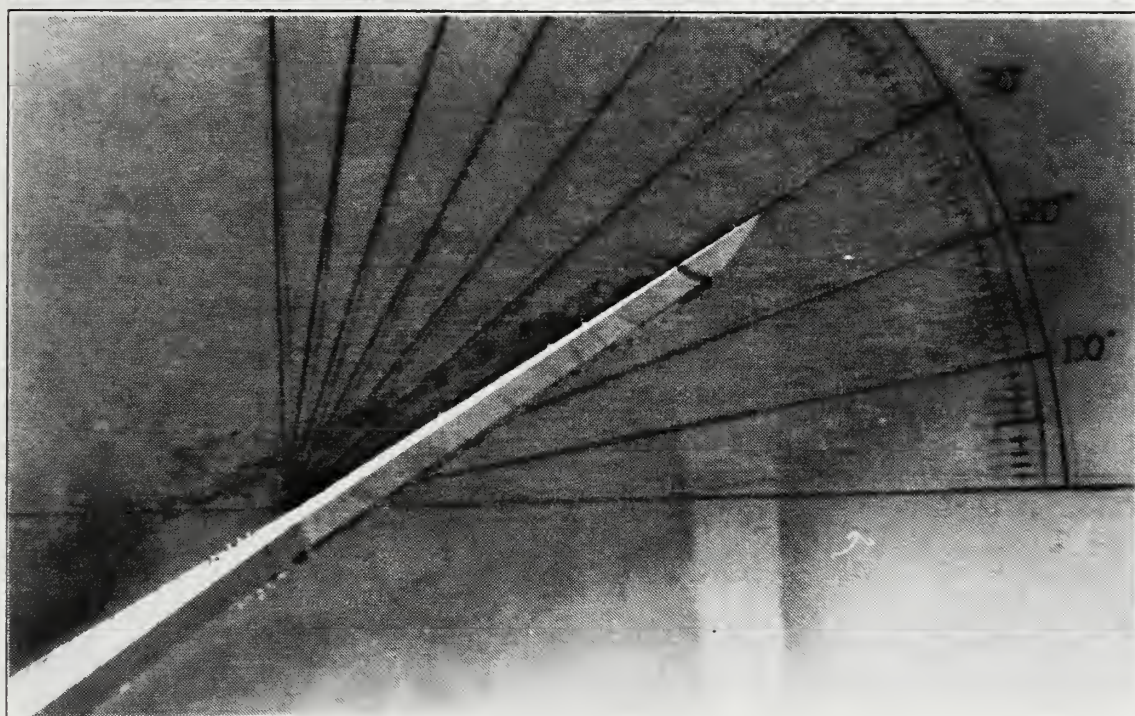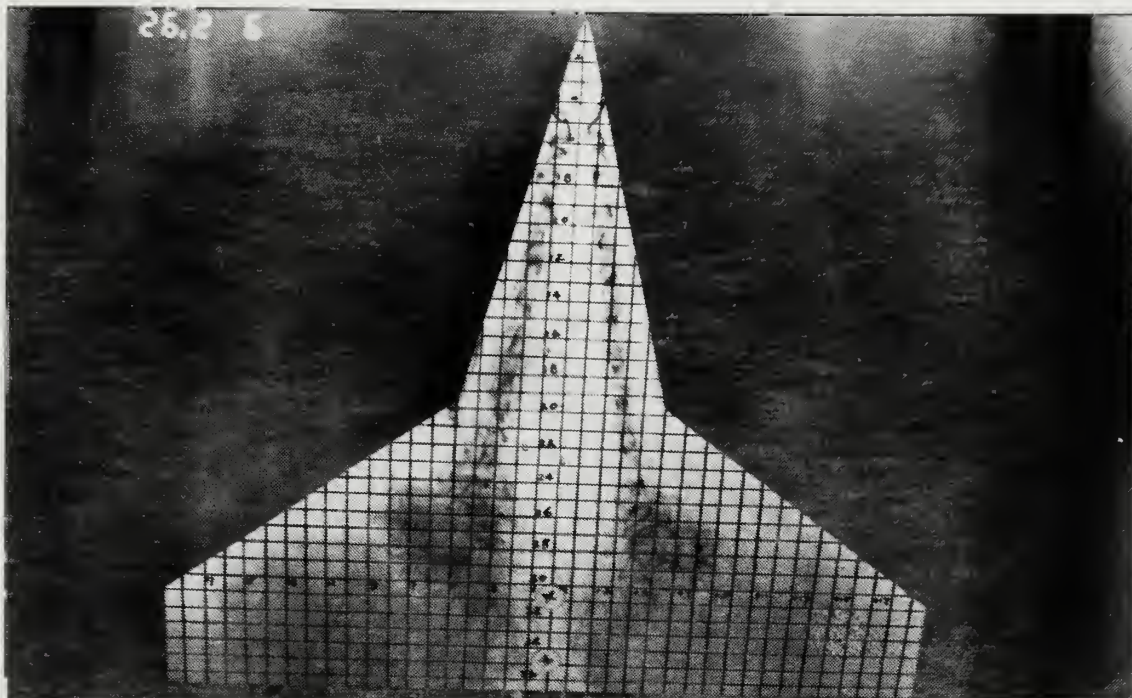
Figure 34. Strake Vortex Flow, Baseline Model,
k=0.06, α=30°
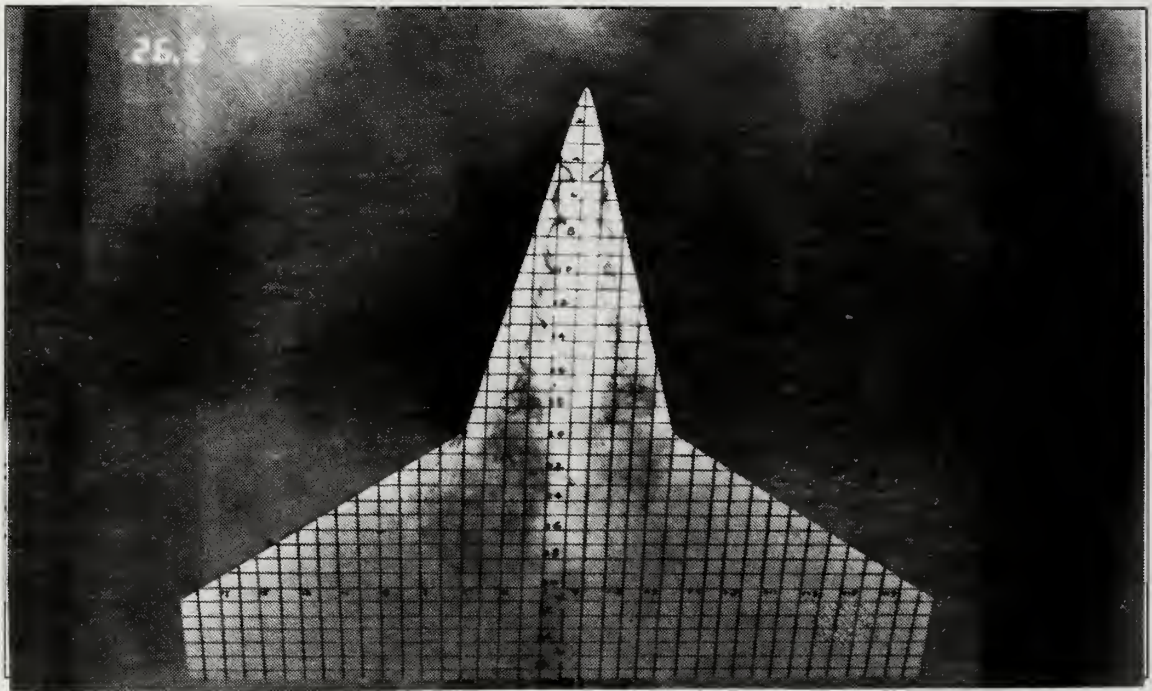
Figure 35. Strake Vortex Flow, Baseline Model, k=0.06, α=40°
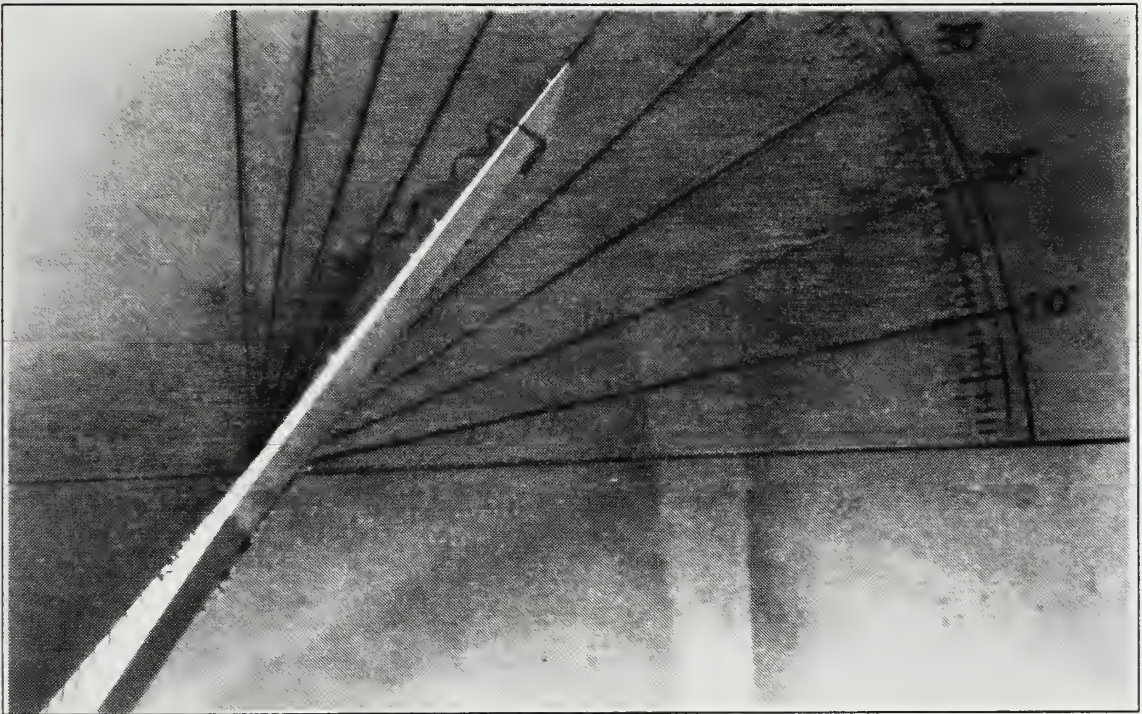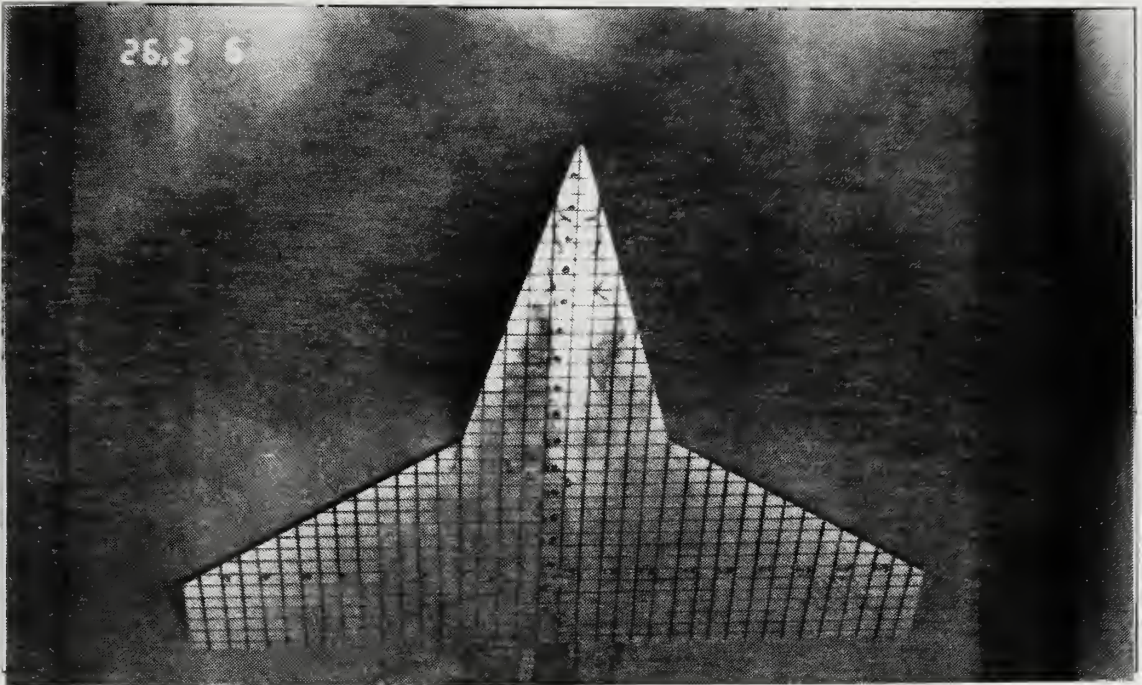
Figure 36. Strake Vortex Flow, Baseline Model,
k=0.06, α=50°

61

Figure 37. Strake Vortex Flow, Baseline Model,
k=-0.06, α=39°
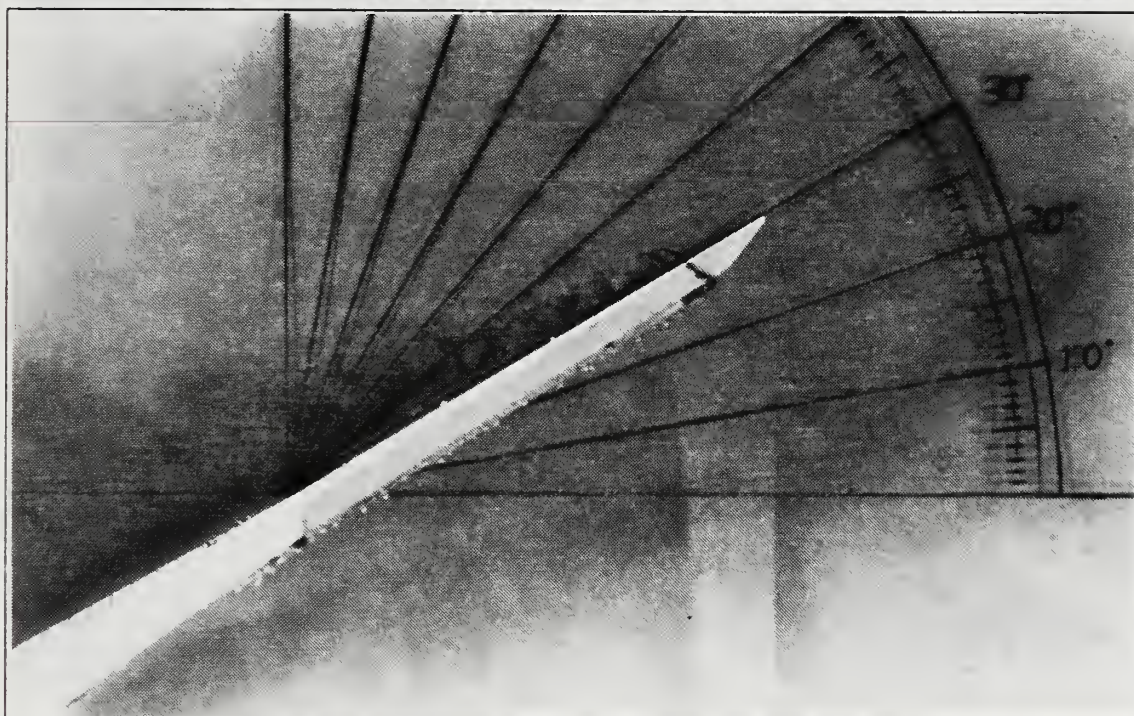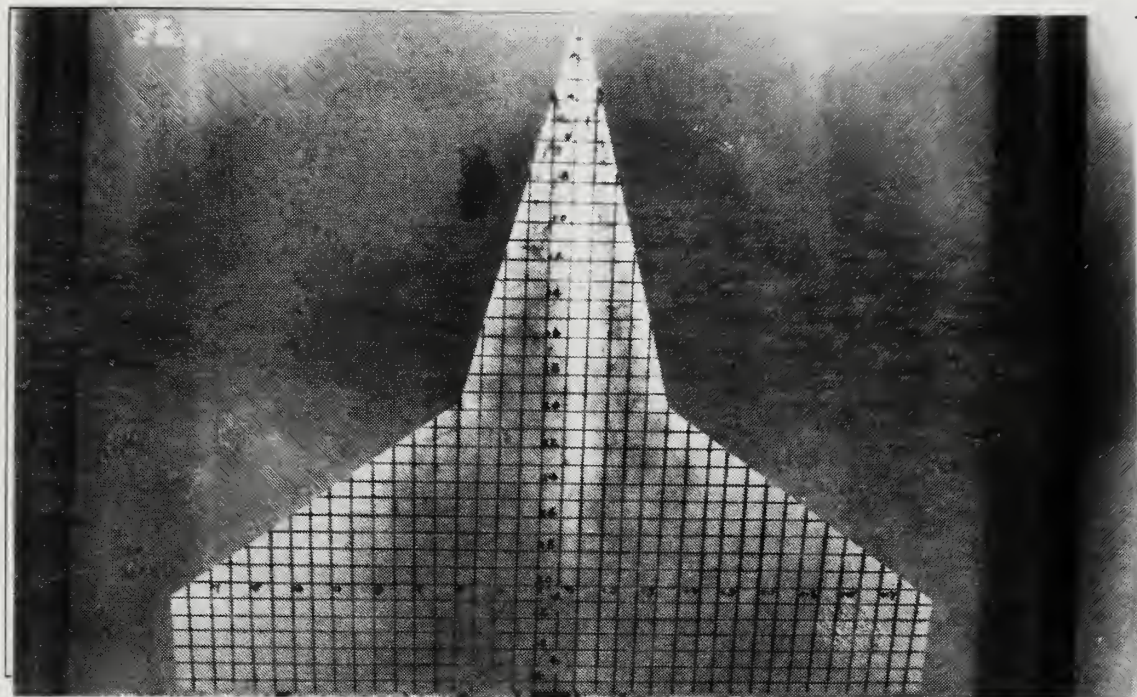
Figure 38. Strake Vortex Flow, Baseline Model, k=-0.06, α=30°
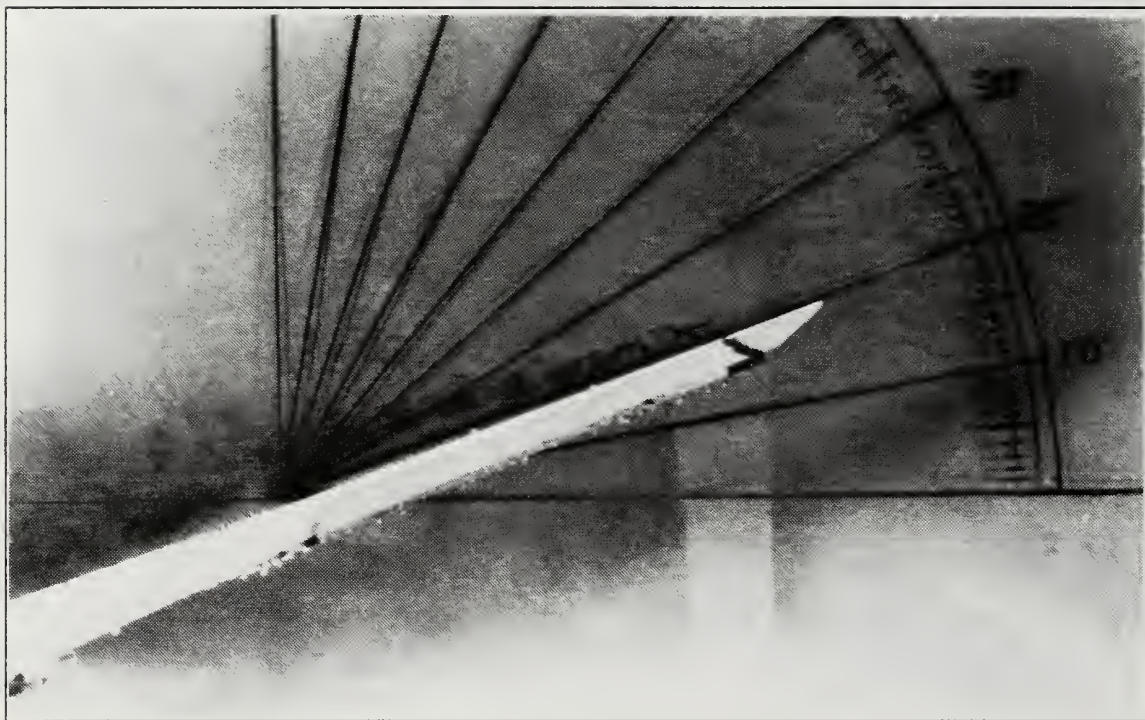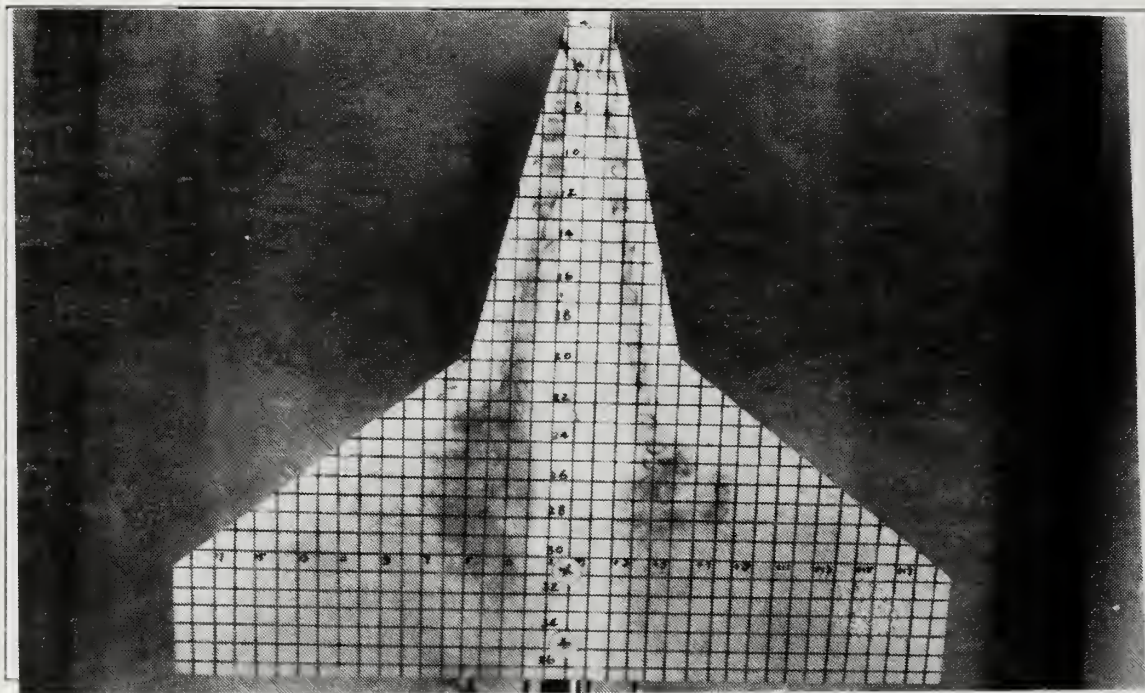
Figure 39. Strake Vortex Flow, Baseline Model,
k=-0.06, α=19°
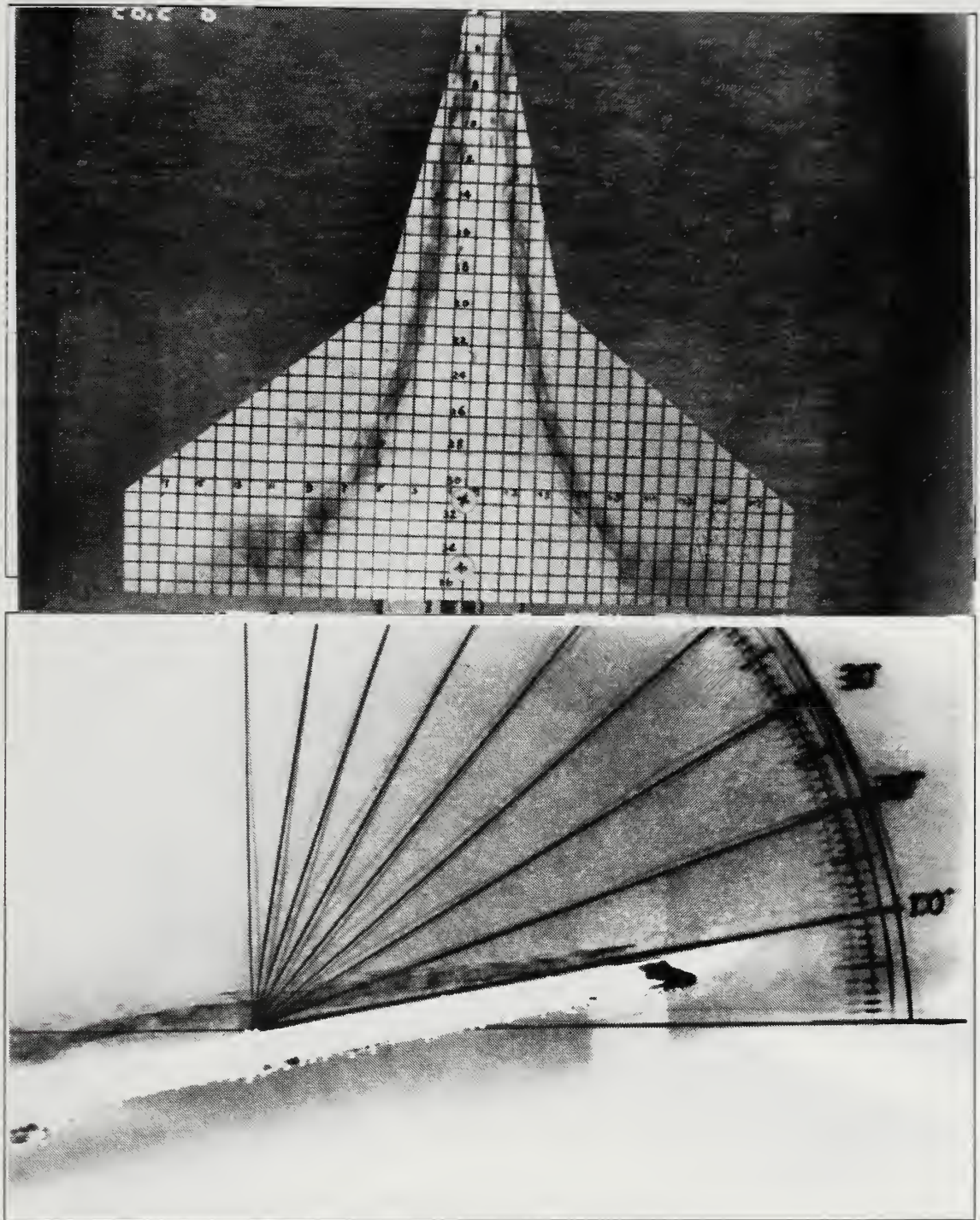
Figure 40. Strake Vortex Flow, Baseline Model,
k=-0.06, α=9°
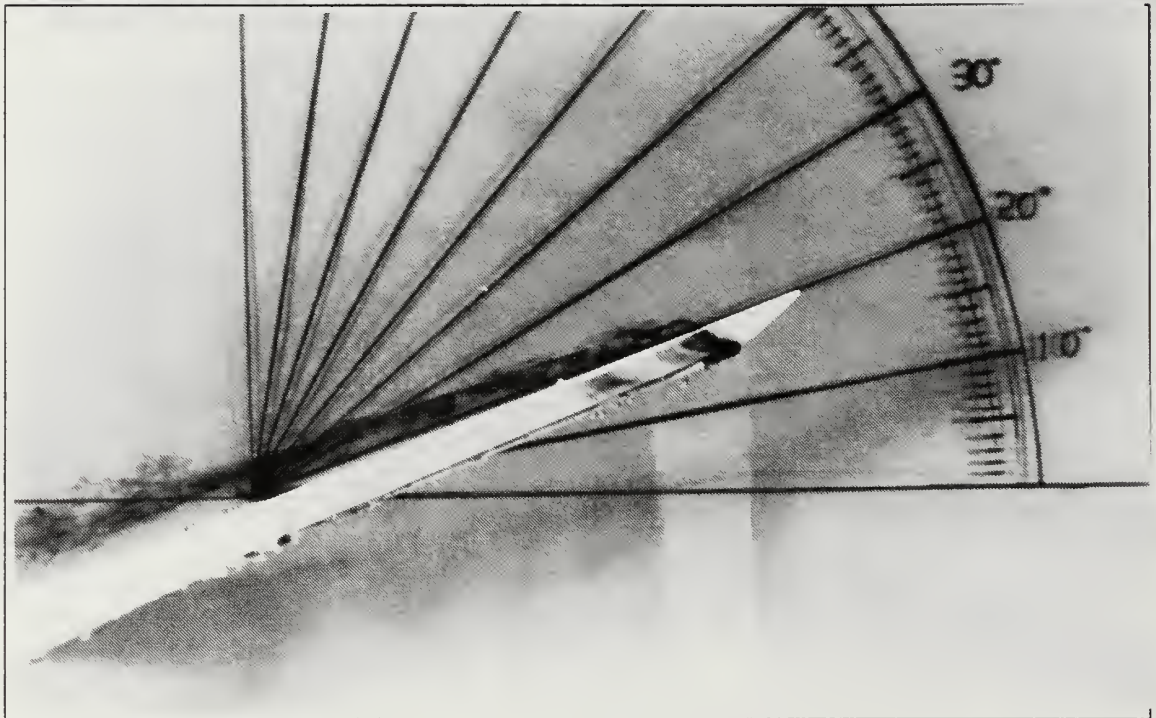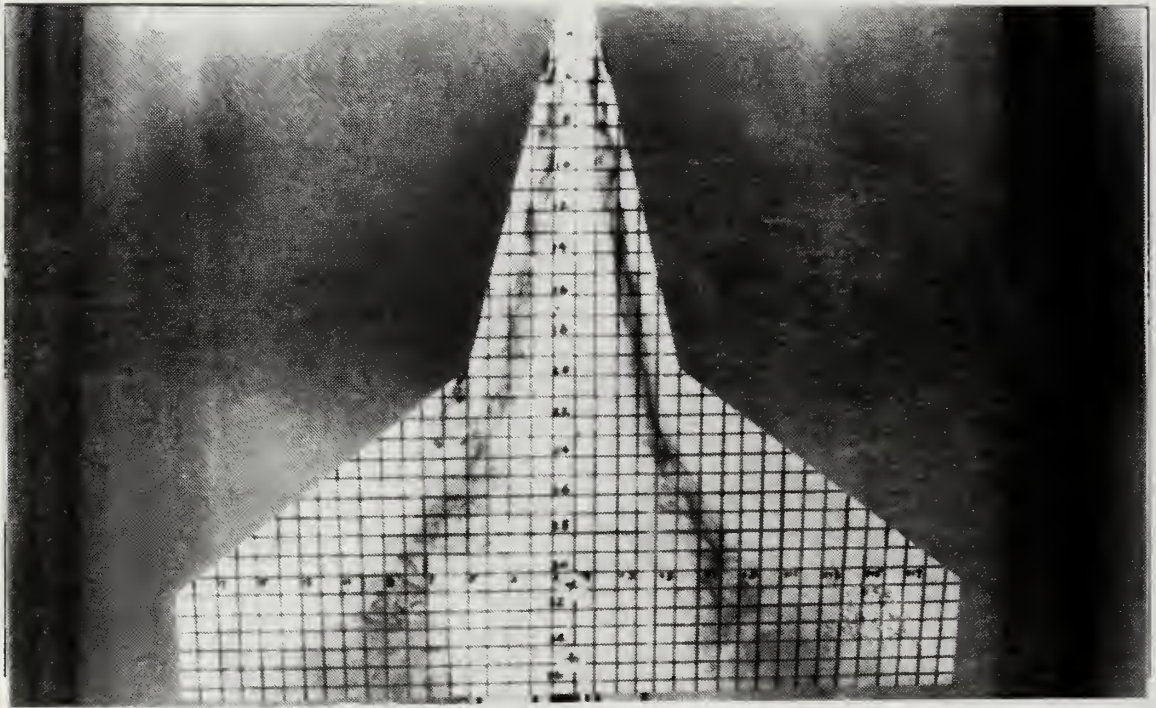
Figure 41. Strake Vortex Flow, Baseline Model,
k=0.13, α=20°
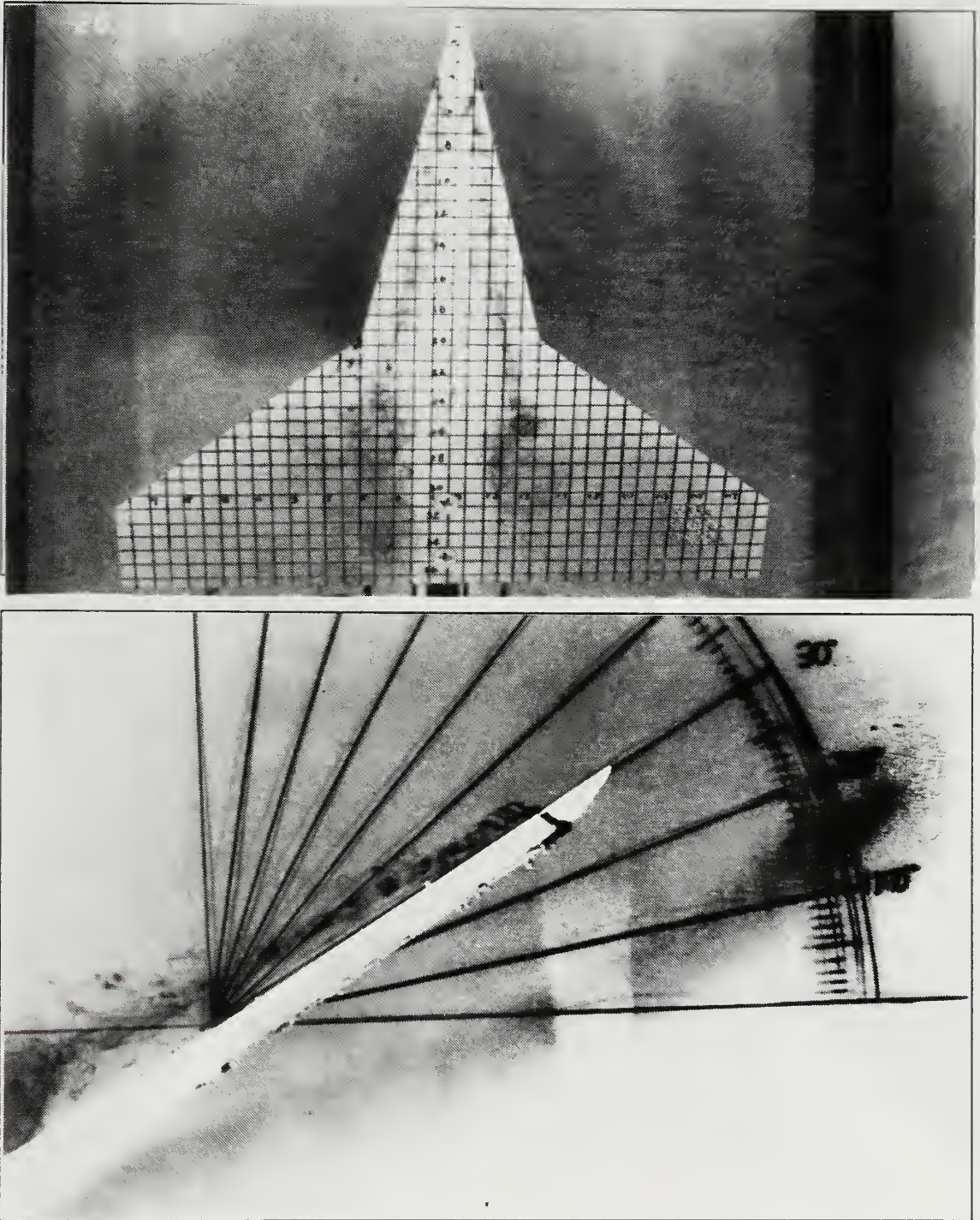
Figure 42. Strake Vortex Flow, Baseline Model,
k=0.13, α=30°
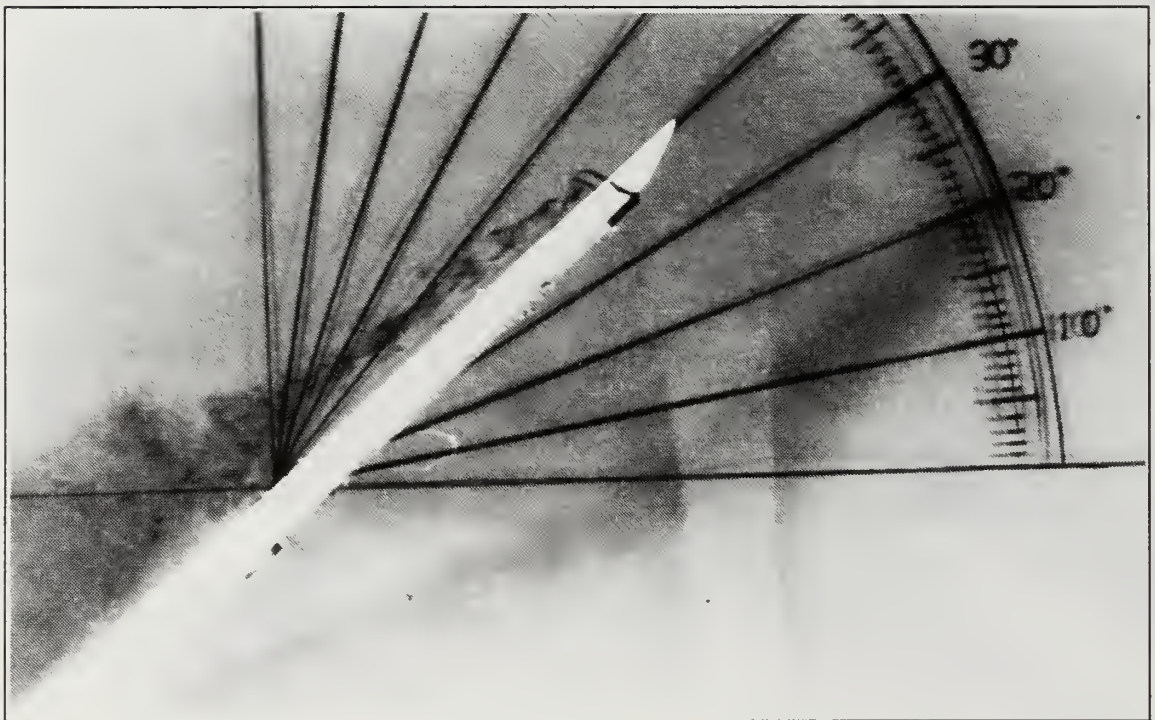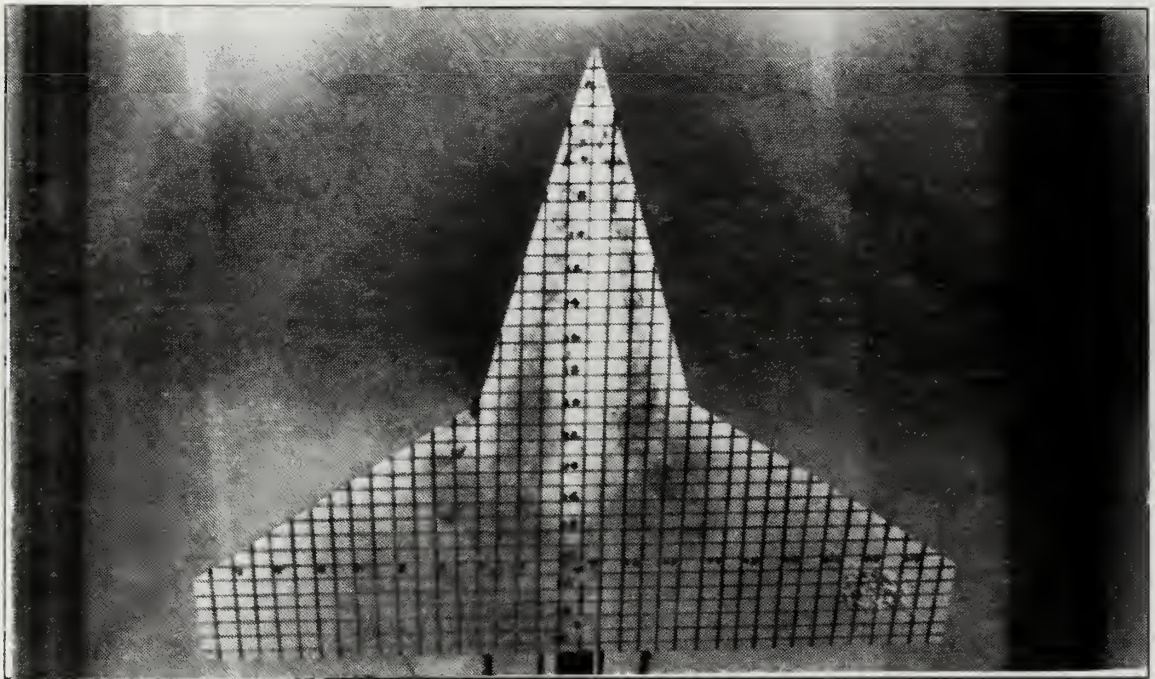
Figure 43. Strake Vortex Flow, Baseline Model,
k=0.13, α=40°
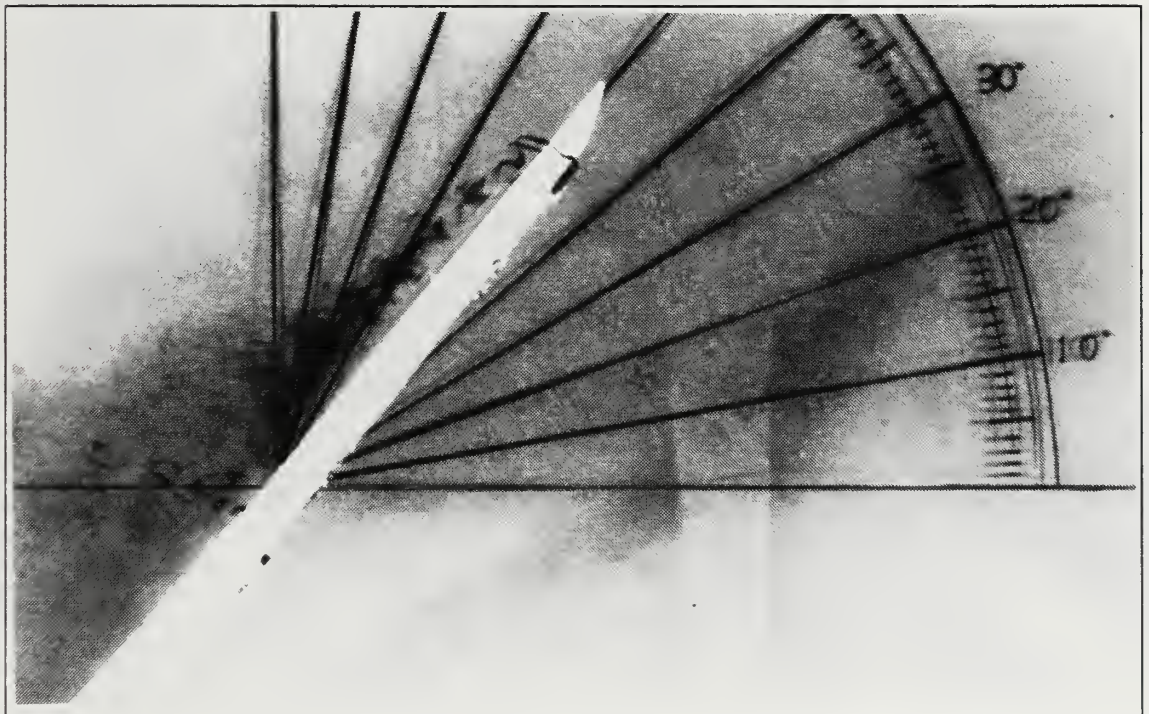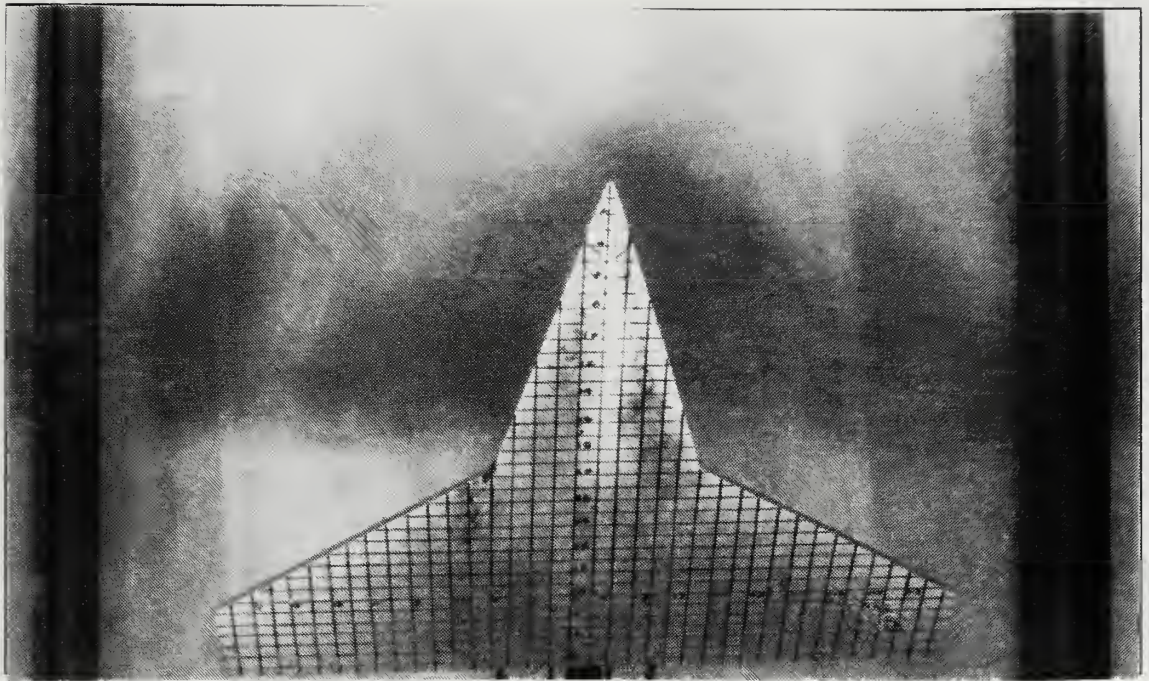
Figure 44. Strake Vortex Flow, Baseline Model,
k=0.13, $\alpha=50°$
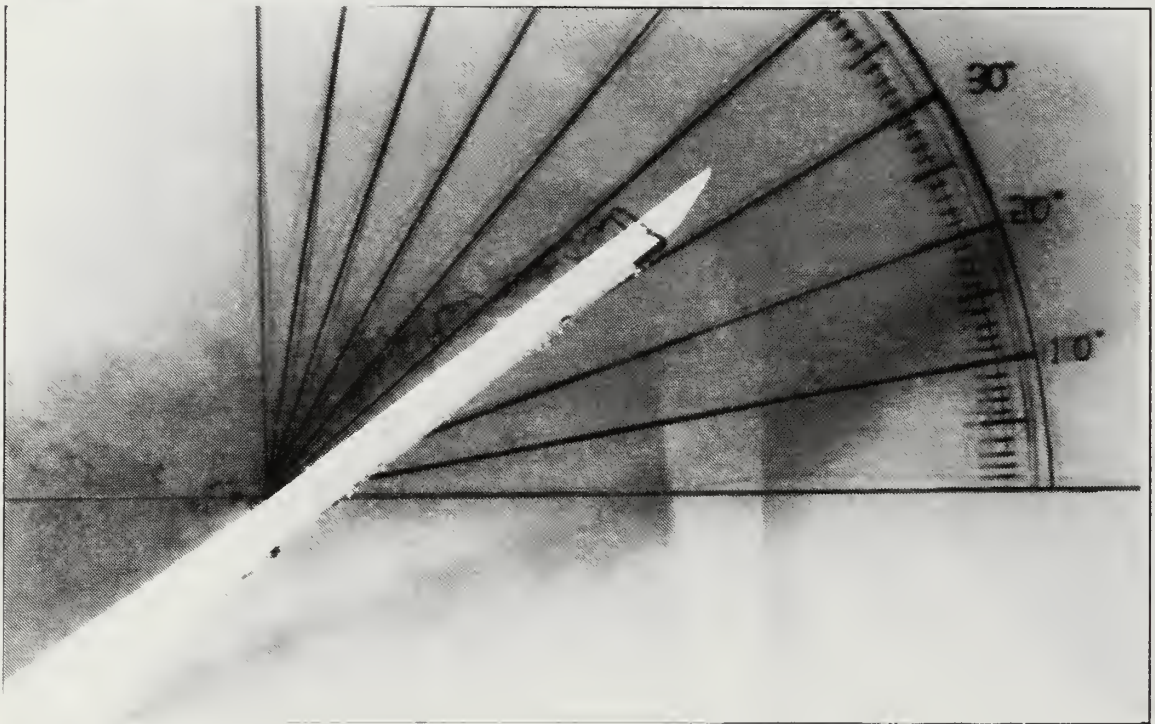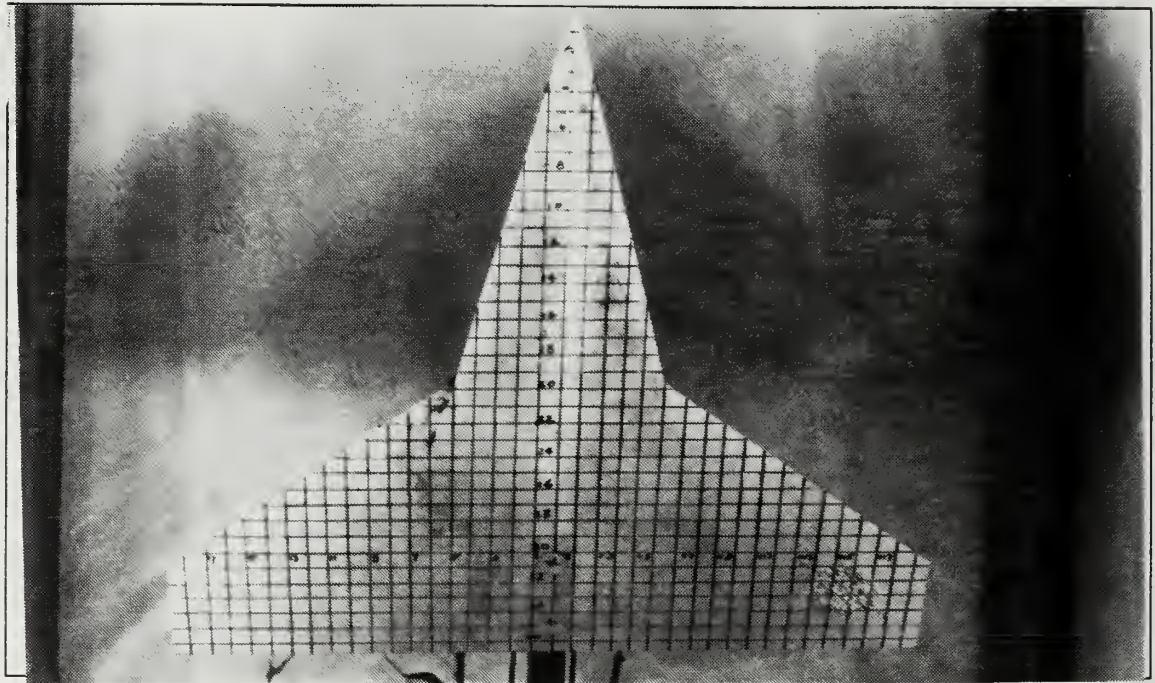
Figure 45. Strake Vortex Flow, Baseline Model,
k=-0.13, α=35°
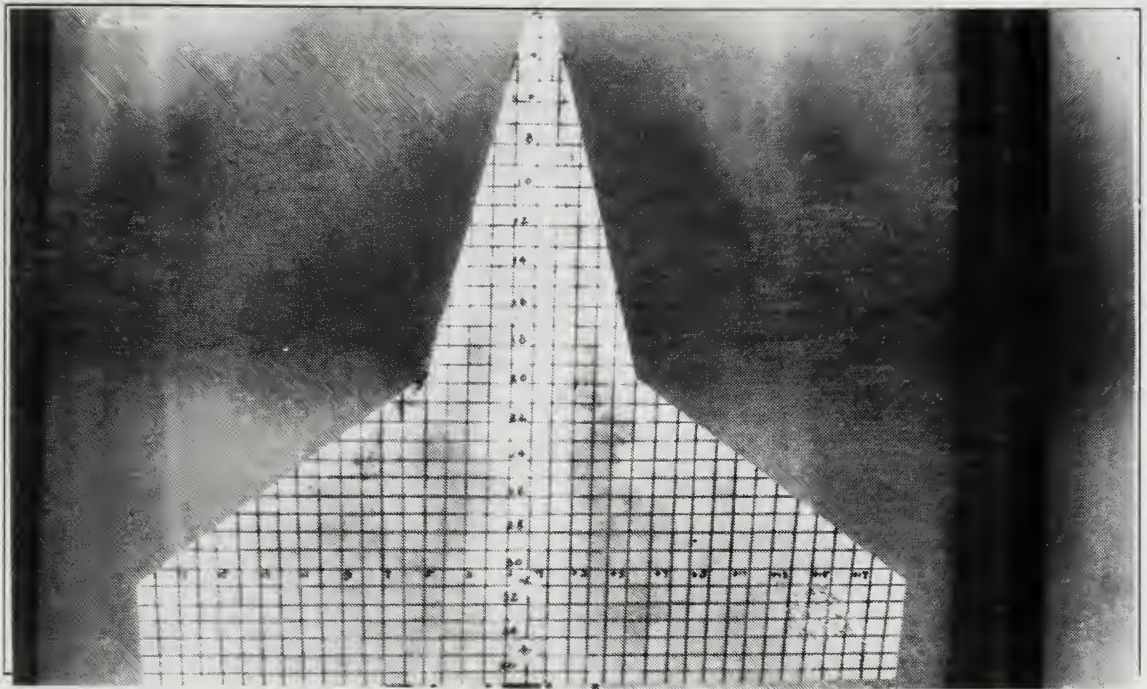
Figure 46. Strake Vortex Flow, Baseline Model,
k=-0.13, α=25°

71
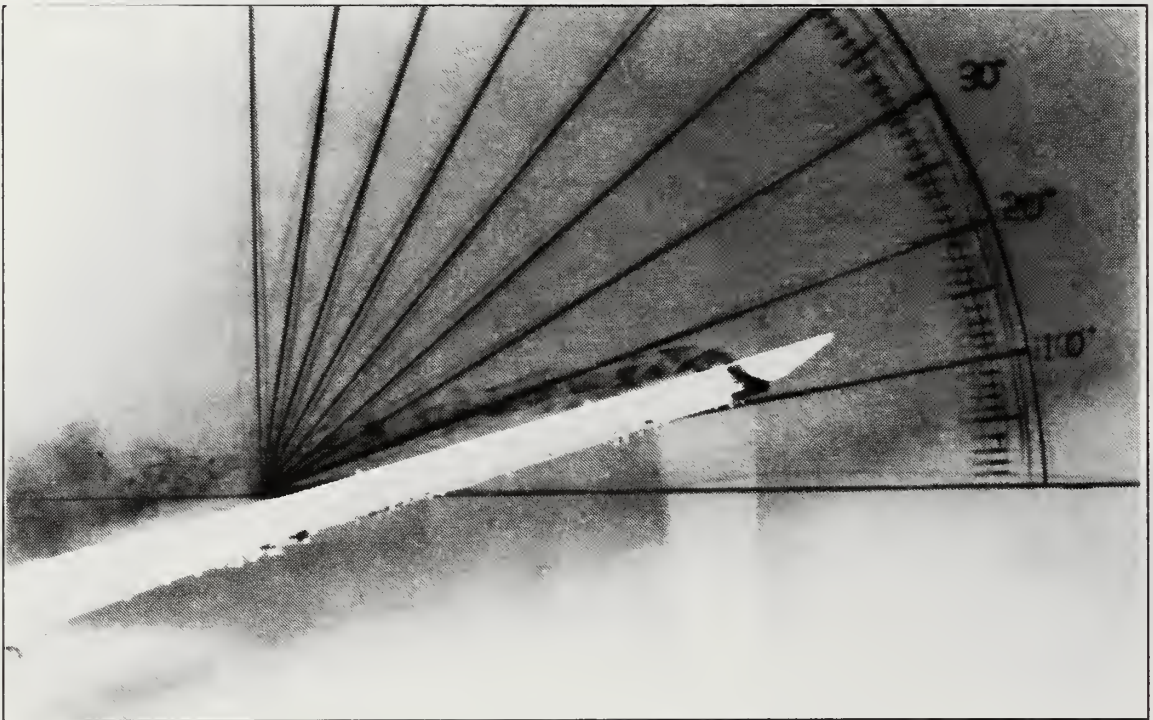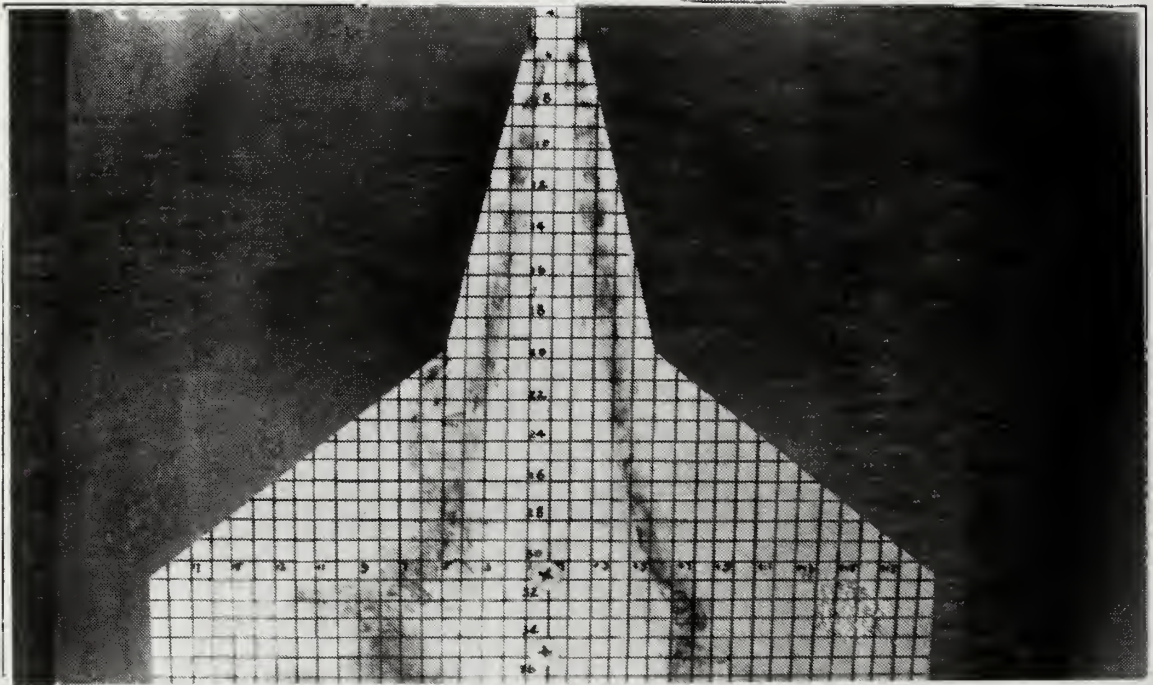
Figure 47. Strake Vortex Flow, Baseline Model,
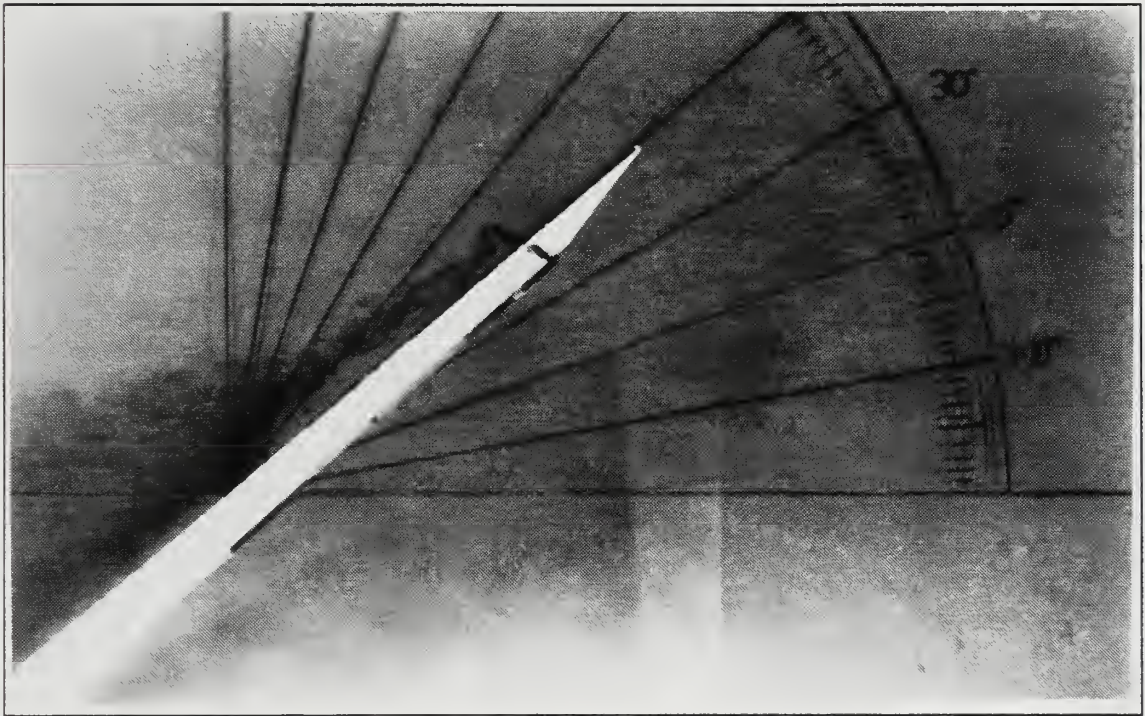k=-0.13, α=15°
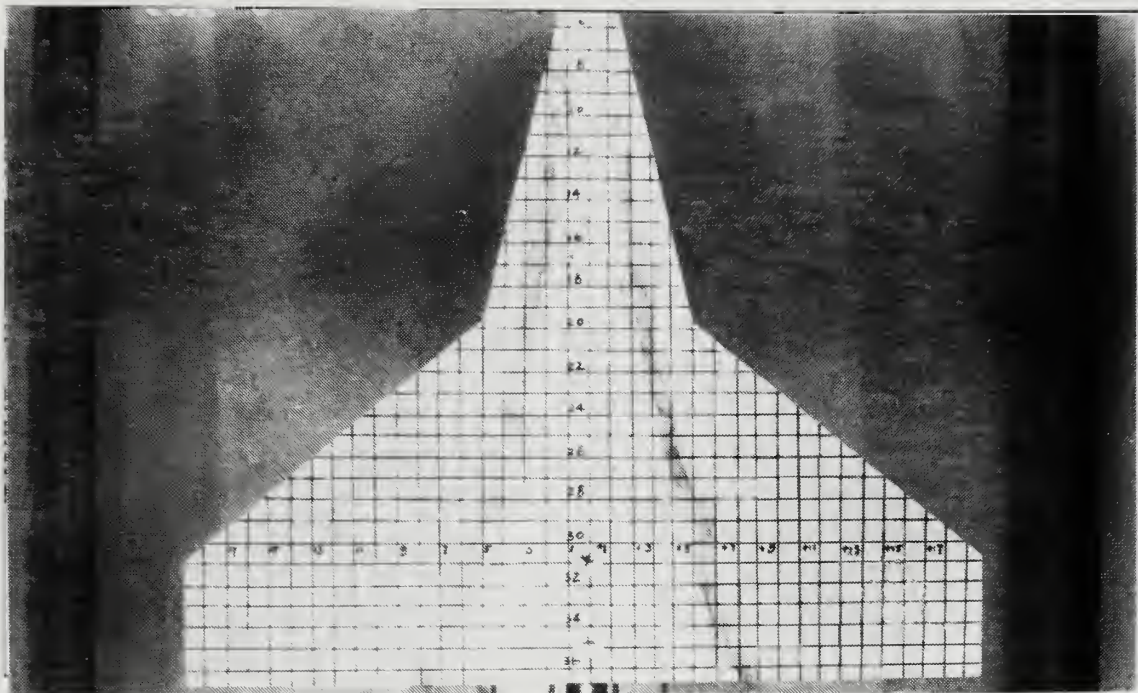
Figure 48. Strake Vortex Flow, Baseline Model,
k=-0.13, α=5°
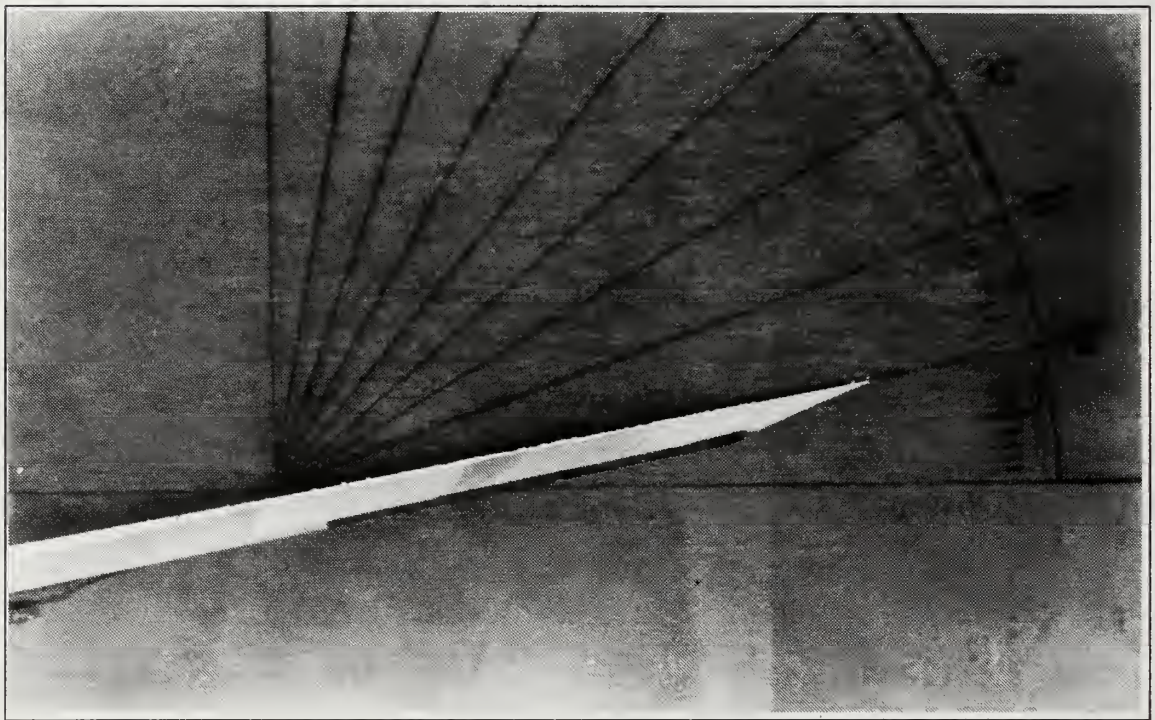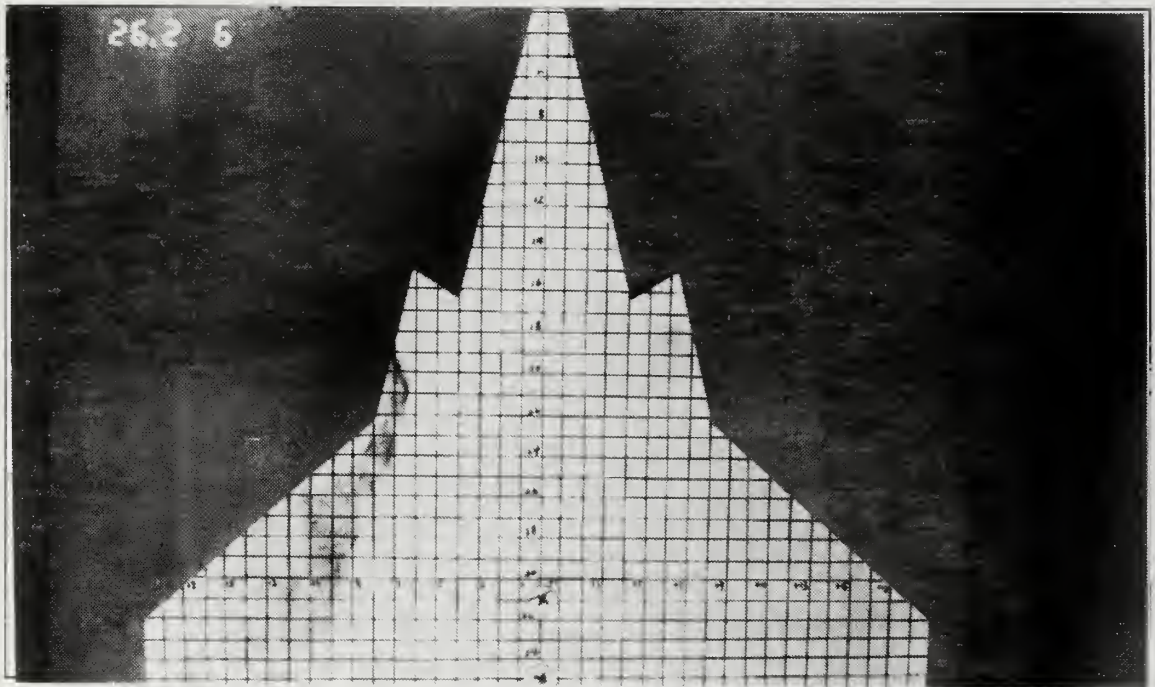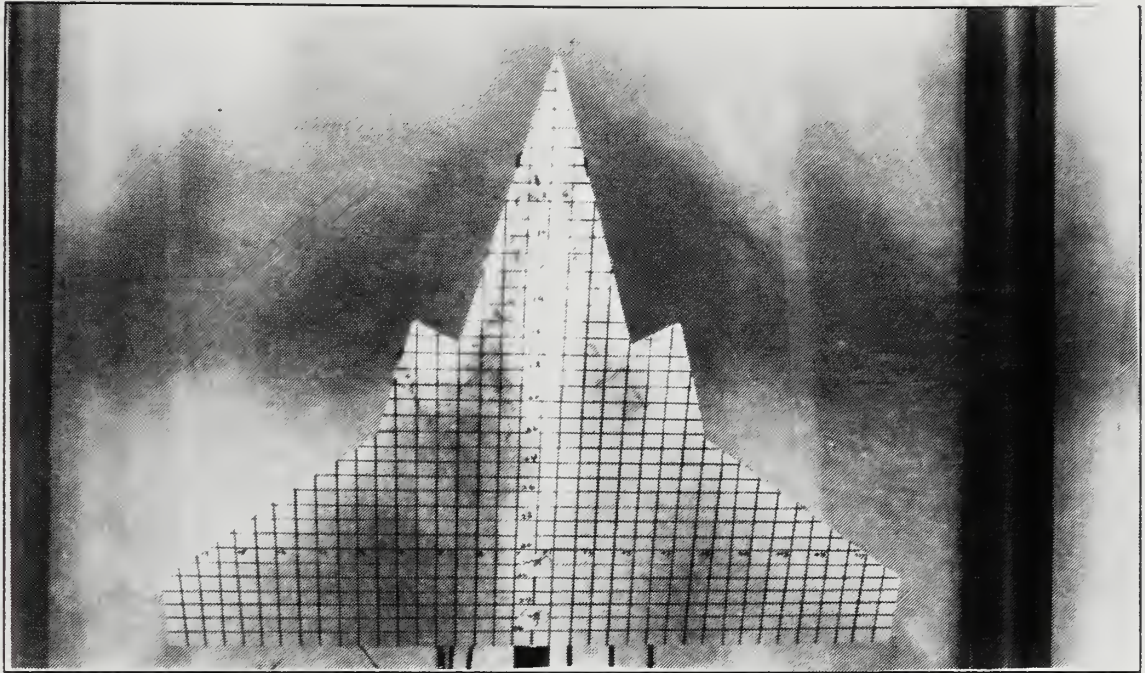
Figure 49. Strake Vortex Flow, Modified Model,
k=0.06, $\alpha=10°$
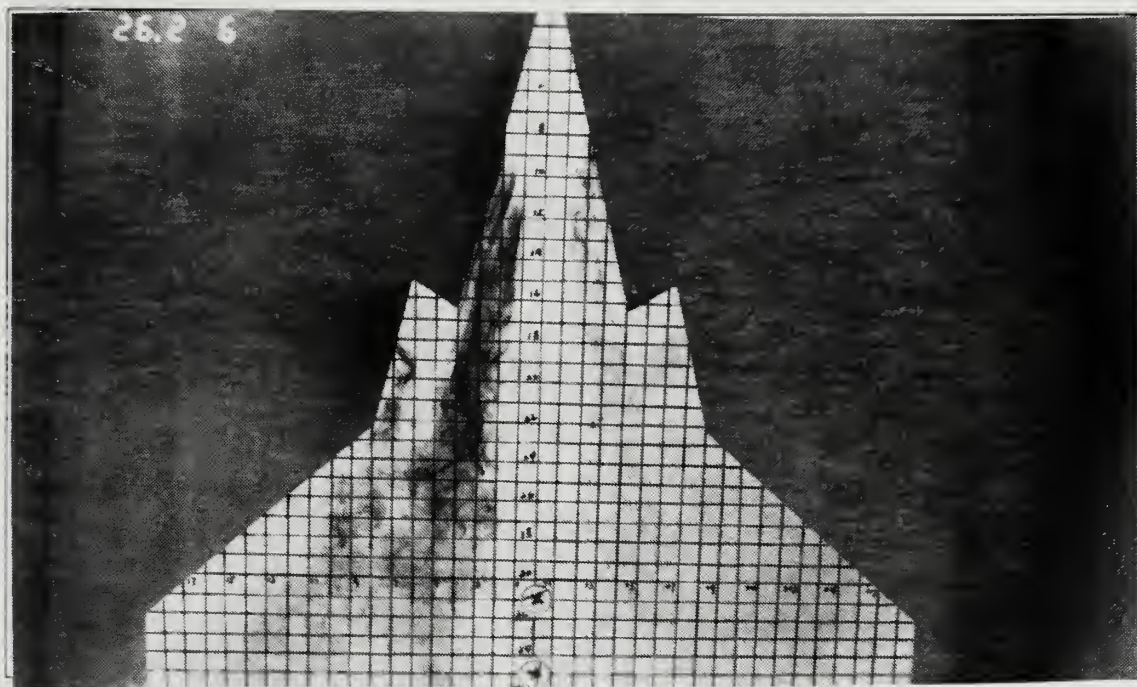
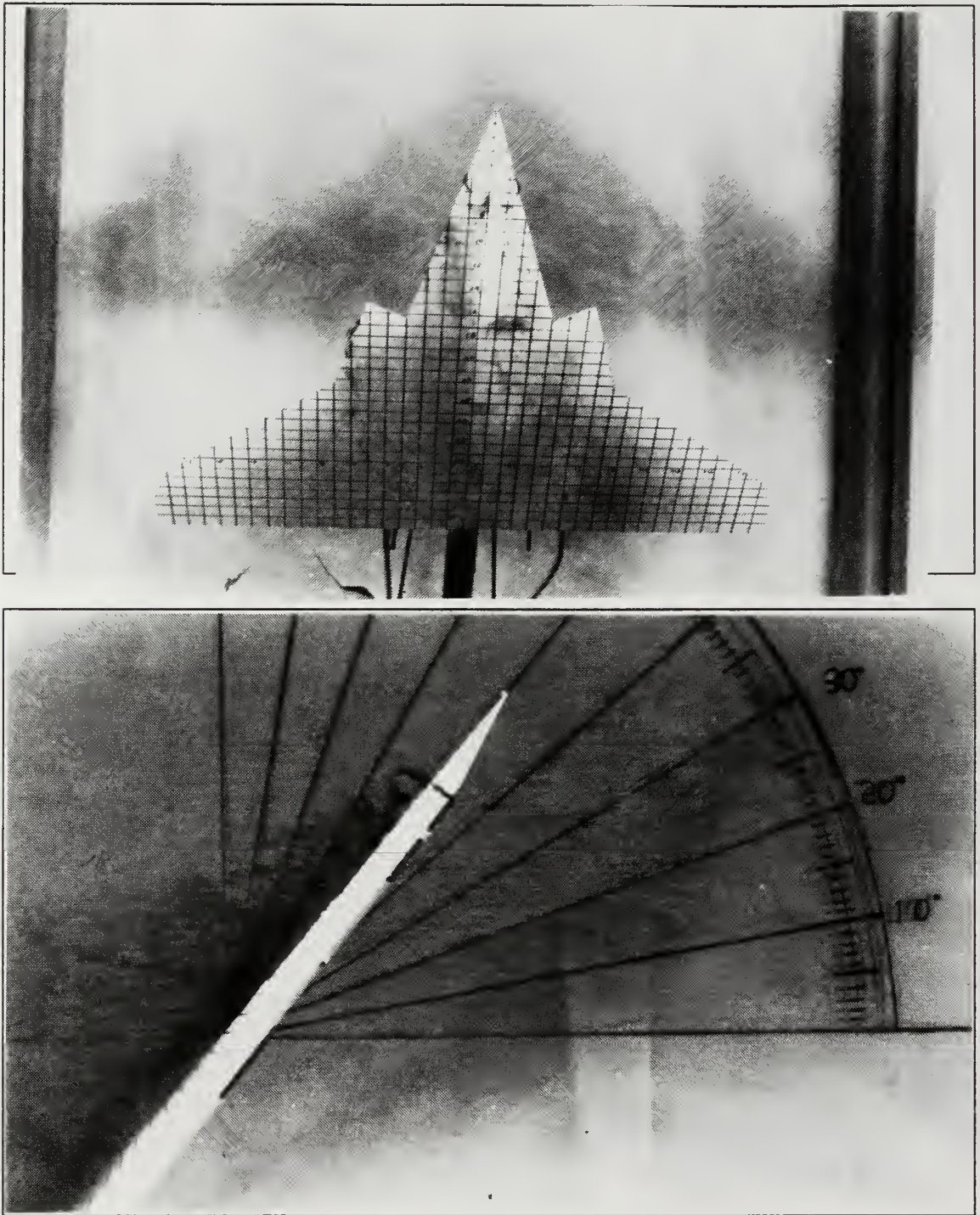Figure 50. Strake Vortex Flow, Modified Model, k=0.06, α=15°
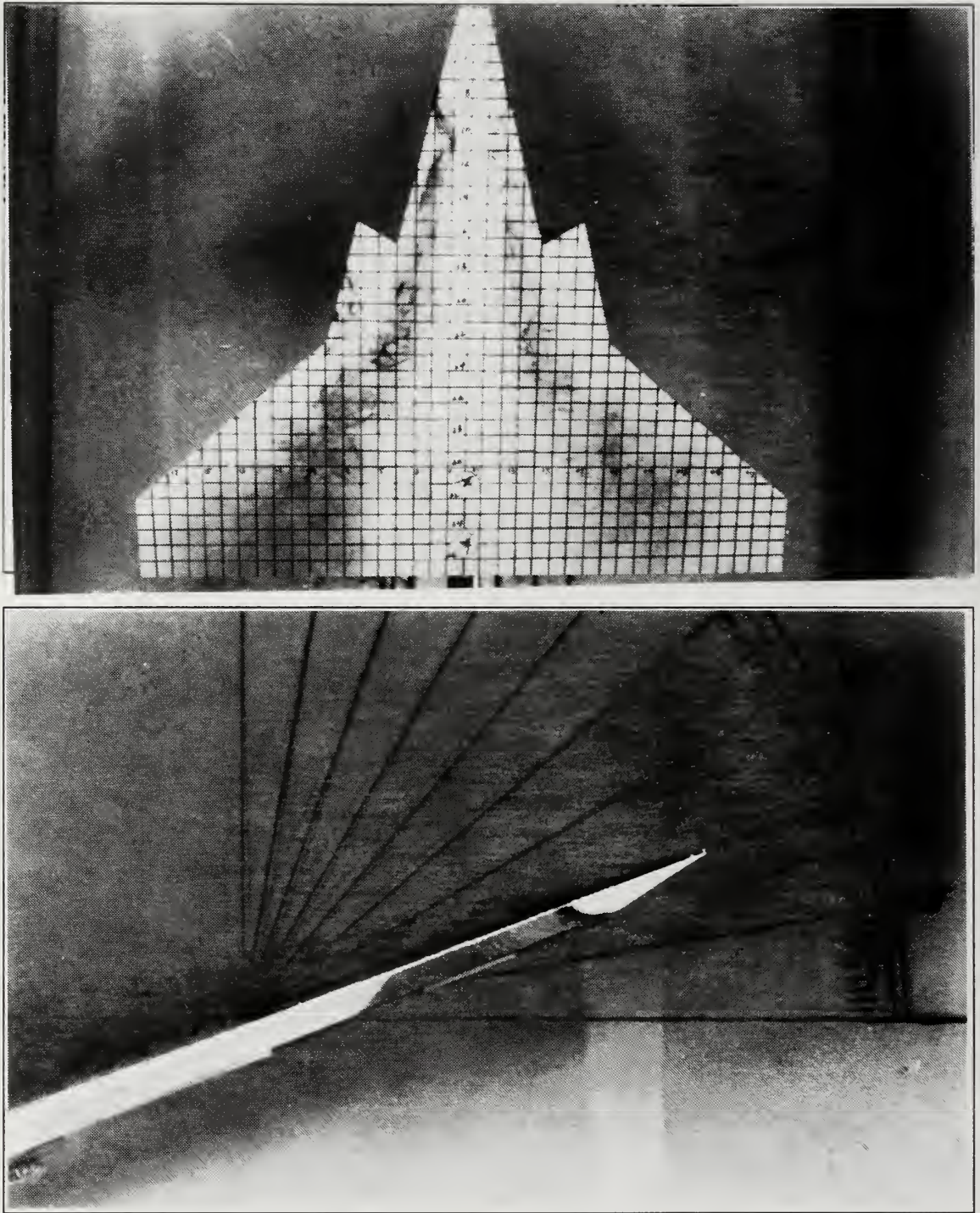
Figure 51. Strake Vortex Flow, Modified Model,
k=0.06, α=20°
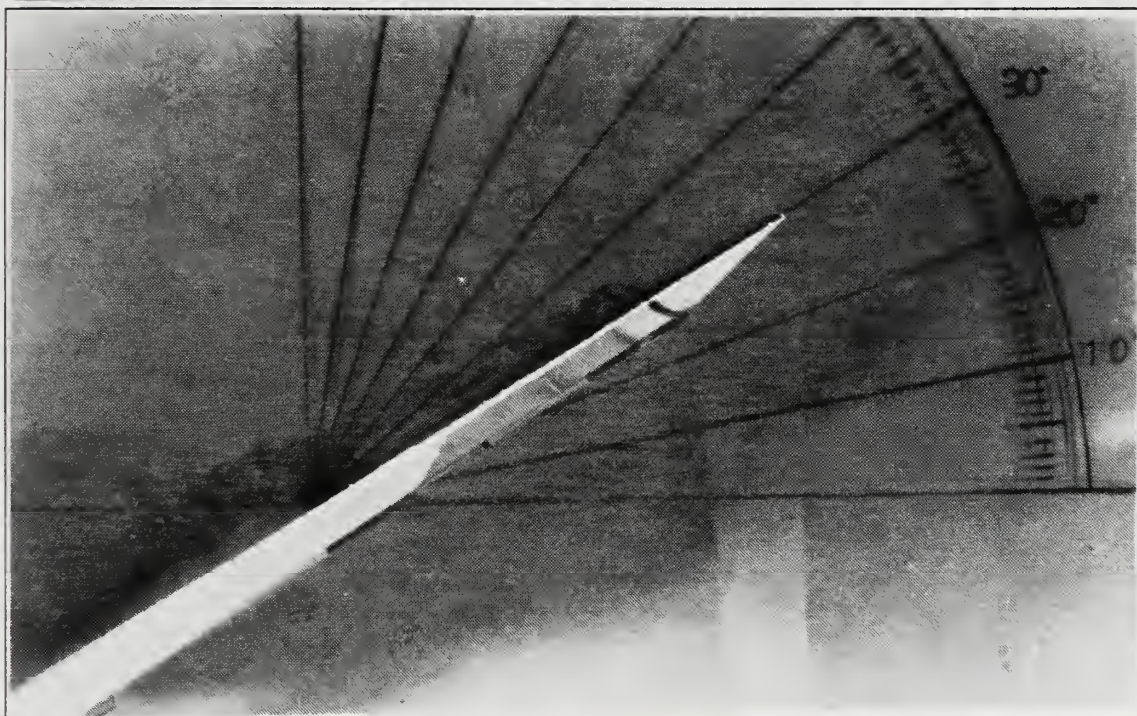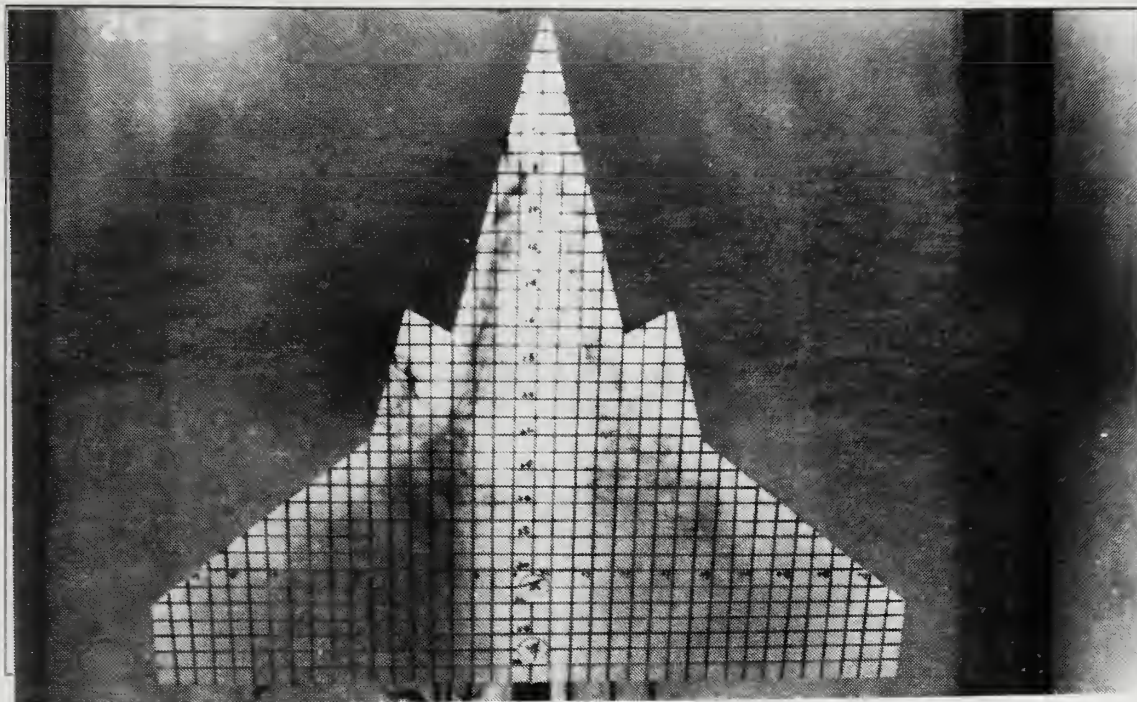
Figure 52. Strake Vortex Flow, Modified Model,
k=0.06, α=30°
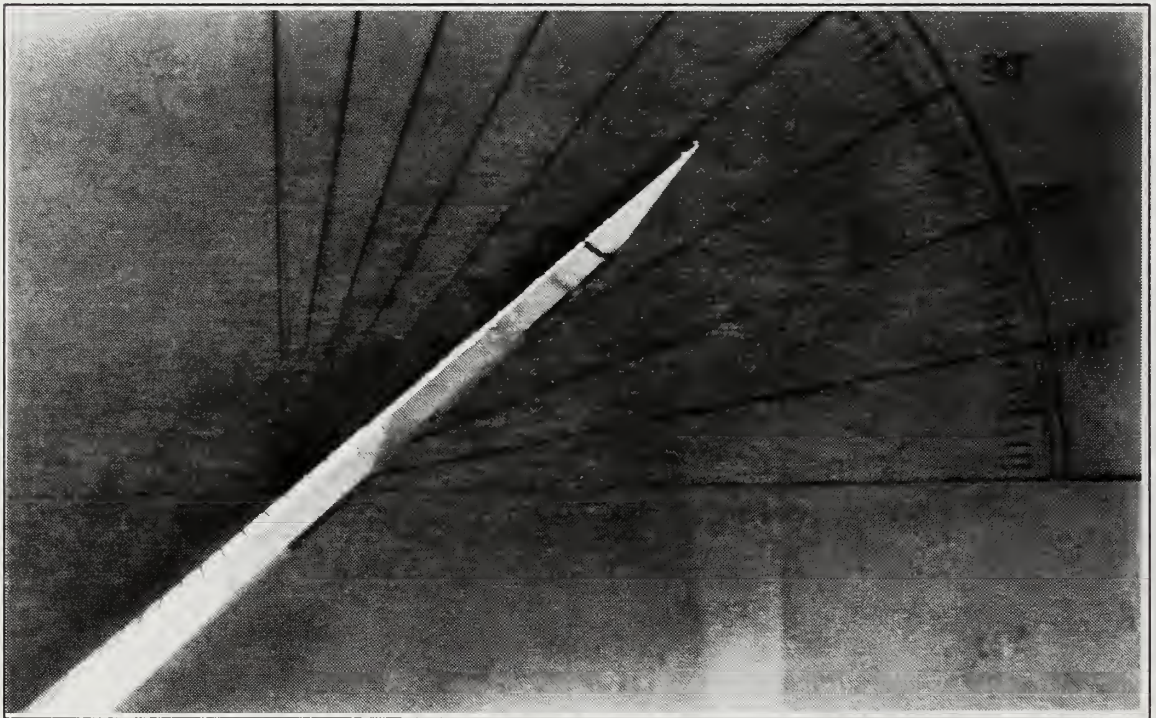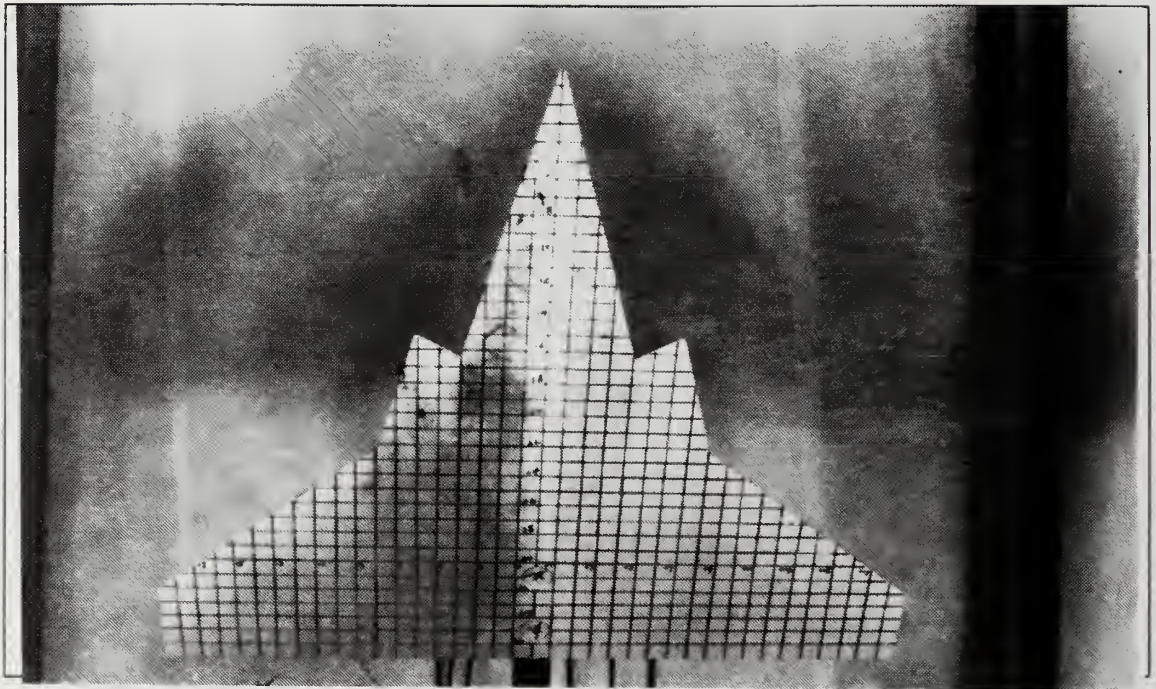
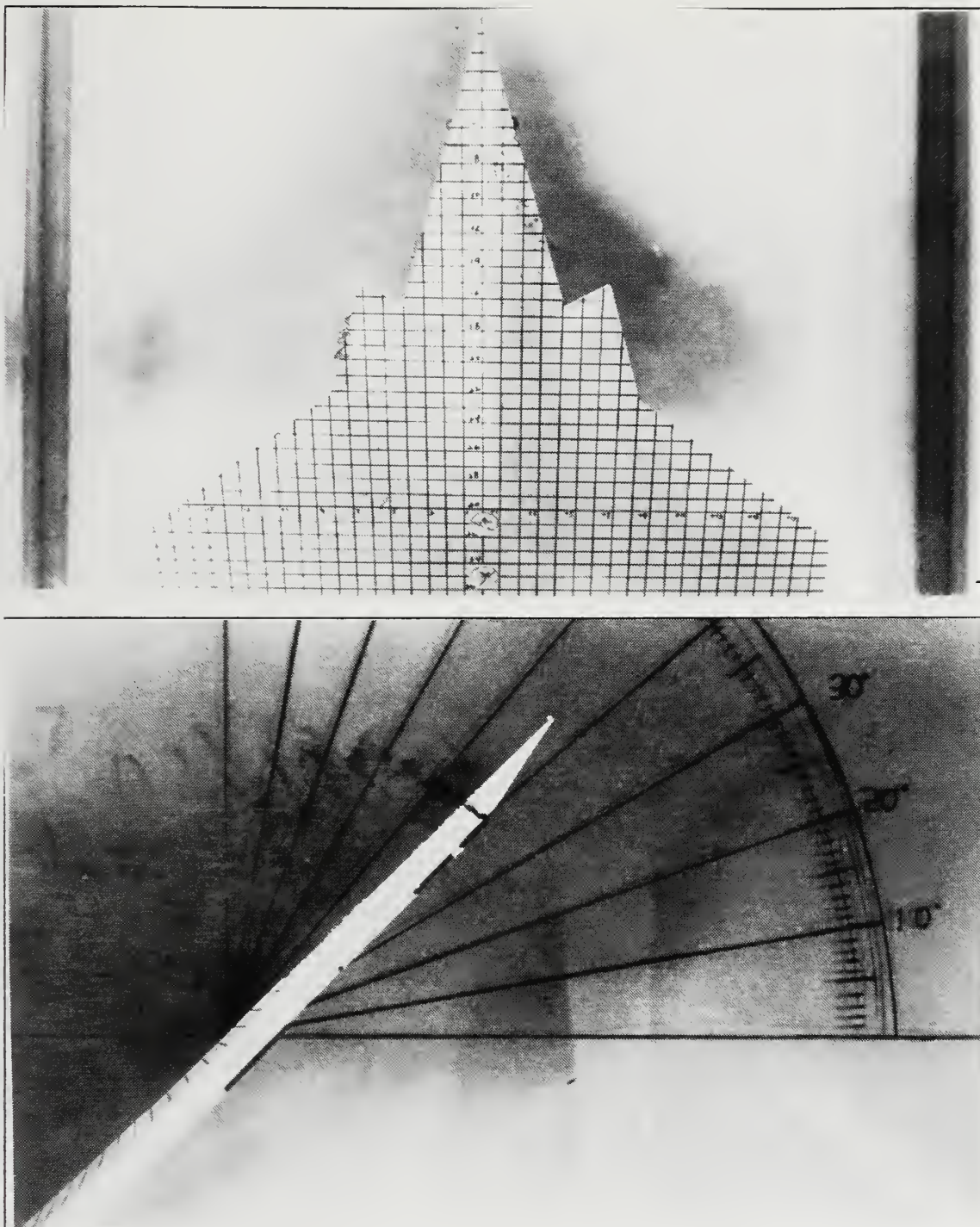Figure 53. Strake Vortex Flow, Modified Model,
k=0.06, α=39°
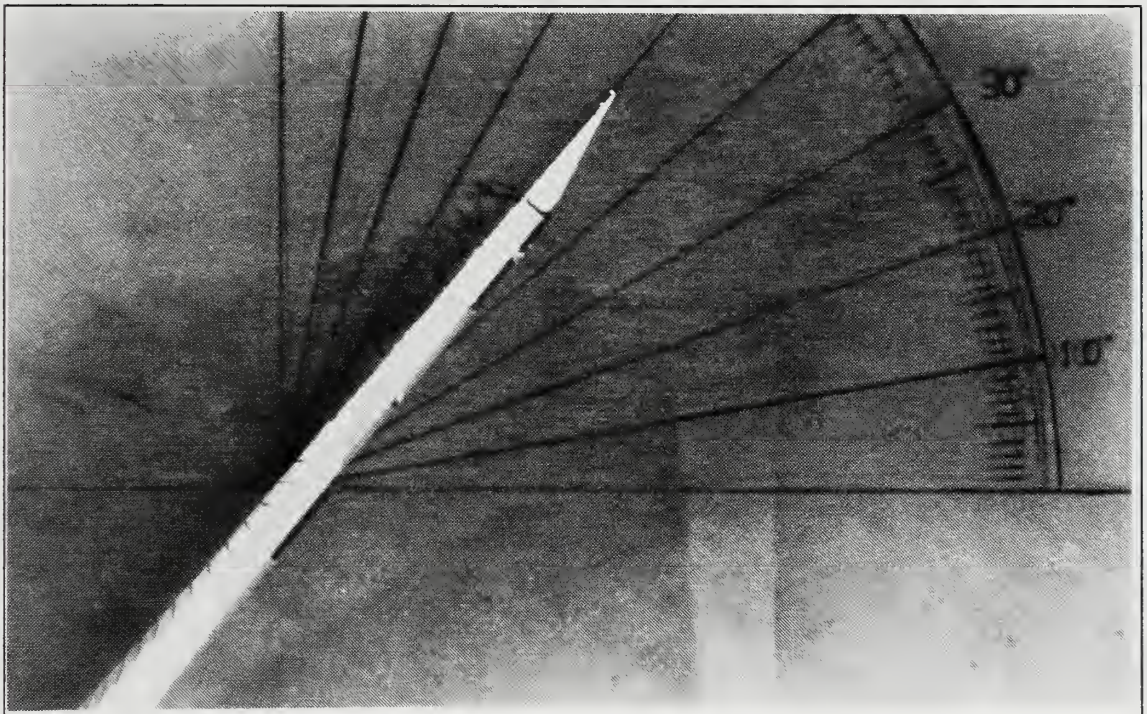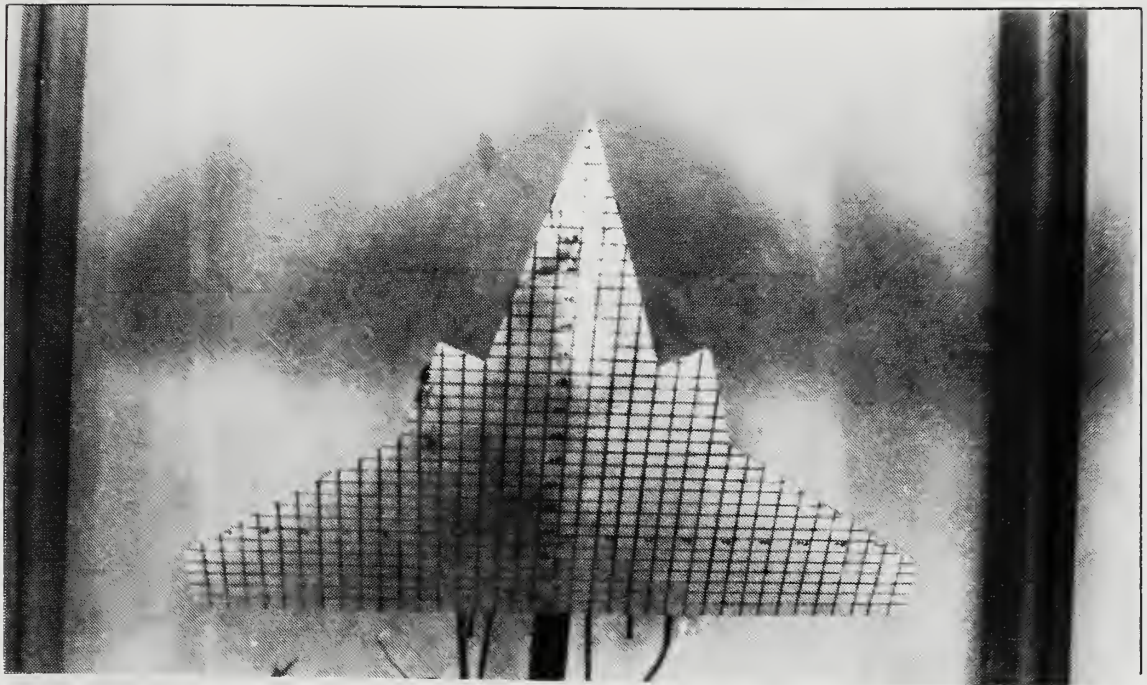
Figure 54. Strake Vortex Flow, Modified Model,
k=0.06, α=50°
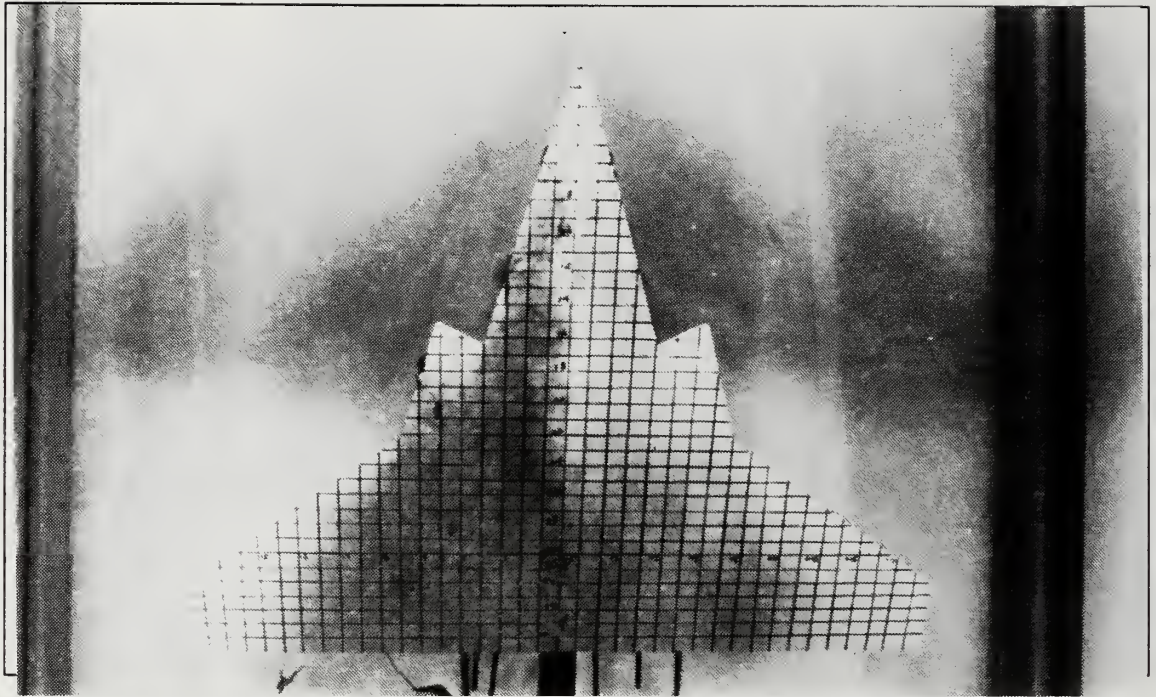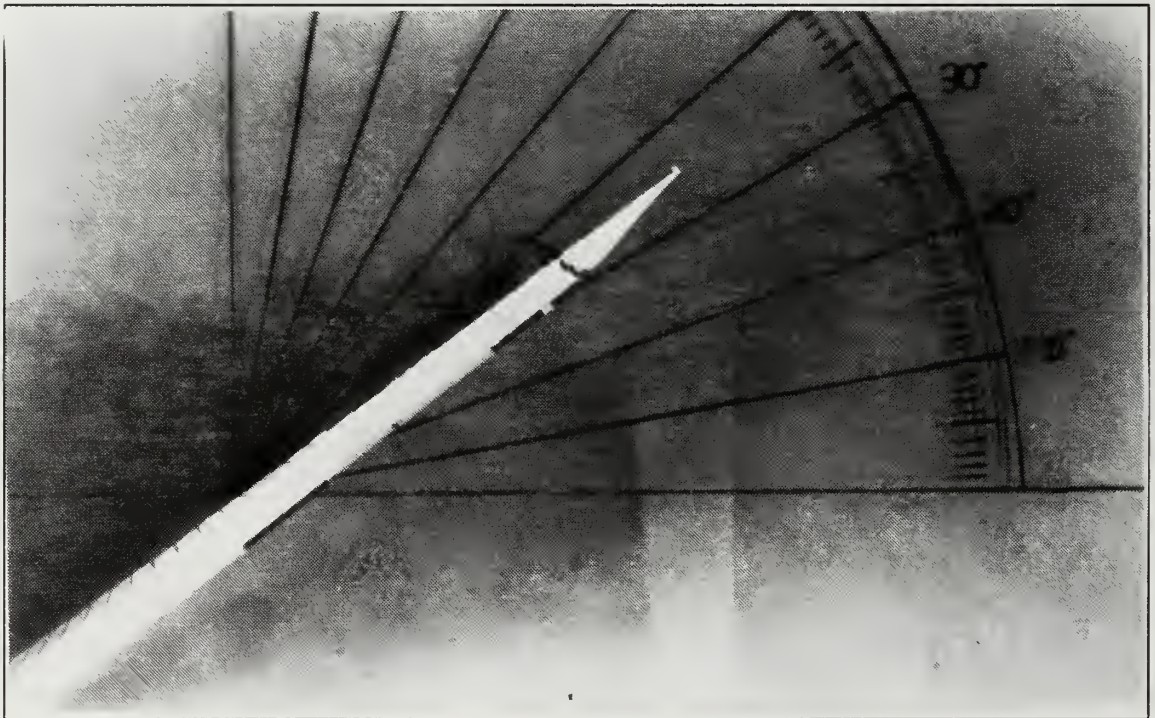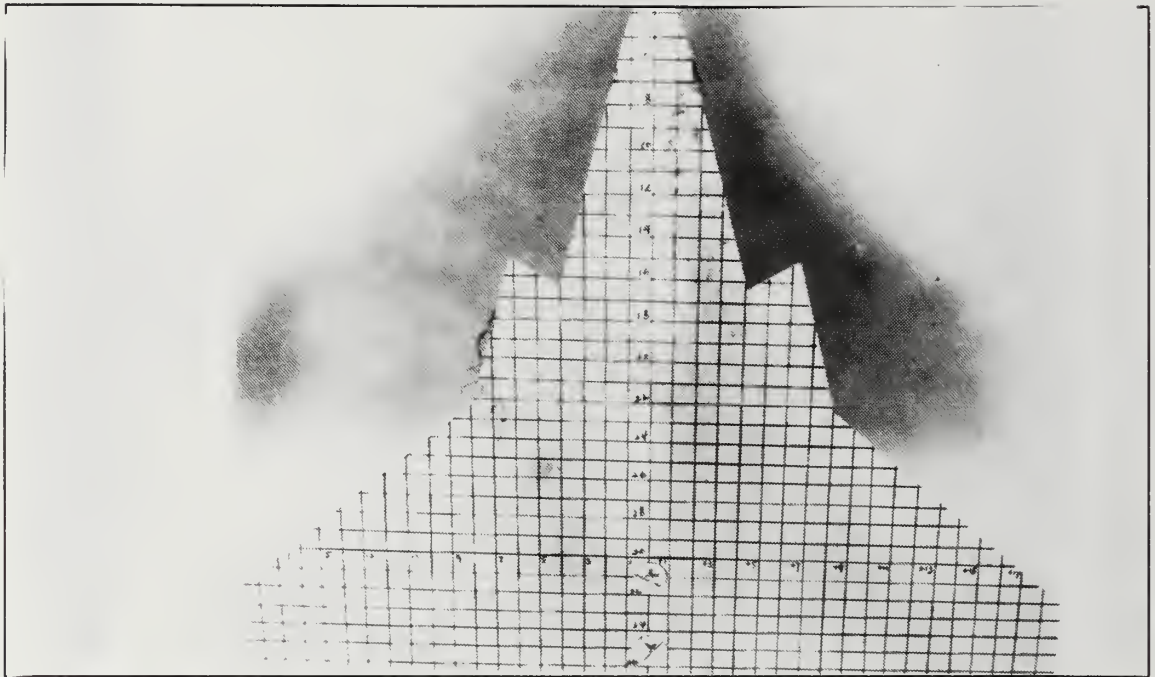
Figure 55. Strake Vortex Flow, Modified Model,
k=-0.06, α=39°

Figure 56. Strake Vortex Flow, Modified Model,
k=-0.06, α=28°

Figure 57. Strake Vortex Flow, Modified Model,
k=-0.06, α=20°

Figure 58. Strake Vortex Flow, Modified Model,
k=-0.06, α=10°

Figure 59. Strake Vortex Flow, Modified Model,
k=0.13, α=10°
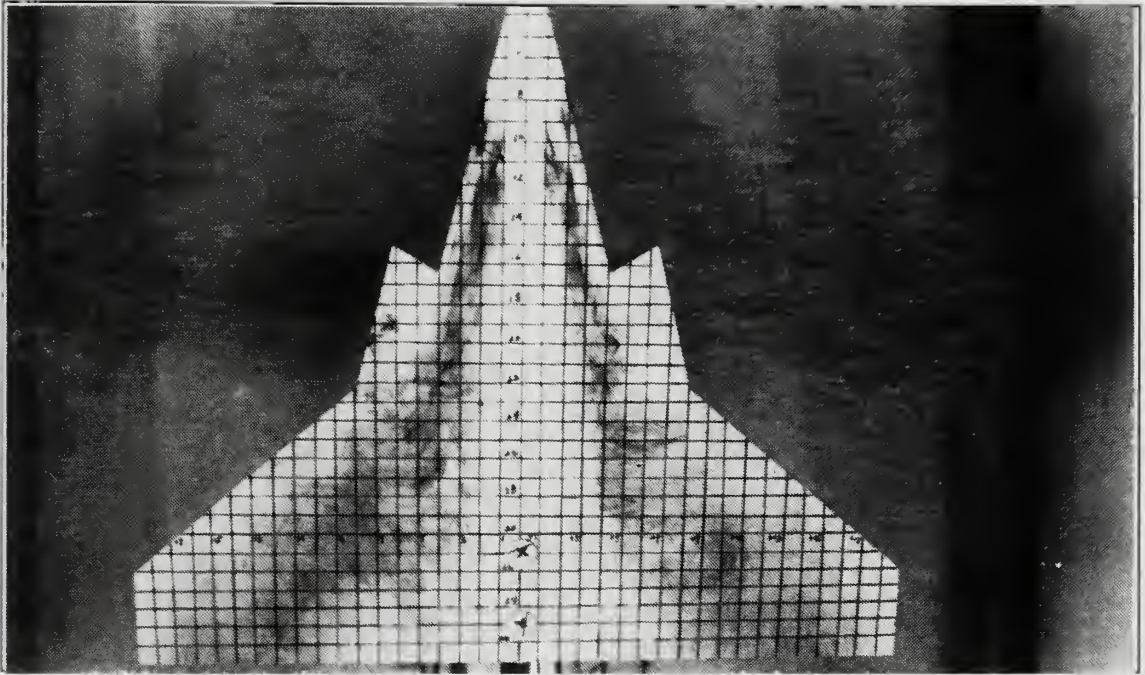
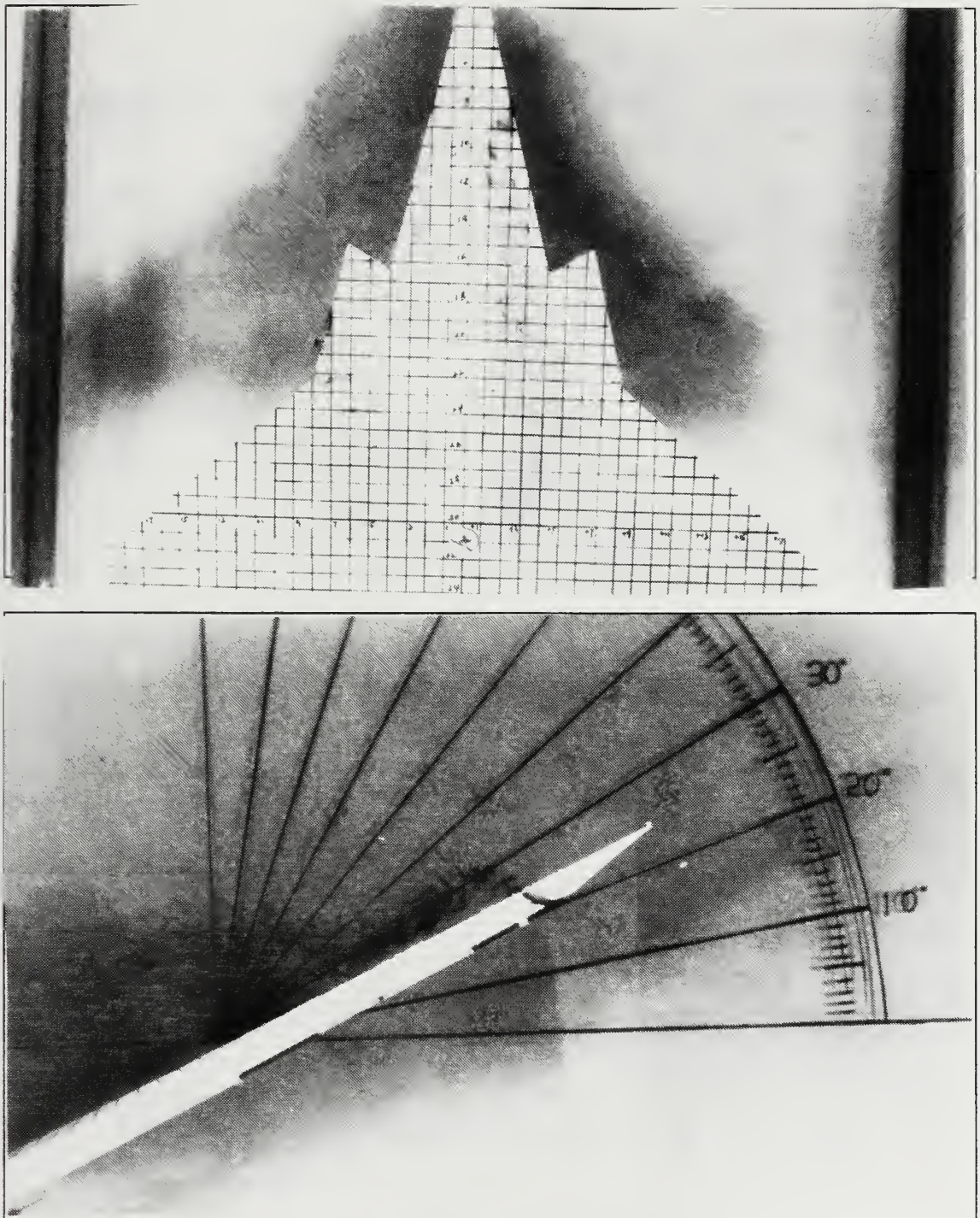Figure 60. Strake Vortex Flow, Modified Model,
k=0.13, α=21°
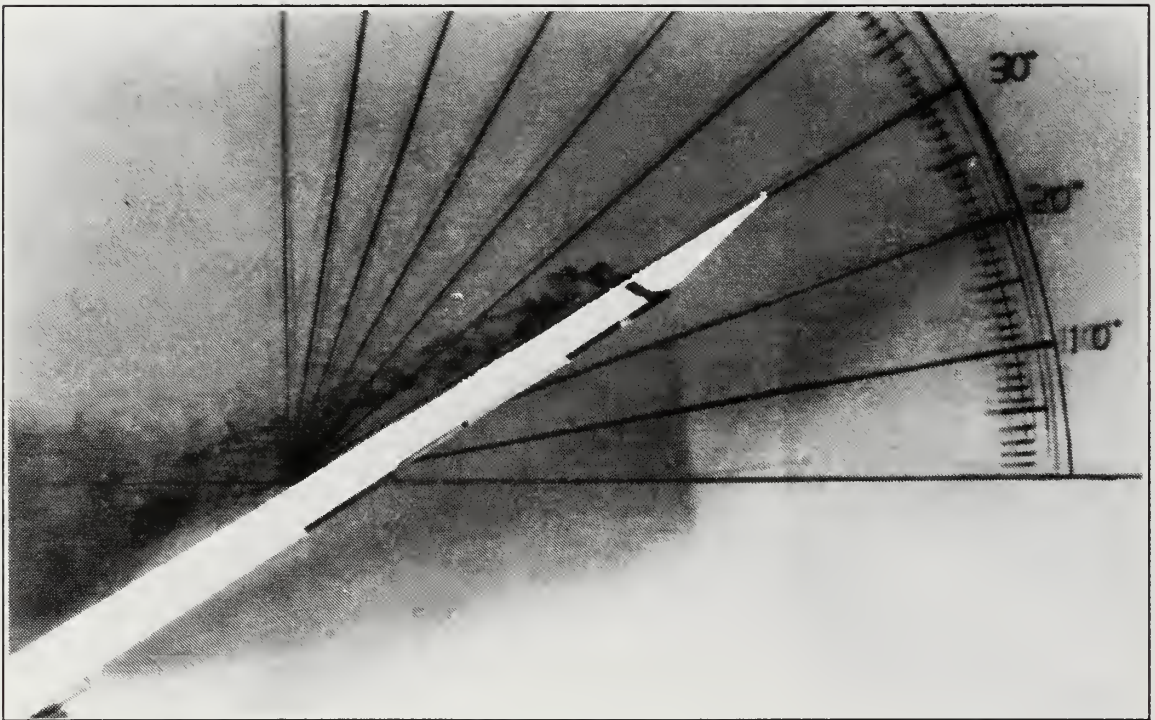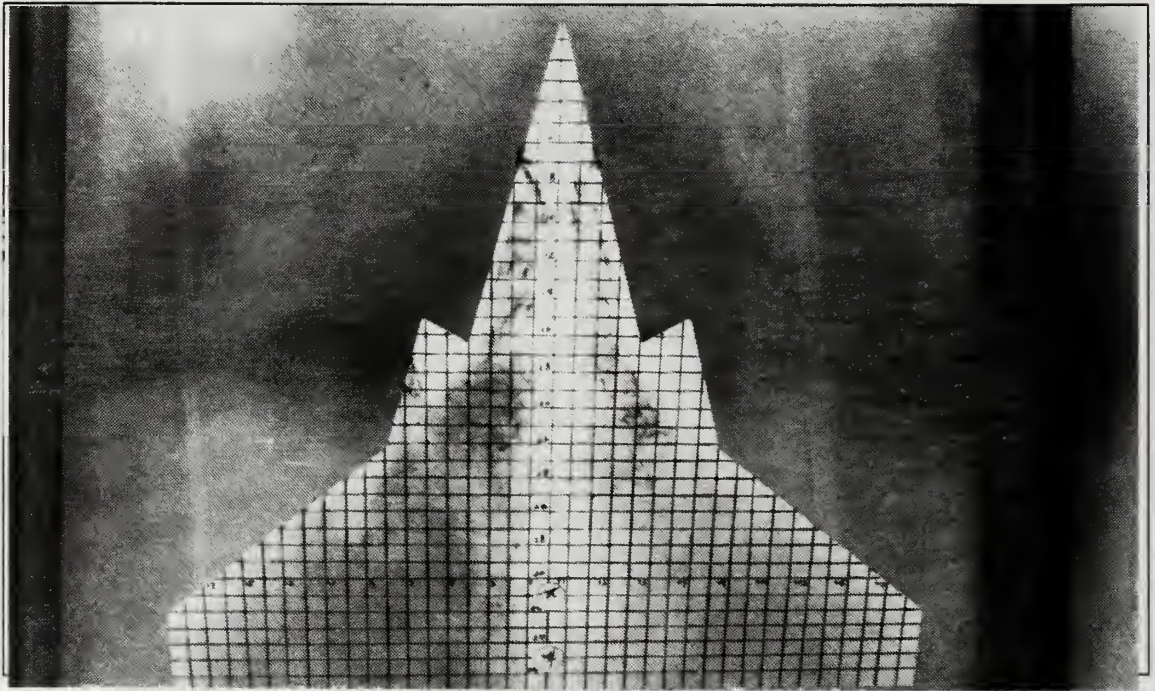
Figure 61. Strake Vortex Flow, Modified Model,
k=0.13, α=30°

Figure 62. Strake Vortex Flow, Modified Model,
k=0.13, α=40°

Figure 63. Strake Vortex Flow, Modified Model,
k=0.13, α=50°

Figure 64. Strake Vortex Flow, Modified Model,
k=-0.13, α=45°

Figure 65. Strake Vortex Flow, Modified Model,
k=-0.13, α=35°

Figure 66. Strake Vortex Flow, Modified Model,
k=-0.13, α=25°

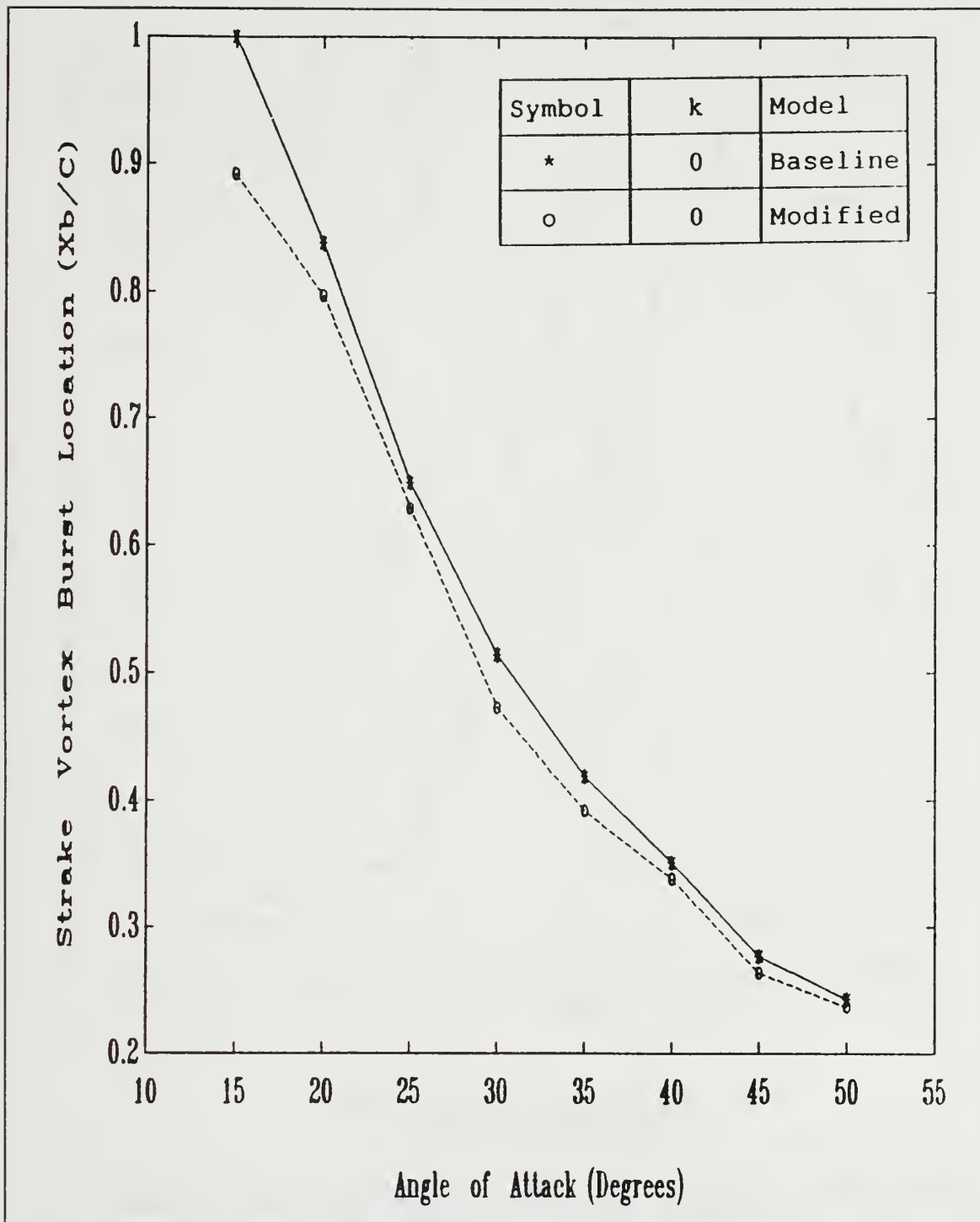# APPENDIX B. EXPERIMENTAL RESULTS (GRAPHS)

FIGURE 67 THROUGH 73

.

Figure 67. Strake Vortex Burst Location for
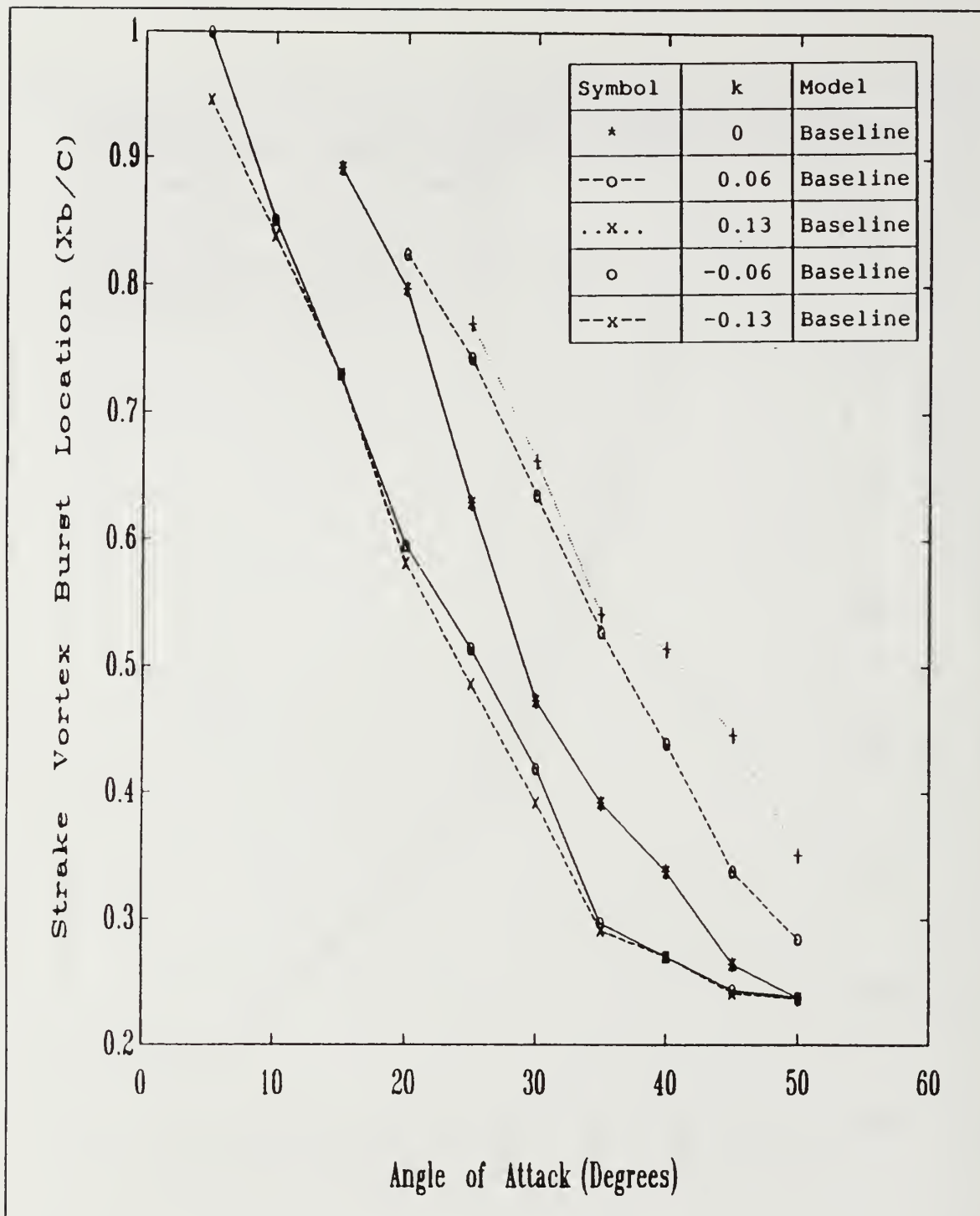Baseline/Modified Models as A Function of AOA for
Static Case

Figure 68. Strake Vortex Burst Location for
Baseline Models as A Function of AOA for
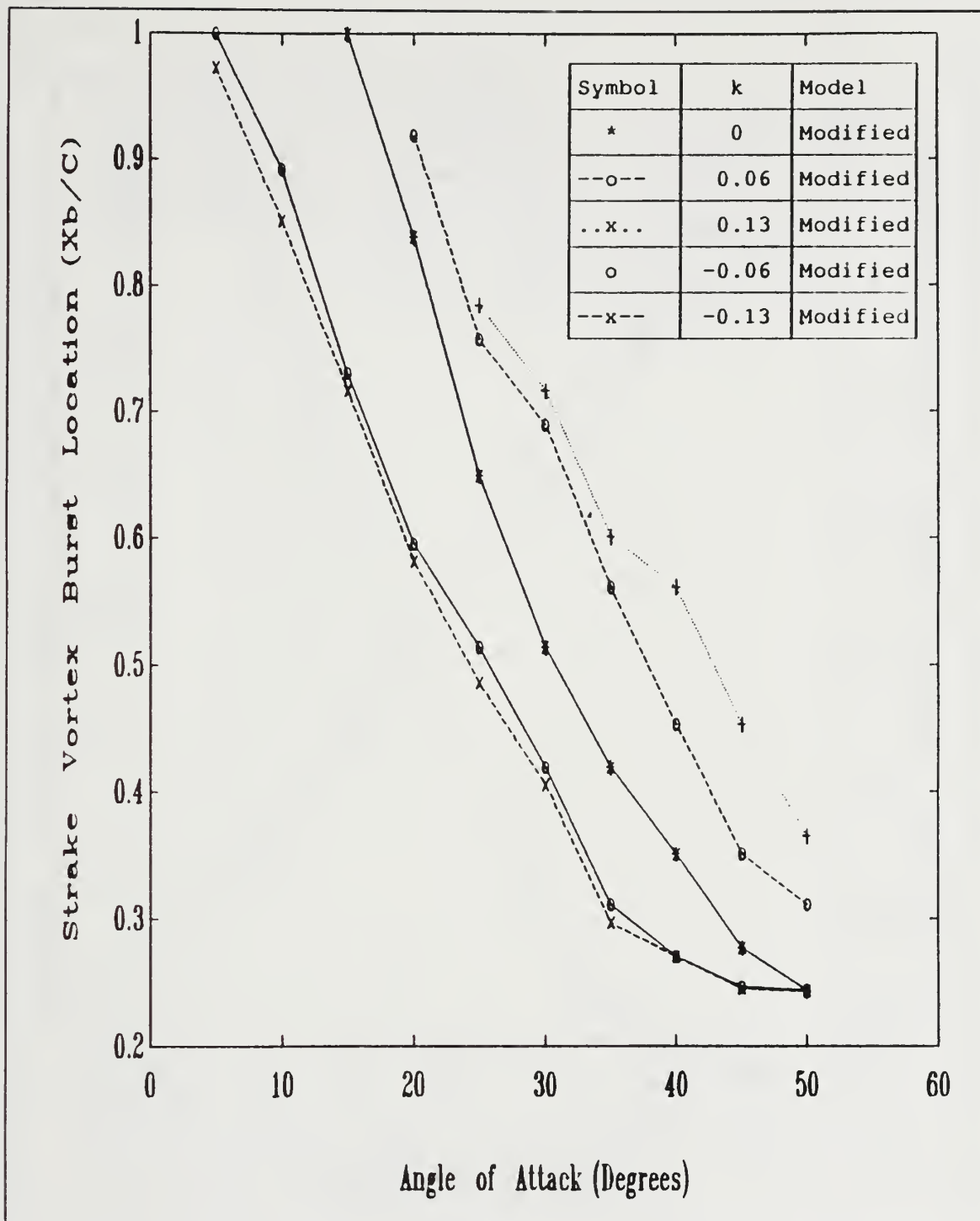Static/Dynamic Case

94

Figure 69. Strake Vortex Burst Location for
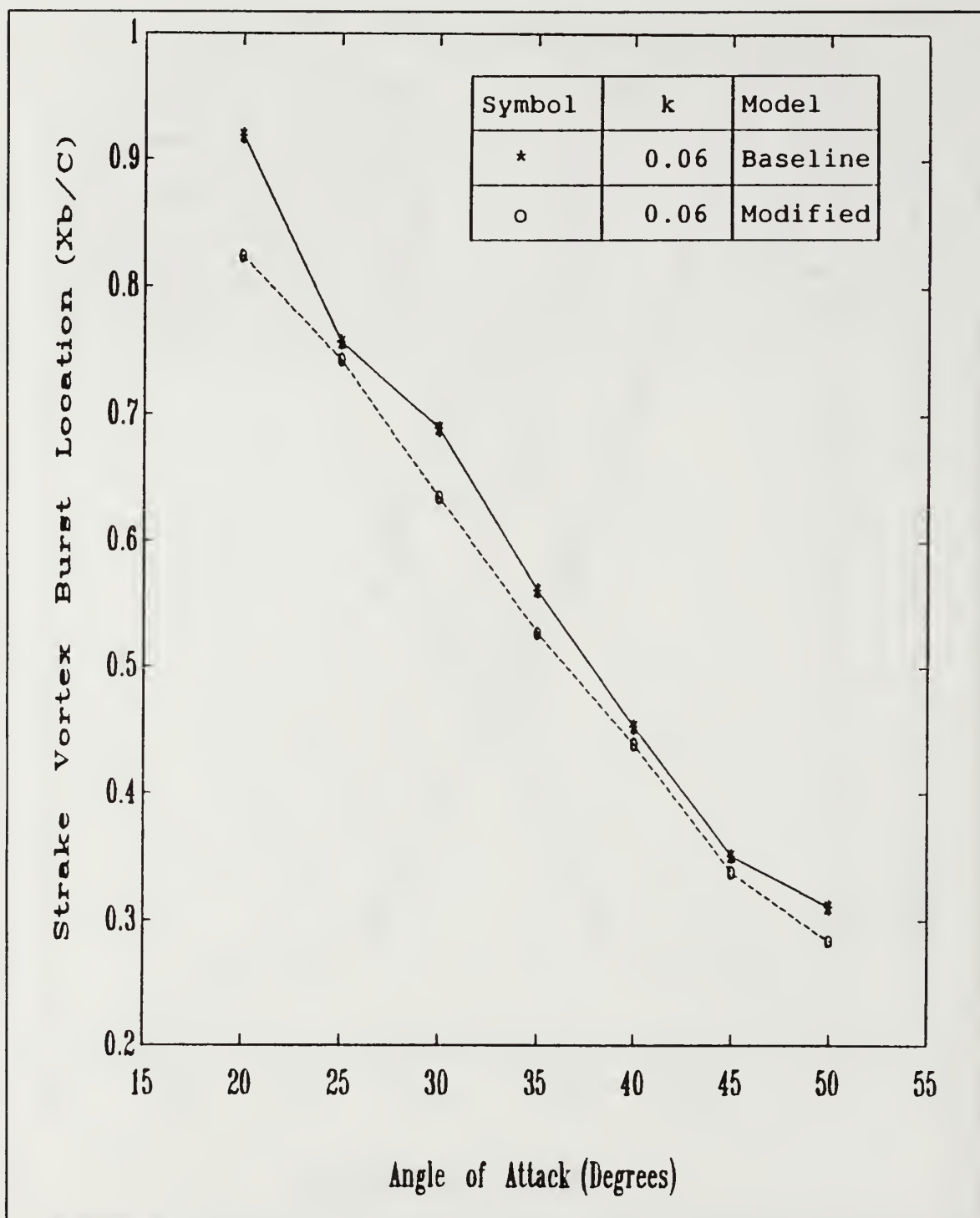Modified Models as A Function of AOA for
Static/Dynamic Case

Figure 70. Strake Vortex Burst Location for
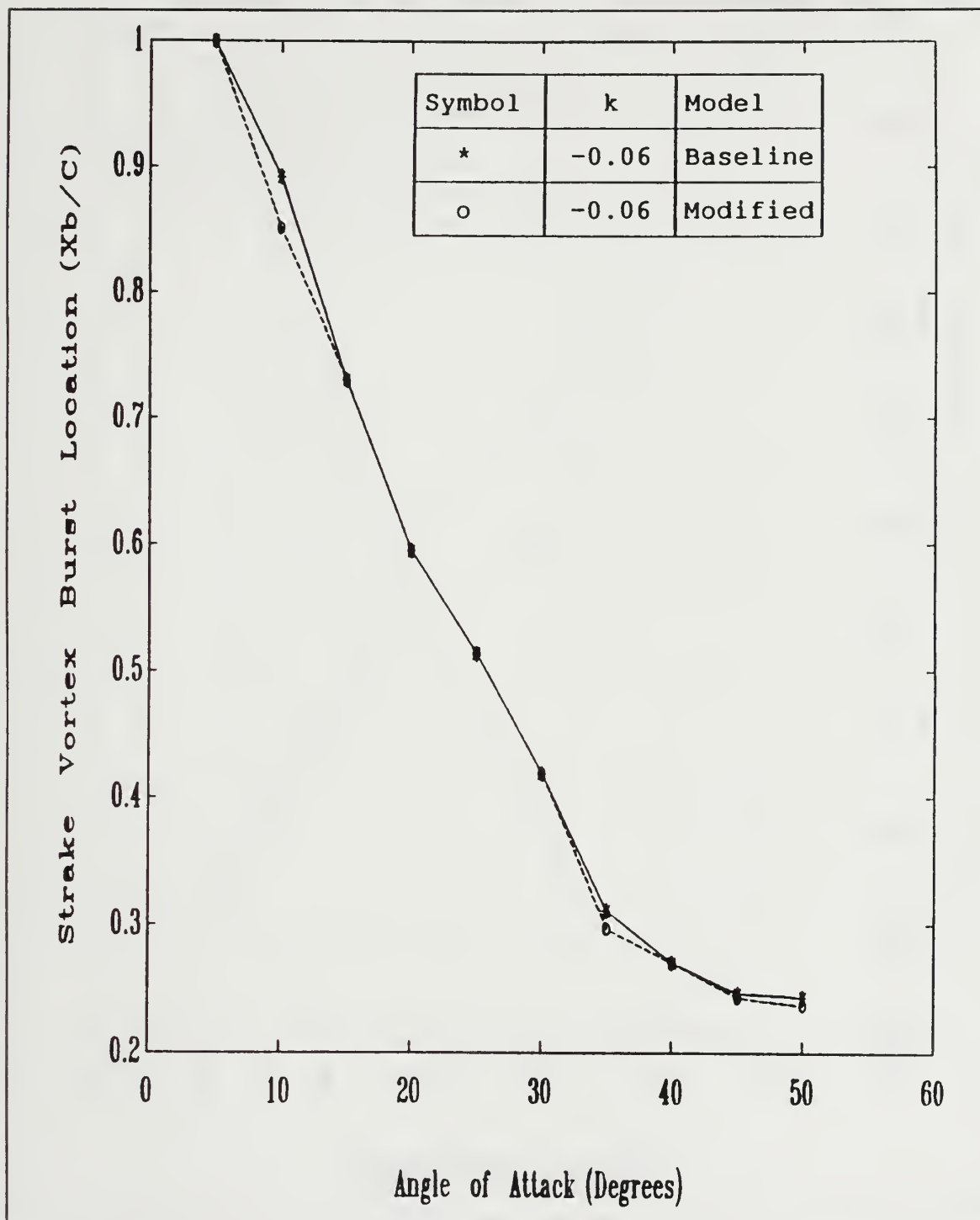Baseline/Modified Models as A Function of AOA for
Dynamic Case, k=0.06

Figure 71. Strake Vortex Burst Location for
Baseline/Modified Models as A Function of AOA for
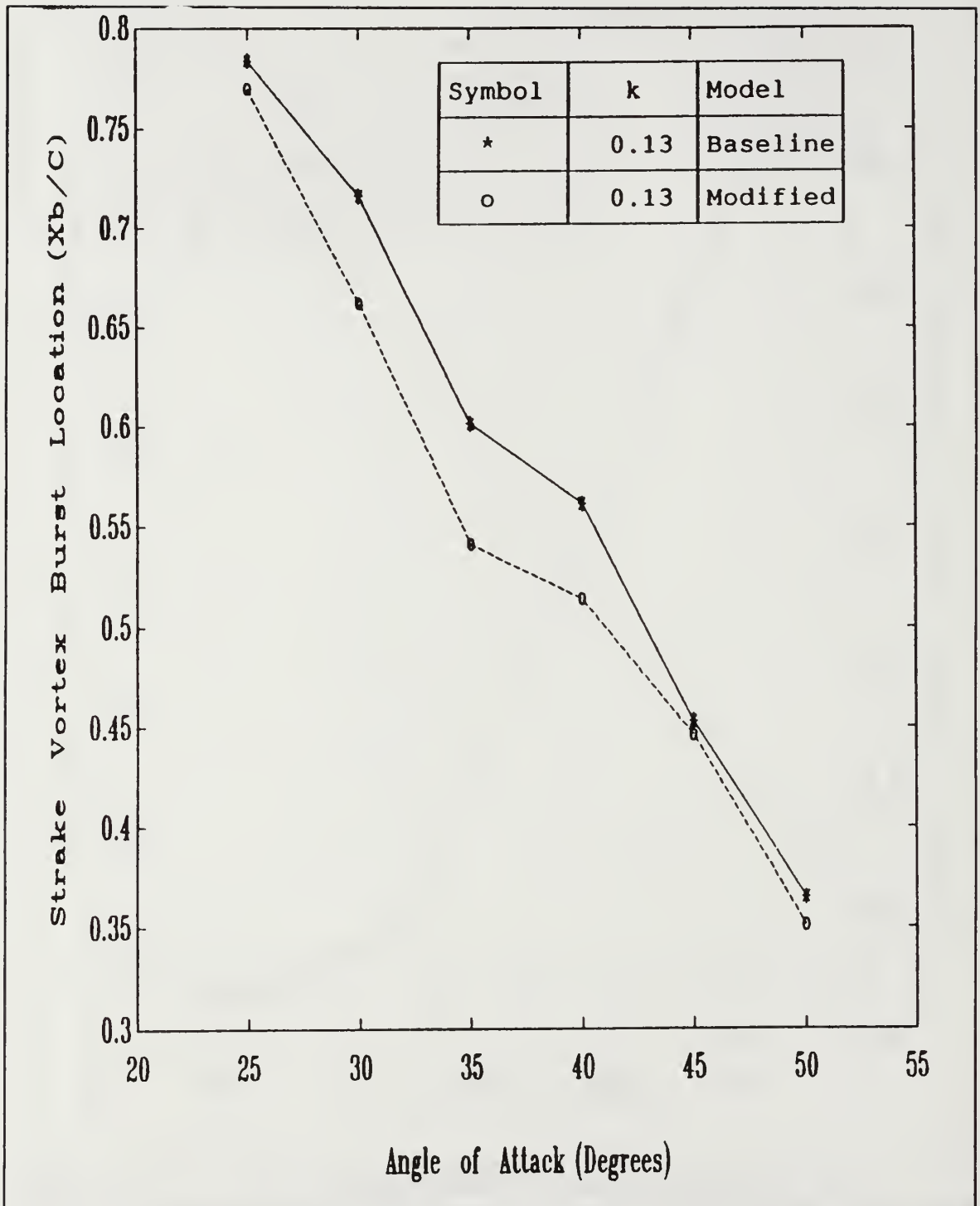Dynamic Case, k=-0.06

Figure 72. Strake Vortex Burst Location for
Baseline/Modified Models as A Function of AOA for
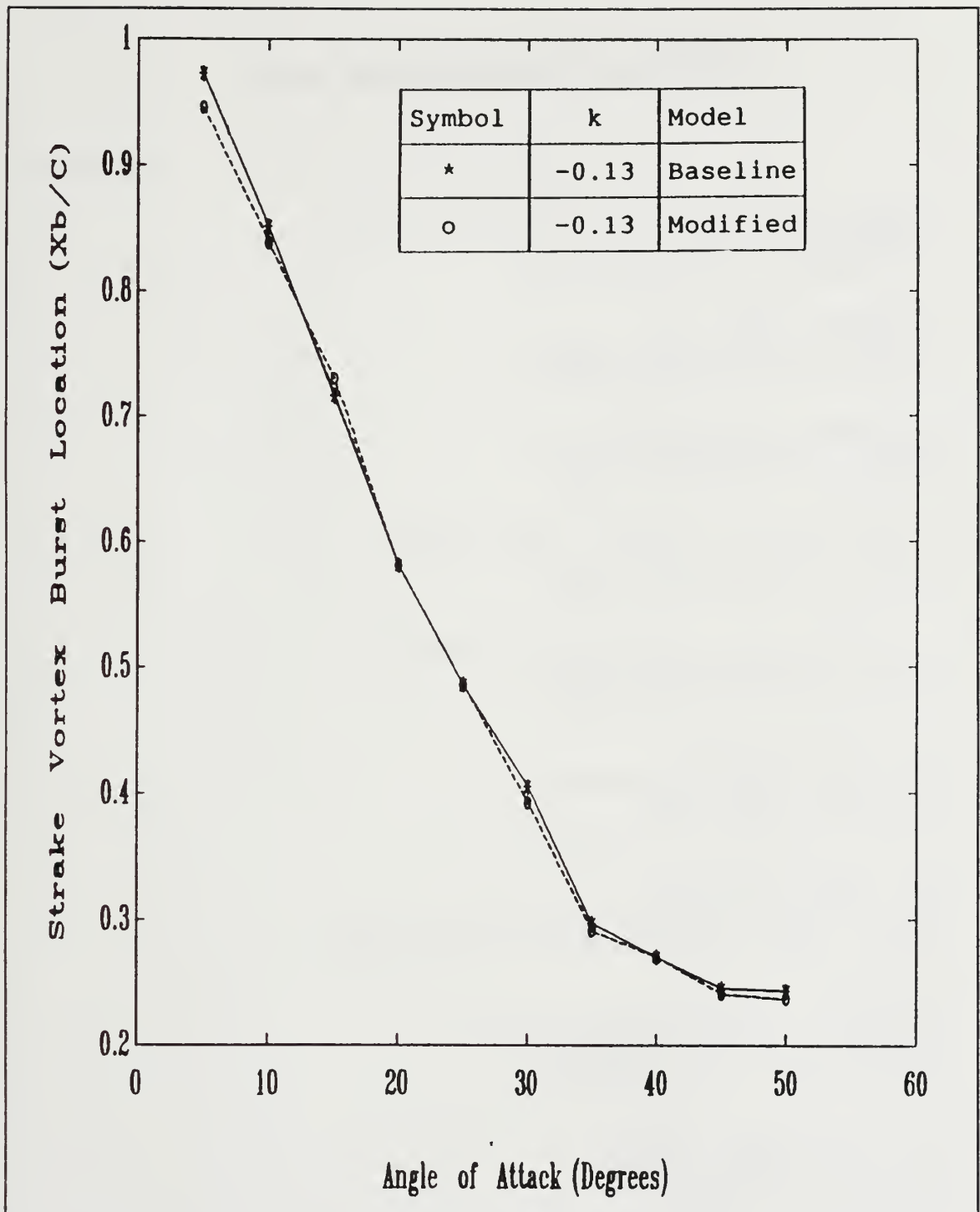Dynamic Case, k=0.13

98

Figure 73. Strake Vortex Burst Location for
Baseline/Modified Models as A Function of AOA for
Dynamic Case, k=-0.13

INITIAL DISTRIBUTION LIST

No.Copies

1. Defense Technical Information Center 2
   Cameron Station
   Alexandria, VA 22304-6145

2. Library, Code 52 2
   Naval Postgraduate School
   Monterey, CA 93943-5002

3. Chairman, Code AA/Co 1
   Naval Postgraduate School
   Monterey, CA 93943-5000

4. Professor S.K. Hebbar, Code AA/Hb 4
   Naval Postgraduate School
   Monterey, CA 93943-5000

5. Professor M.F. Platzer, Code AA/Pl 1
   Naval Postgraduate School
   Monterey, CA 93943-5000

6. CDR. Li Feng-Hsi 2
   5-2 Tsyi Huei 6th Tsuen
   Tsoying, Kaohsiung
   Taiwan, Republic of China

7. Mr. Marvin Walters 1
   Naval Air Development Center
   Street Road, Warminster, PA 18974-5000

8. Michael J. Harris 1
   Aircraft Division Code AIR-931
   Naval Air System Command
   Washington, D.C., 20361-9320

9. Naval Academy Library 1
   P.O. Box 8494, Tsoying
   Kaohsiung, Taiwan
   Republic of China

GAYLORD S